5-6-2014

Gene Expression Profile Reveals the Novel Repression of Heat Shock Protein Expression by TNIP1 in Keratinocytes

Vincent P. Ramirez
vincentpramirez@yahoo.com

Gene Expression Profile Reveals the Novel Repression of Heat Shock Protein Expression by TNIP1 in Keratinocytes

Vincent P. Ramirez, PhD

University of Connecticut, 2014

The TNFα-induced protein 3-interacting protein 1 (TNIP1) protein represses various receptor-mediated signaling pathways, ranging from transmembrane to nuclear receptors. Increased TNIP1 expression results in blocking the TNFα-induced NF-κB activation or repressing peroxisome proliferator activated receptor and retinoic acid receptor activity. These transcription factors play key roles in regulating inflammation and inflammatory diseases. A growing number of references have linked TNIP1 SNPs and increased expression in psoriasis, a chronic inflammatory disease characterized by keratinocyte hyperproliferation and incomplete differentiation. However, TNIP1's exact role is not yet known. To determine the genes and biological functions regulated by TNIP1 in keratinocytes, we overexpressed TNIP1 in cultured keratinocytes and performed a gene expression microarray analysis. Reduced expression of most genes was observed, including several heat shock proteins (HSP). These results suggest TNIP1 could regulate the cell stress response. However, its exact role in this process and the mechanism of the TNIP1-mediated transcriptional repression is not yet characterized.

We examined the TNIP1 repression of HSPA6 (also named HSP70B') to model the repression on all HSPs. Since the transcriptional regulation of HSPA6 has not yet been fully characterized, we examined the factors contributing to its

promoter activation. We found that a novel AP1 site and heat shock element upstream of previously recognized sites contribute to its basal and stress inducibility, respectively. To determine the mechanism of TNIP1's repression on HSPA6, we hypothesized that TNIP1 acts on PPAR, RAR or NF-κB to reduce the expression of HSPs. We observed TNIP1 does not act through these transcription factors, but possibly through a novel, yet uncharacterized pathway. Additionally, we assessed the effect of TNIP1 on keratinocyte proliferation and differentiation. We found that a chronic, but not acute, overexpression of TNIP1 blocks keratinocyte cell growth to possibly through decreasing the HSP chaperone function.

Gene Expression Profile Reveals the Novel Repression of Heat Shock Protein Expression by TNIP1 in Keratinocytes

Vincent P. Ramirez

B.S. University of California, Davis, 2004

A Dissertation

Submitted in Partial Fulfillment of the

Requirements for the Degree of

Doctor of Philosophy

at the

University of Connecticut

2014

APPROVAL PAGE

Doctor of Philosophy Dissertation

Gene Expression Profile Reveals the Novel Repression of

Heat Shock Protein Expression by TNIP1 in Keratinocytes

Presented by

Vincent P. Ramirez, B.S.

Major Advisor _____

Dr. Brian J. Aneskievich

Associate Advisor

_____

Dr. Theodore Rasmussen

Associate Advisor

_____

Dr. Charles Giardina

University of Connecticut

2014

Dedication

To the Ramirez, Pascual, Panganiban and Titong families: thank you for all your support throughout this journey.

Acknowledgements

I would like to give my sincerest thanks to my major advisor Dr. Brian J. Aneskievich for giving me the opportunity to join his laboratory as a graduate student. With his guidance and training, I grew into the scientist I am today. I would also like to thank my associate advisors Dr. Charles Giardina and Dr. Theodore Rasmussen for their time and efforts in advising me throughout my research project. I would especially like to thank Dr. Giardina for his expertise and input on the intricacies and technicalities of the heat shock protein world.

I am thankful for the help and advice given by the past and present members of the Aneskievich lab. First, I would like to thank Carmen Zhang for training me in various aspects of the lab and for starting the microarray project by doing the initial TNIP1-overexpression. I also want to thank the past Aneskievich lab graduate students, Priscilla Encarnacao, Igor Gurevich and Nidhish Francis, for their suggestions and comments to help me with the TNIP1-HSP project. Also, thanks to my undergraduate and Pharm.D mentees Mike Stamatis for generating many of the luciferase constructs used for these experiments, Anastasia Shmukler for performing some of the qPCR and MTS assays, Tom Walcyzk for keeping the lab in perfect condition, and Hank Ng for his assistance with the TSS project. I also could not have completed the project without the work and results generated by Nora McHugh.

I am very grateful to my former supervisors Dr. Sarah Jaw-Tsai for teaching me about pharmacology and pharmacokinetics and encouraging me to

pursue my graduate studies and Michele Bauer for giving me a start in laboratory research.

I would like to acknowledge the financial support I received from the UConn School of Pharmacy, Center for Regenerative Biology, and Molecular and Cellular Biology, and Society of Toxicology, as well as the NIH and UConn Research foundation grants awarded to Dr. Aneskievich.

I would like to thank my family and friends for their support and encouragement throughout my time in graduate school. Lastly, I would like to give a heartfelt thank you to my beautiful and wonderful wife, Alley. Without you by my side to help and support me before and during graduate school, I would not have succeeded. Thank you for all you have done with and for me.

Table of contents

		Page
Title Page		i
Approval Page		ii
Dedication		iii
Acknowledgements		iv
Table of Contents		vi
List of Figures		viii
List of Tables		x
List of Abbreviations		xi
Chapter 1	**Introduction**	1
	Skin anatomy and keratinocyte biology	1
	TNFα-Induced Protein 3-Interacting Protein 1 (TNIP1)	8
	Heat Shock Proteins	20
	Summary	23
Chapter 2	**TNIP1 modulates heat shock protein expression and the stress response**	25
	Abstract	25
	Introduction	27
	Materials and Methods	30
	Results	35
	Discussion	46

Chapter 3	**Transcriptional regulation of HSPA6 in basal and stressed conditions**	50
	Abstract	50
	Introduction	52
	Materials and Methods	55
	Results	62
	Discussion	86
Chapter 4	**TNIP1-HSP mechanism of repression and overall keratinocyte consequences**	92
	Abstract	92
	Introduction	93
	Materials and Methods	96
	Results	100
	Discussion	111
Chapter 5	**Summary, conclusions and future directions**	114
	Summary and conclusions	114
	Future directions	119
Appendix 1	TNIP1 protein expression up to 96 hours	122
Appendix 2	Microarray results from TNIP1 overexpression	123
Appendix 3	Protocol for making HSPA6 promoter constructs	130
Appendix 4	TNIP1 transcriptional start site	136
Appendix 5	Experiment numbers for each figure	138
References		139

List of Figures

		Page
1.1	Illustration of the skin	6
1.2	Illustration of the epidermis and its keratinocyte layers	7
1.3	TNIP1-mediated signaling pathways	17
2.1	Validation of TNIP1 overexpression	36
2.2	TNIP1 overexpression microarray results	38
2.3	Ingenuity Pathway Analysis clustering of genes with significant expression change	39
2.4	DAVID clustering of genes with significant expression change	42
2.5	Effect of TNIP1 overexpression on HSPs in HaCaT KCs	43
2.6	Effect of TNIP1 overexpression on KC differentiation markers in NHEKs	44
2.7	Effect of TNIP1 overexpression on HSPs in NHEKs	45
3.1	Basal and heat-inducible expression of HSPA6 in HaCaT KCs	63
3.2	Basal and heat-inducible expression of HSPA1A in HaCaT KCs	64
3.3	Expression of HSPA6 in various cell types	65
3.4	Native restriction enzyme sites within the HSPA6 3kb promoter	67
3.5	*In silico* analysis of the HSPA6 3kb promoter	68
3.6	Determining the transcriptionally regulated regions within the HSPA6 promoter	71
3.7	Localizing the repressible region within the HSPA6 promoter	72
3.8	Localizing the basal and inducible regions within the HSPA6 promoter	73
3.9	Searching for transcription factor binding sites between -346 to -216 bp region of the HSPA6 promoter	75
3.10	Characterization of the -244 bp AP1 site	76
3.11	EMSA binding analysis of AP1 proteins c-Jun and c-Fos to the -244 AP1 site	77

3.12	Searching for heat responsive elements between -346 to -216 bp region of HSPA6	80
3.13	Characterization of the -284 bp HSE	81
3.14	EMSA binding analysis of HaCaT HSF proteins to the -284 bp HSE	82
3.15	EMSA binding analysis of HaCaT HSF proteins to a consensus HSE	83
3.16	EMSA binding analysis of HeLa HSF proteins to the -284 bp HSE	84
3.17	EMSA binding analysis of HeLa HSF proteins to a consensus HSE	85
4.1	*In silico* analysis of the HSPA6 3kb promoter searching for TNIP1-repressed transcription factors	101
4.2	Analysis of the HSPA6 promoter truncation constructs	102
4.3	Analysis of the HSPA6 promoter deletion constructs	106
4.4	Effect of TNIP1 overexpression on HSPs in heat stressed HaCaT KCs	108
4.5	Effect of “short term” increased TNIP1 levels on HaCaT KCs viability and growth	109
4.6	Effect of “long term” increased TNIP1 levels on HaCaT KCs viability and growth	110

List of Tables

		Page
1.1	TNIP1 and associated diseases	18
1.2	Experimentally altered TNIP1 and the resulting phenotypes	19
2.1	List of qPCR primers for the microarray	34
3.1	Site-directed mutagenesis primer sequences.	60
3.2	Oligomers used for EMSA probes	61
4.1	List of top predicted transcription factor binding sites within the -216 to -70 bp region of the HSPA6 promoter	109

List of Abbreviations

ABIN1	A20 binding and inhibitor of NF-κB
AP1	Activator protein 1
C/EBP	Ccaat-enhancer binding proteins
DAVID	Database for Annotation, Visualization and Integrated Discovery
DNAJA1	HSP40 (homolog), subfamily A, member 1
DNAJB1	HSP40 (homolog), subfamily B, member 1
EMSA	Electrophoretic mobility shift assay
GWAS	Genome wide association studies
HDAC	Histone deacetylase
HSE	Heat shock element
HSF	Heat shock transcription factor
HSP	Heat shock protein
HSPA1A	HSP70, subfamily A, member 1A
HSPA6	HSP70, subfamily A, member 6 (HSP70B')
IKK	Inhibitor of NF-κB kinase
IPA	Ingenuity Pathway Analysis
KC	Keratinocyte
luc	Luciferase
mt	Mutant
MZF1	Myeloid zing finger 1
NEMO	NF-κB essential modulator
NF-κB	Nuclear actor κB
NHEK	Normal human epidermal keratinocyte
NR	Nuclear receptor
PPAR	Peroxisome proliferator activated receptor
RA	Rheumatoid arthritis
RAR	Retinoic acid receptor
RIP140	Receptor interacting protein 140
RXR	Retinoid X receptor
SLE	Systemic lupus erythematosus
SNP	Single nucleotide polymorphism
SRC1	Steroid receptor coactivator 1
SSc	Systemic sclerosis
TNFAIP3	TNFα-induced protein 3
TNFR	TNFα receptor
TNFα	Tumor necrosis factor, alpha
TNIP1	TNFα induced protein 3-interacting protein 1
UBAN	Ubiquitin binding in ABIN and NEMO
VAN	Virion-associated nuclear shuttling protein
WHN	Winged helix transcription factor
ZFX	Zinc finger protein, X-linked

Chapter 1

INTRODUCTION

Skin structure and regulation

Skin anatomy and keratinocyte biology

The skin is the largest organ in our body serving as a first line defense from various environmental stressors, including exposure to UV, heat and chemicals. It is made up of two layers: the outer epidermal layer and the underlying dermal layer (Fig 1.1) *(1, 2)*, each consisting of many specialized cells and structures that contribute to the overall health and protective function of the skin. The outermost layer, the epidermis, is composed of several different cell types, in which approximately 90% are keratinocytes (KC) *(3)*. The remaining cells are melanocytes and Langerhans cells, which contribute to skin pigmentation and protect the skin during infections, respectively. The epidermis can be further subdivided into four major layers – the stratum basale (bottom layer), stratum spinosum, stratum granulosum and stratum corneum (top layer) (Fig 1.2) *(4)*. The process of cornification, when KC proliferate and differentiate from the basal to the cornified cells, is crucial for to generate a tough, resilient barrier to separate the body from the harsh environment *(2)*.

Epidermal and KC homeostasis are regulated by many different endogenous and exogenous factors, including proteins, drugs and UV *(5-7)*. The epidermis is at a constant state of flux where new KCs are produced in the stratum basale, while old, differentiated KCs are sloughed off from the stratum corneum. Proliferative KCs are found in the basal layer, where they are

responsible for repopulating the epidermis. When a KC leaves this layer, a unique form of programmed cell death, cornification, occurs, where there is a turnover of highly specific proteins within each layer of the epidermis, eventually resulting in the KC's death and removal at the top layer *(4)*. Several receptor-mediated pathways regulate the cornification process, including nuclear receptors (NR), tumor necrosis factor alpha (TNFα) receptor (TNFR), epidermal growth factor receptor (EGFR), and toll like receptors (TLR).

Keratinocyte regulation by nuclear receptors

NRs are a superfamily of ligand-activated transcription factors that modulate gene transcription. There are over 45 different NRs, each playing key roles in regulating many biological functions and processes *(8)*. Many different NRs, including but not limited to peroxisome proliferator activated receptors (PPAR) and retinoic acid receptors (RAR), contribute to KC differentiation process. Equally important to the transcriptional activity of ligand-bound NRs are the coregulator proteins they interact with. Coregulators, which are classified as either coactivators or corepressors, directly bind NRs through specific amino acid motifs. As their name might suggest, coactivators increase NR transcriptional activity, facilitated by NR ligand binding. Corepressors, on the other hand, mediate the repression of NRs, typically, in absence of a ligand. The regulation of NRs, and the possible effect on their target genes, could have a great effect on KC homeostasis *(9)*.

The PPAR subfamily of NRs has been shown to enhance KC proliferation and differentiation. Ligands for PPARs range from endogenous lipids and their derivatives to exogenous therapeutic chemicals targeting a specific subtype(s) of PPAR. KCs express all three subtypes (α, β/δ and γ) of PPARs in both basal and suprabasal KCs *(10)*. Pharmacological stimulation of PPAR β/δ or γ by isoform specific ligands resulted in stimulating KC differentiation, suggesting a pro-differentiation role in skin physiology *(11, 12)*. On the other hand, PPARα activation results in a thinner epidermis, where KC proliferation is blocked but differentiation is induced *(13)*. Since each PPAR isoform plays a role in normal KC differentiaton and proliferation, its potential role in KC-related diseases were also characterized. Psoriasis is classically recognized as epidermal keratinocyte hyperproliferation with incomplete differentiation, incomplete barrier formation, and immune cell infiltration *(14)*. In psoriasis, PPAR ligand treatment reduced the inflammation and restored normal KC physiology *(15-17)*.

In contrast to PPARs, the two isoforms of RAR (α and γ) were characterized in the skin to represses KC proliferation and differentiation. Treatment with retinoids, the ligands for RARs, has shown to prevent proper KC differentiation, where the top, cornified layer does not fully form *(18)*. Because of this repressive effect, retinoids have been used to treat hyperproliferative inflammatory diseases, including psoriasis *(19)*. Since the activation of either RAR or PPAR can lead to drastic changes in skin proliferation and differentiation in both normal and diseased skin, understanding the mechanisms involved in

these regulating NRs activation and repression is crucial to potentially target these receptors to maintain or modulate KC homeostasis.

TNFα receptor and keratinocyte cornification

The fate of KC proliferation and differentiation in both normal and inflamed conditions can also be regulated by altering the TNFR-initiated signaling pathway. TNFR is a key transmembrane protein to activate the transcription factor NF-κB, which contributes to promoting KC terminal differentiation. Classically, the activation of NF-κB is initiated by TNFR and is largely dependent on a series of phosphorylation and ubiquitination steps on various cytoplasmic proteins. Typically, ubiquitination is part of the proteasome-mediated protein degradation pathway; however, there are proteins, including NF-κB essential modulator (NEMO; also named inhibitor of NF-κB kinase gamma; IKKγ), whose ubiquitination results not only in protein breakdown but also in protein-protein interaction and enzyme activation *(20)*. Although not an enzyme itself, ubiquitinated NEMO interacts with IKKα and IKKβ in the IKK complex and facilitates activation of these kinases. The ubiquitination of NEMO is essential in this pathway because without it, the subsequent degradation of IκB and nuclear translocation of NF-κB will be blocked. When NF-κB activation was prevented in mice, a thickening in the suprabasal KCs was observed; alternatively, when NF-κB was overexpressed, a hypoplastic epidermal layer was seen *(21)*. In addition to activation of NF-κB, TNFR stimulation results in increased expression of pro-inflammatory cytokines, including IL-6 and IL-8, which are also involved in regulating KC proliferation *(22)*. These results indicate that the activation of

TNFR and NF-κB contribute to the generation of a normal, stratified epidermal layer. Overall, understanding the regulatory proteins involved in the TNFR and NR pathways is essential to determine the possible fate of epidermal KCs. Our lab discovered and characterized a novel NR corepressor, TNFα-induced protein 3 (TNFAIP3)-interacting protein 1 (TNIP1), and aimed to examine its potential function(s) in KC biology.

Figure 1.1

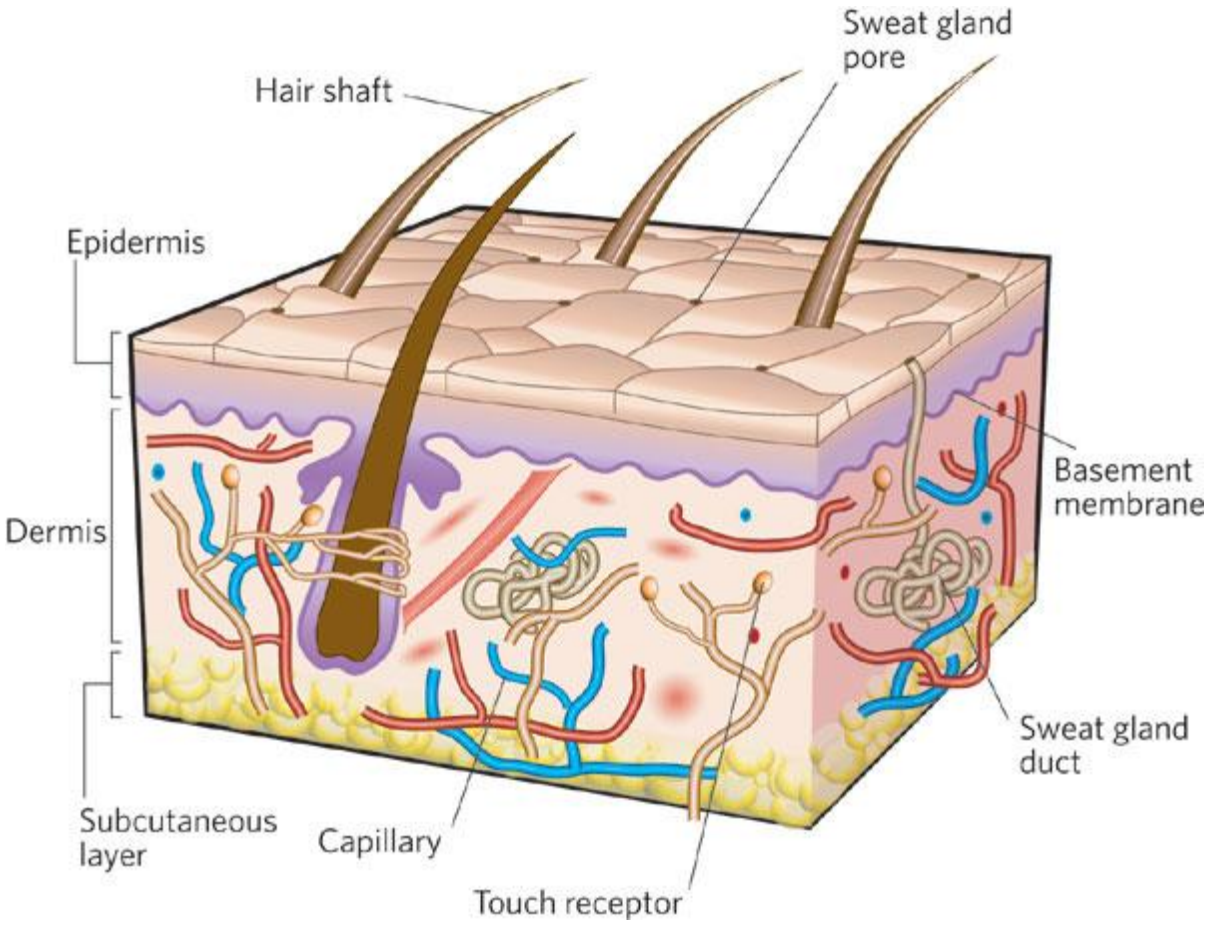

Figure 1.1. Illustration of the skin. The general structure of the skin is shown, including the thick dermal layer and the thin epidermis. Part of the subcutaneous layer is also show. The related structures are also illustrated. Original image from *(1)*.

Figure 1.2

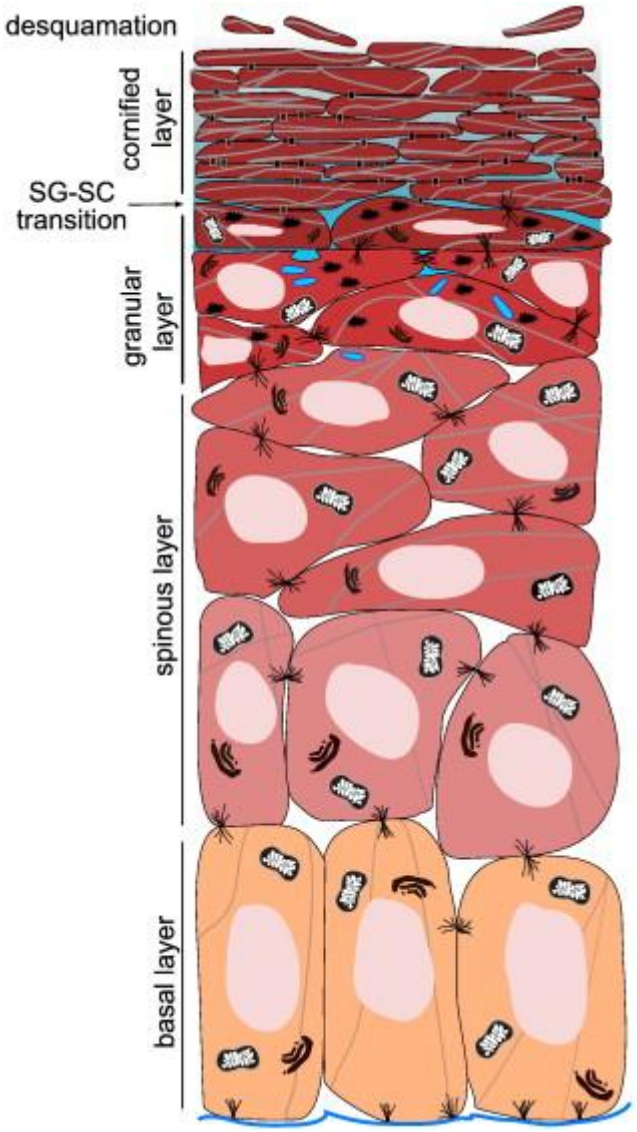

Figure 1.2. Illustration of the epidermis and its keratinocyte layers. Keratinocyte proliferation begins at the basal layer (stratum basale) where new cells can begin to move out of is layer to differentiate. The process of cornification is shown as the cells transition to become the cornified layer (stratum corneum). Original image from *(4)*.

TNFα-induced protein 3-interacting protein 1 (TNIP1)

TNIP1 is a corepressor of PPARs and RARs

Prior work in our laboratory discovered TNIP1 (also known as ABIN-1, Naf1 and VAN) as a novel coregulator of ligand-bound PPARs and RARs (Fig 1.3) *(23, 24)*. The requirement for ligand presence for TNIP1-NR interaction suggested TNIP1 as a NR coactivator. Intriguingly, the effect of TNIP1 interaction with NRs resulted in repression of these receptors' activities. TNIP1's direct binding to PPARs and RARs is facilitated by specific amino acid motifs within the TNIP1 sequence. TNIP1 exhibits a strong subtype preference amongst PPARs (γ > β/δ >>> α) and RARs (α >> γ) *(23, 24)*, however it does not interact with the PPAR and RAR heterodimer partner retinoid X receptor (RXR). Additionally, TNIP1 had no effect on the activities of other NRs, such as estrogen receptors α and β, androgen receptor, and progesterone receptor (Encarnacao and Aneskievich, unpublished). The decrease in PPAR and RAR activity was not due to a reduction in NR expression levels, *(23-25)* supporting the interpretation that the repressive effect was due to TNIP1 alterating NR transcriptional activity.

As a NR coregulator, TNIP1 is in a still relatively small class of corepressors of agonist-bound NRs exemplified by this group's archetype, receptor interacting protein 140 (RIP140) *(26)*. Unlike RIP140 *(27)*, we found no association between TNIP1 and chromatin remodeling histone deacetylase (HDAC) enzymes. Rather, TNIP1 attenuates receptor activity acting through a different mechanism to halt excessive receptor activation either by toxic ligand levels or exposure to the ligand at inappropriate times. Additionally, even under

normal ligand conditions, coregulators may contribute to a combinatorial approach to NR regulation, providing for a finer level of control over receptor activity instead of the all-on or all-off effect of typical coactivators or corepressors. Furthermore, TNIP1 repression is partially relieved by over-expression of the NR coactivator steroid receptor coactivator 1 (SRC1) suggesting that interference with coactivator recruitment by liganded NRs is a mechanism of TNIP1 repression *(23)*.

The repressive effect observed on NRs indicates TNIP1 could play key roles in regulating KC proliferation and differentiation. Since ligand activation of PPAR and RAR results in changes KC cornification, altered TNIP1 expression could lead to significant changes in KC differentiation.

TNIP1 blocks TNFα Receptor induced NF-κB activation

Increased TNIP1 expression levels have also led to decreased activation of NF-κB via the TNFR (Fig 1.3). TNIP1 over-expression inhibits NF-κB signaling downstream of TRAF2 at the level of IKK, specifically NEMO. There is a direct physical interaction *(28)* between TNIP1 and NEMO (in addition to TNIP1 and A20). When TNIP1 levels are experimentally increased, A20-mediated removal of ubiquitin from NEMO is likely facilitated, decreasing the activity of the IKK complex, blocking NF-κB gene regulation *(28, 29)*.

In addition to the interaction with NEMO, TNIP1 can also prevent NF-κB activation through decreasing the pool of one of the NF-κB subunits -- p50 (Fig 1.3). NF-κB is a homo- or hetero-dimeric transcription factor consisting of

proteins in the Rel family. The p50 and p65 complex is the most common NF-κB dimer, with the p50 subunit derived from proteolytic processing of the precursor, and IκB protein, p105. Endogenous *(30)* and overexpressed *(31)* TNIP1 was found to bind and inhibit the processing of p105 resulting in a reduction of active p50. While the two proteins can physically interact, this is not an absolute requirement for the effect on p105. Interestingly, for any effect TNIP1 may have on intracellular signaling, increases in p105 expression significantly increased TNIP1 half-life *(31)*. This protein-protein interaction could prevent NF-κB activation in two ways: (1)decreasing available p50 to form an active NF-κB dimer and (2)increasing TNIP1 expression to prevent IKK activation.

Further upstream of NEMO or Complex II, TNIP1 was found to interact with the TNFR. Haas and colleagues identified the various intracellular proteins recruited post TNFR ligand binding, including the IKK trimeric complex and TNIP1 *(32)*. Although the specific details of how TNIP1 associates with the complex were not elucidated, mechanisms of NEMO's association in this complex were discussed. NEMO's ubiquitin binding domain, UBAN, facilitates the recruitment of the complex to other ubuquitinated TNFR bound proteins, such as RIP1 and TNFR-associated factor 2 (TRAF2). Given that TNIP1 also has the same UBAN domain, it is likely that its presence in the TNFR complex is mediated through TNIP1's ability to bind ubiquitin chains.

Implication for TNIP1 at the genetic level

Current connections between TNIP1 and human pathologies are found in

several diseases and tissues including psoriasis, a chronic inflammatory skin disease. These associations derive from high throughput approaches such as genome-wide association studies (GWAS) and expression microarrays *(33-39)* (Table 1.1). Whether through sequence variations or expression levels, these approaches have linked TNIP1 with psoriasis, systemic lupus erythematosus (SLE), systemic sclerosis (SSc), rheumatoid arthritis (RA) and leukemia/lymphoma. Additionally, the inflammation-associated defects observed using both *in vitro* and *in vivo* experimental systems are consistent with current reports of TNIP1 alterations associated with human auto-immune and chronic inflammatory diseases (Table 1.2). TNIP1's wide tissue distribution *(24, 25, 40)* and involvement in a number of receptor-mediated signaling pathways *(41)* would likely extend impact of its altered function to non-immune cells. For instance, we found TNIP1 antibody staining in both stratified cutaneous and mucosal epithelial cells and germinal centers of human tonsil *(25)*. More clearly defined roles for TNIP1 in normo- and patho-physiology will benefit from organ- and cell-specific knockout systems.

The *TNIP1* gene has been implicated in psoriasis, SLE and SSc through at least three independent GWAS reports. In each case however, the strongest disease-associated single nucleotide polymorphisms (SNP) were in non-coding regions. In the psoriasis study *(34)*, despite strong association with the disease (P-value 1×10^{-20}) and ~1.5 fold increase in TNIP1 expression between lesioned and uninvolved skin (i.e., tissues from the same individual), the SNP was several kilobases upstream from the *TNIP1* locus, indicating the TNIP1 promoter

sequence may be altered, possibly affecting TNIP1 expression.

Similar to psoriasis, SNPs in non-coding TNIP1 regions were also disease associated with SSc. Three different TNIP1 SNPs were identified in European populations in the second GWAS report for SSc *(39)*. Intriguingly, when TNIP1 mRNA and protein levels were assessed from cultured dermal fibroblasts of SSc patients, a ~1.7-fold decrease was observed. A separate GWAS study also identified SNPs in SLE. Two TNIP1 intronic SNP variants were found in SLE patients from Chinese Han, Caucasian, and Japanese populations, with the latter two groups having the same SNP *(35, 36, 38)*. Unlike the altered expression of TNIP1 in psoriasis and SSc, there was no TNIP1 mRNA change associated with this SLE SNP *(38)*. However, Kawasaki and colleagues suggested the SNP location in intron 1 could impact TNIP1 splicing possibly affecting the use of alternative exons 1A and B with exon 2 and thereby contributing to the numerous splice variants of TNIP1 *(42-44)* with as yet unrecognized consequences. Far from being innocuous spacers between coding regions of genes, introns are now recognized as possible sites of transcription-regulating factors at the DNA level and/or potential effectors of splicing at the RNA level *(45, 46)*. Likewise, proximal or intergenic regions, especially those covering the disease-associated gene's promoter/enhancer region, may affect expression levels or tissue-specific expression *(47)*. Most recently, copy number variations were reported for TNFAIP3 and TNIP1 suggesting other forms of genome-wide analyses could prove productive in relating these genes to the disease states *(48)*.

Through physical association with TNFR pathway, the molecular

mechanisms of TNIP1's function to inhibit NF-κB-dependent gene transcription may explain its potential role in inflammatory and immune-related diseases. Deregulation of this pathway can result in a myriad of diseases and disorders, including but not limited to the progression of arthritis and psoriasis, and yet, controlled TNFR signaling can lead to differentiation and immunomodulation in equally diverse cell types *(49, 50)*. As previously mentioned for leukemia-lymphoma *(43, 51)* and psoriasis *(34, 52)*, TNIP1 association with disease states need not be limited to variants in its protein sequence. Wild-type TNIP1 could still play a key role in pathologies or as a pharmacologic target if its levels were altered.

TNIP1 sequence variants at the mRNA and protein level

In addition to gene analysis, TNIP1 mRNA expression has been analyzed from several human cell lines and tissues. Several splice variants having either 5' truncated ends or lacking specific exons were detected in samples derived from patients with acute myeloid leukemia (AML) *(43)*. Although variant 5' ends have been mapped to the use of alternative first exons, the 3' truncations described in these samples are the first of their kind to be reported. Most of the splice variants did not confer changes in amino acid sequence. However, one variant lacking exons 16 and 17 was less effective at reducing NF-κB activity. Decreased TNIP1 mRNA levels, for with full-length or splice variants, were observed in AML patient samples post chemotherapy treatments. Separately, several TNIP1 mutations have been detected in gastrointestinal diffuse large B cell lymphomas *(51)*.

These sequence alterations are either point or frame-shift mutations, the latter resulting in a protein truncation. One mutant in particular, causing a glutamic acid to lysine change (E476K), lost its NF-κB inhibitory properties; other missense mutations did not alter this TNIP1 property. Thus, sequence variations, either at the mRNA level possibly affecting message stability, exon content, or amino acid sequence could impact ultimate TNIP1 protein function. Additionally, we should consider that there could be functional consequence to even wild-type TNIP1 protein if its levels or post-translation processing, e.g. phosphorylation were altered.

Increased expression of TNIP1

In contrast to other TNIP1 associated diseases, the connection between *TNIP1* and RA appears strictly at the expression level, not at a susceptibility locus or nucleotide mutation. Three SNP type GWAS reports *(38, 53, 54)* concluded loci-disease association(s) did not meet the cut-offs used for the analyses. However, when compared to knee synovial membrane biopsies from osteoarthritis patients, similar samples from patients with RA showed a 2.5-3.5 fold TNIP1 mRNA increase. Osteoarthritis and RA are referred to as non-inflammatory versus inflammatory forms of the disease, respectively. Consistent with this inflammatory association, TNIP1 was one of the genes with increased expression following TNFα treatment of cultured synovial fibroblasts *(33)*. Nevertheless, TNFα-increased TNIP1 expression may be tissue specific by following one of multiple post-TNFα-receptor signaling pathways. For instance,

retrovirus-mediated increases in NF-κB signaling, one of several post-TNFα-receptor consequences, did not increase TNIP1 expression in dermal fibroblasts but did in epidermal keratinocytes *(55)*. TNIP1 upregulation in response to signaling from inflammatory mediators coupled with dampening of NF-κB activity, at least in experimental systems, suggests its dysregulation may be contributory and/or consequential to cytokine signaling.

Non-coding changes in TNIP1 and possible connections to disease

The quandary of how TNIP1 non-coding region SNPs affect psoriasis, SLE and SSc is much the same as for any other extra-exonic sequence changes associated with disease. Sequence alterations in promoter regions, even those distant to transcription start sites may affect transcription factor binding and, in turn, mRNA production. Likewise, SNPs in non-coding regions may alter transcript conformation resulting in changes in its stability, translational efficiency, or interaction with RNA regulatory factors *(56)*. Thus even the wild-type TNIP1 protein sequence at altered levels could impact the associated disease states given the ability of TNIP1 to modulate post-receptor signaling as detailed below. In the case of RA, experiments using fibroblast-like synoviocytes show wild-type TNIP1 increases pro-inflammatory cytokines, potentially advancing the disease *(57)*. In this vein, as psoriasis, SLE, and RA are at least in part regulated *(58)* by receptor pathways (TNFR) modulated by TNIP1, TNIP1 itself could be a focal point for clinical intervention. This possibility is again echoed by TNIP1 corepression of nuclear receptors currently used as therapeutic targets (RAR)

(59) or suggested for such use (PPAR) *(60, 61)* for treatment of psoriasis or other inflammatory diseases *(62)*. However, a discrepancy arises in TNIP1's inhibitory effect on TNFR signaling and increasing pro-inflammatory cytokines in RA. We hypothesize that TNIP1 could regulate these molecules through a separate pathway distinct from TNFR *(57)*. Therefore, while several targets have been elucidated, it is plausible that other TNIP1-mediated pathways have not yet been discovered.

Figure 1.3

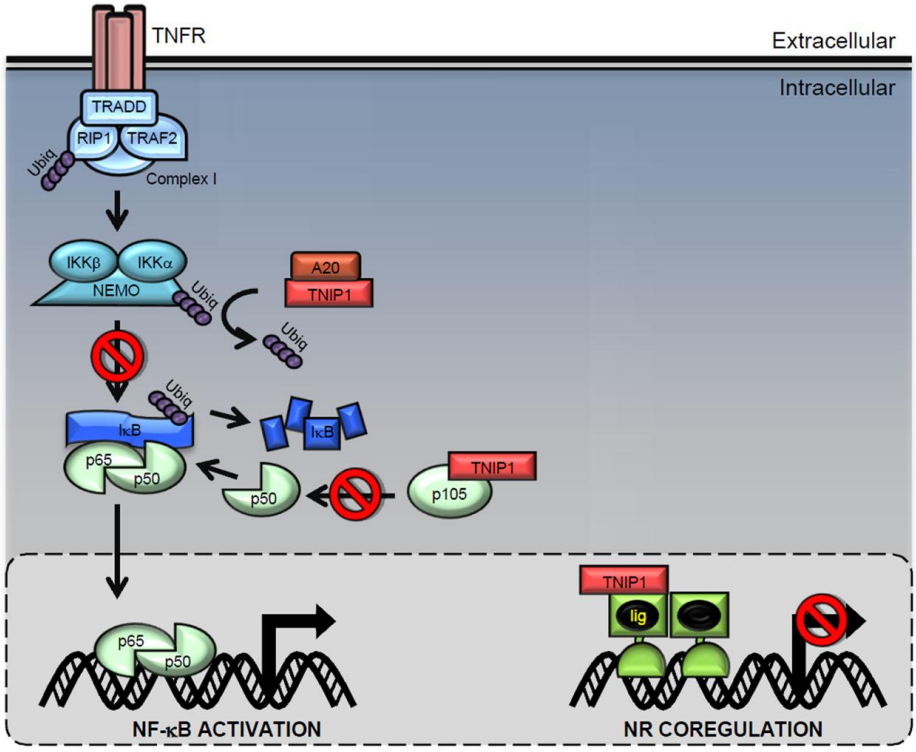

Figure 1.2. TNIP1-mediated signaling pathways. (Left) In the TNFR-induced NF-κB activation pathway, intracellular proteins are recruited to the TNFR to form complex I, which facilitates the phosphorylation and subsequent activation and polyubiquitination of NEMO. IκB is then targeted for degradation, allowing the p65/p50 NF-KB heterodimer to translocate into the nucleus. TNIP1 inhibits NF-KB activation by preventing NEMO's polyubiquitination. Additionally, TNIP1 blocks the processing of p105 to the NF-KB subunit p50, therefore decreasing the available pool of NF-KB. (Right) TNIP1 represses nuclear receptors transcriptional activity. Upon ligand-NR binding, TNIP1 exerts its inhibitory effects on either PPAR or RAR. Red (ᘔ) denotes TNIP1's inhibitory functions.

Table 1.1. TNIP1 and associated diseases

Disease	**TNIP1 Association**	**Experimental Approach**	**Reference**
Psoriasis	Intronic SNP; Increased expression	GWAS; Gene expression microarray	Nair et al. *(34)*; Psoriasis Consortium *(52)*; Ellinghaus et al. *(63)*
Psoriatic Arthritis	Intronic SNP	GWAS	Bowes et al.*(64)*
Systemic Lupus Erythematosus	Intronic SNP	GWAS	Kawasaki et al. *(38)*
Systemic Sclerosis	Intronic SNP	GWAS	Allanore et al. *(39)*
Leukemia-Lymphoma	Splice Variants	RT-PCR and sequencing	Shiote et al. *(43)*
Leukemia-Lymphoma	Point or frameshift mutations	PCR and sequencing	Dong et al. *(51)*
Rheumatoid Arthritis	Increased expression	Gene Expression microarray	Gallagher et al. *(33)*

Table 1.2. Experimentally altered TNIP1 and the resulting phenotypes

Experimental Model	**Phenotype**	**Reference**
Overexpression of WT TNIP1 in vivo via adenoviral tail vein delivery	Protection from TNFα/Galactosamine induced acute liver failure	El Bakkouri et al. *(65)*
Overexpression of WT TNIP1 in vivo via adenoviral intratracheal delivery	Protection from allergen induced airway inflammation	Wullaert et al. *(66)*
Mouse knockout by BAC recombineering and Cre mediated excision to delete sequences including exons 12-15	1 in 40 mice were live-born; Embryonic lethal at day 18.5; Anemic; Hypocellular livers; Increased apoptosis in embryonic livers	Oshima et al. *(67)*
Gene trap mutation mouse model	1 in 40 mice were live-born; Embryonic lethal at day 18.5; Live-born mice die within 40 days post-birth; Enlarged lymph nodes and spleen	Zhou et al. *(68)*
Mouse knock-in model mutating TNIP1's UBAN domain	Development of lupus-like autoimmune disease within 5 months; Enlarged lymph nodes and spleen;	Nanda et al. *(69)*
Overexpression of WT TNIP1 in vitro in Saos-2 osteosarcoma cells	Protection from trichostatin A induced apoptosis	Zhang et al. *(70)*

Heat shock proteins

Heat shock proteins and the skin

Epidermal KCs serve as the primary barrier between the numerous environmental chemicals and toxins and the body *(71)*. These cells are likely to respond through a number of mechanisms and proteins to protect them from toxicity or death. Heat shock proteins (HSP) are a superfamily of molecules involved in protecting cells from numerous stress events. Initially discovered in *Drosophila* after incubating in increased temperatures *(72)*, increase HSP expression was observed in response to toxic chemical and UV light assaults across all cell types and organisms *(71)*. HSPs were reported to refold of denatured proteins and block protein aggregation, therefore preventing cell death. However, further characterization of many HSPs revealed constitutive expression of several family members. These constitutively expressed HSPs account for their availability in “house-keeping” chaperone function *(73)*.

Different HSP subfamilies, which are classified according to their molecular weight *(73)*, are found in the skin. The HSPA family (also named HSP70) has been well studied in KC biology. Members of this family are observed in both unstressed and stressed KCs *(74, 75)*. Several family members have mostly similar with some distinct functions in the cell with regards to the proteins they can interact with and fold. HSPA1A (HSP70) is the best known HSPA family member. This protein is expressed in KCs, but can still be highly stress induced. The HSPA1A chaperone function is vital in unstressed conditions, while its expression in stress-induced cells is crucial to prevent cell

death. Targeting HSPA1A to reduce its expression using an antisense oligomer induced cell death and inhibited cell growth *(76)*. A closely related family member, HSPA6 (HSP70B') expression is also observed in both conditions. While these two proteins are key to cell protection in stressed conditions, each can bind specific proteins with higher affinity than others. For example, HSPA6 is more effective at binding and refolding p53, whereas it does not interact with HSPA1A-specific protein substrates from the peroxisome *(77, 78)*. However, both proteins are important to normal cell homeostasis because specific knockdown of either HSP resulted in reduced cell survival following thermal or chemical stress. Furthermore, decreasing the expression of both HSPs led to a greater reduction in cell survival, suggesting both are important in cell protection *(79)*. Additionally, increased expression of HSPA1A led to enhanced cell growth and proliferation, suggesting it may regulate this process. In KC specific tissues, increased expression of several HSPs, including HSPA1A, was observed in psoriatic lesions *(80)*. While the exact function of HSPs in psoriasis is yet unknown, it is speculated that the increased expression could be a result of inflammation within the keratinocytes. Regardless, this observation could indicate a functional role for HSPs in the pathogenesis of inflammation.

Expression and transcriptional regulation of heat shock protein A6

The expression of HSPA6 is less characterized and understood compared to other HSPs. HSPA6 mRNA and protein expression is highly induced following either thermal, chemical or UV stress in all cells examined *(81, 82)*. In non-

stressed conditions, HSPA6 production is variable, from none detected to low expression levels *(79, 81, 82)*. This could possibly be dependent on cell type and growth condition differences *(83)*. Currently, the transcriptional regulation of HSPA6 has mostly been characterized using a minimal ~287 bp promoter *(84-86)*. To date, a functional activator protein 1 (AP1) site and heat shock response element (HSE) have been characterized. Additionally, a predicted TATA box was found, but not yet analyzed. Initial work from our laboratory observed high expression levels of HSPA6 in basal, unstressed conditions. This level was further increased in response to thermal stress (Ramirez et al 2014, submitted). These findings may indicate HSPA6, like HSPA1A, plays key roles in normal, stressed and diseased KCs to possibly modulate the pathogenesis of skin related diseases.

Summary

Proper regulation of epidermal KC homeostasis is essential to generate a functional barrier to separate the possible environmental stressors from our body. Outlined in this chapter are only some of the proteins involved in regulating the proliferation and differentiation of KCs in both normal and diseased states. We, and others, characterized TNIP1 as one of those possible factors. TNIP1 can directly or indirectly repress the activity or activation of transcription factors involved in KC proliferation and differentiation. Sequence alterations and expression level changes were observed in several inflammatory diseases, including those affecting KC growth. However, TNIP1's exact role in these diseases are not yet understood. In the research presented on this dissertation, we sought to characterize the transcriptional and cellular outcomes of increased TNIP1 expression in human KCs to possibly contribute in understanding TNIP1's role in normal or diseased skin.

Using a gene microarray analysis to examine the transcriptional expression changes in TNIP1-overexpressing cultured KCs, this research validated TNIP1's role in the previously mentioned associated inflammatory diseases. Expression of TNFR- and NR-regulated genes was also reduced following increased TNIP1 exposure, confirming TNIP1's repressive effect on these pathways. Interestingly, we observed the novel repression of genes associated in regulating the cell stress response, HSPs. Choosing one HSP (HSPA6), we examined the potential mechanism of how TNIP1 could repress a family HSPs. We determined that the transcriptional repression of HSPA6 is not

through previously characterized TNIP1 factors, suggesting TNIP1 could regulate a yet uncharacterized pathway. In addition to the possible transcriptional changes involved with TNIP1, we assessed the overall cellular consequence of increased TNIP1 levels. This work suggests that a chronic, but not acute, overexpression of TNIP1 results in reduced growth of cultured KCs. These results indicate that TNIP1 could regulate KC growth and differentiation, possibly through repression of HSP expression.

Chapter 2

TNIP1 Modulates Heat Shock Protein Expression and the Stress Response

Abstract

A vast number of cellular responses to environmental and physiological signals are regulated by various receptor-initiated pathways, which in turn are modulated by a diverse set of regulatory proteins. TNFα-induced protein 3-interacting protein 1 (TNIP1) is one such protein; it inhibits both transduction by transmembrane receptors, such as the TNFα-receptor, and by nuclear receptors PPAR and RAR activity. Despite their cytoplasmic versus nuclear signaling, these receptors play key roles in regulating inflammation and inflammatory diseases. Interestingly, a growing number of references through GWAS and expression studies have implicated TNIP1 in chronic inflammatory diseases such as psoriasis and rheumatoid arthritis. However, TNIP1's exact role has yet been determined.

To characterize the specific genes and pathways affected by TNIP1, we overexpressed TNIP1 in HaCaT keratinocytes. Using a gene microarray analysis, we observed reduced expression of most genes altered. These results not only validated previously determined TNIP1-repressed pathways and biological processes, but also revealed novel TNIP1-affected pathways, such as the cell stress response. Specific proteins involved in this process, heat shock proteins (HSP), showed reduced mRNA and protein expression following increased TNIP1 levels. When TNIP1 levels were increased in normal human epidermal keratinocytes, the repression of HSPs were only observed in differentiating

keratinocytes. Additionally the induction of one keratinocyte differentiation marker, involucrin, was blocked by TNIP1. This may indicate that keratinocyte differentiation may be slowed by increased levels of TNIP1. Keratinocytes rely on HSPs for both chaperone and stress recovery functions, during differentiation and inflammation. Their reduced expression by TNIP1 could compromise cell function, possibly affecting KC homeostasis.

Introduction

TNFα-induced protein 3-interacting protein 1 (TNIP1) is an intracellular regulatory protein that blocks or represses various signaling pathways involved in normal cell physiology and the pathogenesis of several inflammatory diseases, such as psoriasis, systemic lupus erythematosus and rheumatoid arthritis *(34, 38, 87)*. These pathologies share a hyper inflammatory nature, in part, resulting from dysregulation of a diverse group of receptor-mediated signaling pathways, possibly involving altered TNIP1 levels or functions. For instance, increased levels of TNIP1 were observed in skin samples from patients with psoriasis, a chronic inflammatory disease characterized by keratinocyte (KC) hyper-proliferation and incomplete differentiation. Research from our laboratory determined TNIP1 as a ligand-dependent nuclear receptor corepressor, specifically of peroxisome proliferator activated receptor (PPAR) and retinoic acid receptor (RAR) *(23, 24)*. Work from other laboratories characterized TNIP1 blocking transmembrane receptor-initiated cascades, such as TNFα receptor (TNFR) *(28, 31, 88)*, epidermal growth factor receptor (EGFR) *(89)*, and toll-like receptor (TLR) *(69, 90)*, resulting in the reduced activation of NF-κB, Elk-2 and C/EBPβ, respectively. Overall, TNIP1 can be classified as a direct or indirect repressor of transcription factor activation or activity (for a recent review on TNIP1, refer to *(41)*). Although TNIP1's association in these cascades and diseases has been observed, the consequences and specific genes affected by increased TNIP1 have not yet been established. To assess the role TNIP1 plays in KC biology, we performed a gene microarray using samples from TNIP1-

overexpressing cultured KCs. The gene clustering analysis not only confirmed TNIP1's association in known inflammatory diseases and processes, but it also found a novel pathway involved in TNIP1 signaling — the cell stress response centering on heat shock proteins (HSP).

HSPs are molecular chaperones initially discovered *(72)* for their protective roles during cellular stress by preventing protein unfolding and aggregation *(71, 73)*. Under basal, unstressed conditions, these proteins aid in new protein folding and shuttling. Similar to other cell types, epidermal keratinocytes have basal and stress inducible levels of HSPs *(74, 80, 91)*. Because the keratinocytes are a first line barrier between various environmental stressors and the body, HSPs are key to protecting keratinocytes from the damage caused by cellular stressors, including UV exposure, chemical treatment or increased thermal changes *(71)*.

The HSPA (also named HSP70) family is well known and widely studied in skin biology. In unstressed skin, HSPA1A, the best-characterized member of this family, is primarily found in the major cell type in the epidermis, KCs, but not other cell types, such as melanocytes and fibroblasts *(92)*. Pharmacologic repression of HSPA1A expression in keratinocytes resulted in reduced resistance to UV treatment *(93)*. Further, increased expression of HSPA1A is observed in psoriatic lesions *(80)* and wound healing *(94)*, suggesting a potential role for these chaperones in these pathologies. The expression of a close relative of HSPA1A, HSPA6 (also named HSP70B'), has recently been established in KCs *(74)*. This protein has some similar protective functions compared to HSPA1A

(79) although each has distinct protein substrates as examined through protein binding with endogenous or experimentally expressed proteins. HSPA6 has preferential binding to unfolded p53, but has no effect on HSPA1A protein subtrates, luciferase enzyme and peroxisomal proteins *(77, 78)*. It is speculated that HSPA6 may act as a backup response to stressors, whereas HSPA1A is the primary response. Regardless, siRNA-mediated knockdown of either HSP resulted in decreased cell survival post thermal and chemical stress, indicating both HSPs are crucial for cell protection *(79)*.

In this chapter, we examined the cell signaling effects and gene transcriptional changes due to overexpression of recombinant TNIP1. Although TNIP1 was previously shown to block pathways initiated by nuclear and transmembrane receptors *(23, 24, 28, 31, 88)*, this repression was assessed using reporter gene constructs, not through quantifying the expression of endogenous target genes. To determine the specific genes, we performed a gene microarray analysis of TNIP1-overexpressed HaCaT KCs to confirm the biological functions and pathways associated with TNIP1, as well as to search for novel pathways altered by TNIP1. In addition to affecting pathways involved in inflammation and cell death, increased TNIP1 affected a not yet characterized TNIP1-associated pathway, regulation of the stress response. We observed reduced levels of several heat shock proteins (HSP), including HSPA1A and HSPA6. These results could suggest a novel TNIP1 function in modulating the cell stress response.

Materials and Methods

Cell Culture

HaCaT KCs *(95)* were cultured in 37°C with 5% CO_2 humidified incubator in a 3:1 DMEM/F12 media containing 10% FBS (Thermo Scientific HyClone, Logan, UT), 100U/ml penicillin, and 100 mg/ml streptomycin. The cells were plated on 6- or 24-well plates at a density of 6.8 x 10^5 or 1.5 x 10^5 cells per well, respectively. Twenty-four hours after, cells were infected with an adenovirus construct expressing TNIP1 (Ad-TNIP1) or LacZ as a control (Ad-LacZ) at an multiplicity of infection (MOI) of 500 using Polybrene infection reagent (Millipore, Billerica, MA) *(96)*. Sixteen hours post-infection, the viral mixture was aspirated and media replaced. Twenty-four hours post-infection, cells were collected for total RNA using the RNeasy kit (Qiagen, Valencia, CA) or protein using RIPA lysis buffer (10 mM Tris, 150 mM NaCl, 1% deoxycholic acid, 1% Triton, 0.1% SDS).

Normal human epidermal keratinocytes (NHEK) were cultured in 37°C with 5% CO_2 humidified incubator in a KBM-Gold supplemented with KBM-Gold Bullet Kit (Lonza Biologics Inc, Hopkinton, MA) at passage number 2-4. Cells were plated on 6-well plates at 9.5 x 10^4 cells per well. Forty-eight hours after, cells to be collected from low calcium (0.1 mM) media were infected with Ad-TNIP1 or Ad-LacZ (control) at an MOI of 50 (assuming one cell doubling time has occurred)using Polybrene infection reagent. Twenty-four hours after infection, the cells cultured in low calcium medium were collected for total RNA using the RNeasy kit (Qiagen) or protein using RIPA lysis buffer, while the media for the

the cells grown in high calcium was replaced with fresh media supplemented to a final concentration of 1.2 mM calcium. Forty-eight hours after, high calcium cultured cells were infected with Ad-TNIP1 or Ad-LacZ (control) at an MOI of 50 (assuming a total of 4 cell doubling times have occurred) using Polybrene infection reagent. Twenty-four hours after infection, the cells cultured in high calcium medium were collected for total RNA using the RNeasy kit (Qiagen) or protein using RIPA lysis buffer.

Microarray

Total RNA isolated from LacZ- or TNIP1-expressing adenovirus infected cells was provided to the University of Connecticut Health Center Molecular Core Facility for microarray analysis. The microarray was performed using the Illumina Human WG-6 3.0 Expression Bead Chip and analyzed using the GenomeStudio software (Illumina, San Diego, CA). Significantly altered genes were determined using a fold change of ≥ 2 and a p-value ≤ 0.05 (DiffScore = 13). Functional grouping and analysis was performed using Ingenuity Pathway Analysis online software (Ingenuity Systems, www.ingenuity.com) and the Database for Annotation, Visualization and Integrated Discovery (DAVID) web-accessible program *(97, 98)*.

Real-Time quantitative PCR analysis

Reverse transcription was performed using aliquots from the total RNA used for the microarray using the iScript reverse transcriptase (BioRad, Hercules, CA).

Gene expression changes were analyzed using POWER SYBR green master mix (Life Technologies, Grand Island, NY). Real-time PCR was performed using Applied Biosystems 7500 Fast Real-Time PCR system. Data analysis was carried out on ABI 7500 software using the ΔΔCT method. The primer sequences used and reaction conditions are listed on Table 2.1. All data was normalized to the ribosomal proten L13a (RPL13a) *(99)*.

Immunoblot analysis

Whole-cell lysates were prepared in RIPA buffer and the protein concentration was determined using the 660 nm Protein Assay (Thermo Pierce). Ten micrograms of protein were separated by SDS/PAGE, transferred to nitrocellulose membranes, rinsed with nanopure water and treated with Qentix (Thermo Scientific Pierce). Blots were incubated in blocking buffer consisting of 5% (w/v) non-fat dried milk, phosphate-buffered saline, and 0.1% Tween 20, then probed with HSP70B' antibody (ADI-SPA-754) at 1:1000 dilution (Enzo Life Sciences, Farmingdale, NY) or anti-HSPA1A antibody (ADI-SPA-810) at 1:1000 dilution (Enzo Life Sciences) *(82, 83)* followed by HRP (horseradish peroxidase)-conjugated secondary goat anti-mouse antibody at 1:10,000 dilution (PerkinElmer, Branford, CT). Blots were subsequently probed with β-actin antibody (ab8227) at 1:5,000 dilution (Abcam, Cambridge, MA) followed by HRP-conjugated secondary goat anti-rabbit antibody at 1:20,000 dilution (PerkinElmer). Between probing steps, blots were washed with 0.2% Tween20 in phosphate-buffered saline. Detection of binding was determined with enhanced

chemiluminescence reagents (Thermo Scientific Pierce). Band signals were digitally captured and analyzed using the Kodak image station CCF and Carestream molecular imaging software.

Statistical Analysis

Data was analyzed using Prism Software version 5 (GraphPad) (La Jolla, CA). Student's T-test was use to compare between pairs. Statistical significance was defined as $p \leq 0.05$.

Table 2.1 List of qPCR primers

Primer name	**Primer sequence 5’ to 3’**
HSPA6, forward	CTC CAG CAT CCG ACA AGA AGC
HSPA6, reverse	ACG GTG TTG TGG GGG TTC AGG
IL6, forward	GGT ACA TCC TCG ACG GCA TCT
IL6, reverse	GTG CCT CTT TGC TGC TTT CAC
DNAJB1, forward	GAG GAA GGC CTA AAG GGG AGT
DNAJB1, reverse	AGC CAG AGA ATG GGT CAT CAA
HSPA1A, forward	AGG TGC AGG TGA GCT ACA AG
HSPA1A, reverse	ATG ATC CGC AGC ACG TTG AG
RARRES3, forward	CAA GAG CCC AAA CCT GGA G
RARRES3, reverse	TAT ACA GGG CCC AGT GCT CAT
NFKBIA, forward	AAC CTG CAG CAG ACT CCA CT
NFKBIA, reverse	ACA CCA GGT CAG GAT TTT GC
DNAJA1, forward	TCA AAC CCA ATG CTA CTC AGG A
DNAJA1, reverse	TCC ACC CTC TTT AAT TGC CTG T
RNASE7, forward	GGA GTC ACA GCA CGA AGA CCA
RNASE7, reverse	CAT GGC TGA GTT GCA TGC TTG A
MAKP13, forward	TGC TCG GCC ATC GAC AA
MAKP13, reverse	TGG CGA AGA TCT CGG ACT GA

Results

TNIP1 overexpression analysis using a gene microarray

To determine the effect of increased TNIP1 levels in keratinocytes (KC), recombinant TNIP1 was overexpressed in HaCaT KC, a human immortalized, but non-tumorigenic KC cell line which retains the KC differentiation properties *(95)*. Using an adenoviral vector expressing either TNIP1 (Ad-TNIP1) or control gene LacZ (Ad-LacZ) at a MOI=500, a ~11-fold increase of TNIP1 protein was observed twenty-four hours after adenoviral infection (Fig 2.1). Increased expression of TNIP1 was further examined at 48, 72 and 96 hours post-infection. Expression of TNIP1 did not change throughout these later timepoints (data not shown). The mRNA changes at 24 hours post-infection was chosen for the microarray to reduce the chances of gene expression changes due to further downstream protein expression changes.

Increased TNIP1 results in repression of a majority of genes

To assess the possible direct repressive effect on TNIP1 on target genes' transcription, we extracted total RNA lysates from the Ad-LacZ and Ad-TNIP1 infected cells twenty-four hours post-infection for a gene microarray analysis. Using the Illumina whole genome expression array, we observed 139 significantly regulated genes using cutoffs of 2-fold and a p-value ≤ 0.05. We plotted these results and observed that 136 genes' expression was reduced, while only 3 genes were increased (Fig 2.2, top panel). The volcano plot shows log2-fold change in mRNA expression between the control and TNIP1-

Figure 2.1

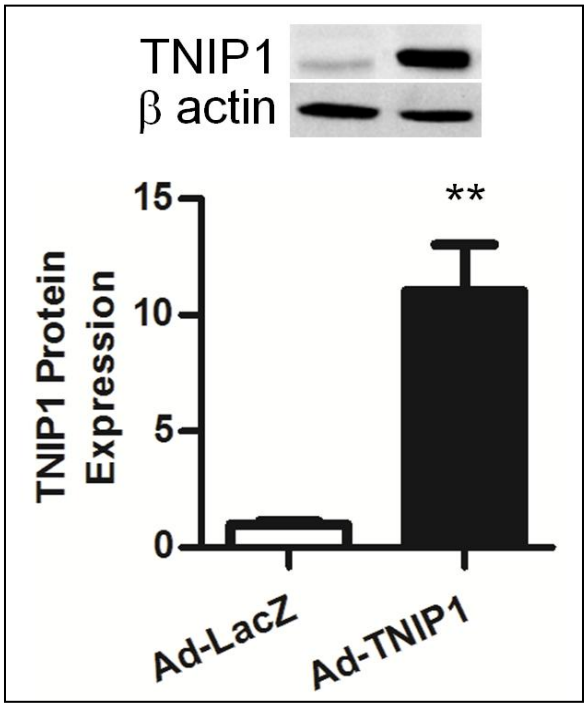

Figure 2.1. Validation of TNIP1 overexpression. Expression and quantitation of TNIP1 protein in control (Ad-LacZ) or TNIP1-overexpressed (Ad-TNIP1) HaCaT KCs. Statistical significance was determined using Student's t-test, ** $p < 0.01$. Bars are mean + SEM from experimental triplicates.

overexpressed samples on the x-axis and the negative log of the DiffScore (transformed p-value) on the y-axis. Each point on the plot represents a single gene.

To validate the use of the microarray, we performed a qPCR analysis of selected genes. Genes which were maximally reduced (HSPA6 and IL-6) and increased (RNase7 and MAPK13) were among those chosen. Additionally, we chose previously determined nuclear receptor and NF-kB regulated genes (RARRES3 and NFKBIA, respectively) (Fig 2.2, bottom panel). A similar trend in gene reduction and induction was observed comparing the microarray and qPCR.

Determining the biological functions and pathways affected by increased TNIP1

To determine the biological processes most relevant to our TNIP1 overexpression microarray, we used two pathway analyses and clustering web-accessible programs, Ingenuity Pathway Analysis (IPA) and the Database for Annotation, Visualization and Integrated Discovery (DAVID). The IPA analysis can group the significantly altered gene list by biological function and toxicological pathways affected. The top associated biological functions affected by increased TNIP1 levels include cancer, cell death, inflammatory diseases and gene expression (Fig 2.3, top panel). The IPA pathway clustering analysis showed that pathways involving PPAR and RAR activation were affected in the microarray (Fig 2.3, bottom panel). Further, pathways previously unknown to be regulated by TNIP1 were affected, especially stress associated pathways.

Figure 2.2

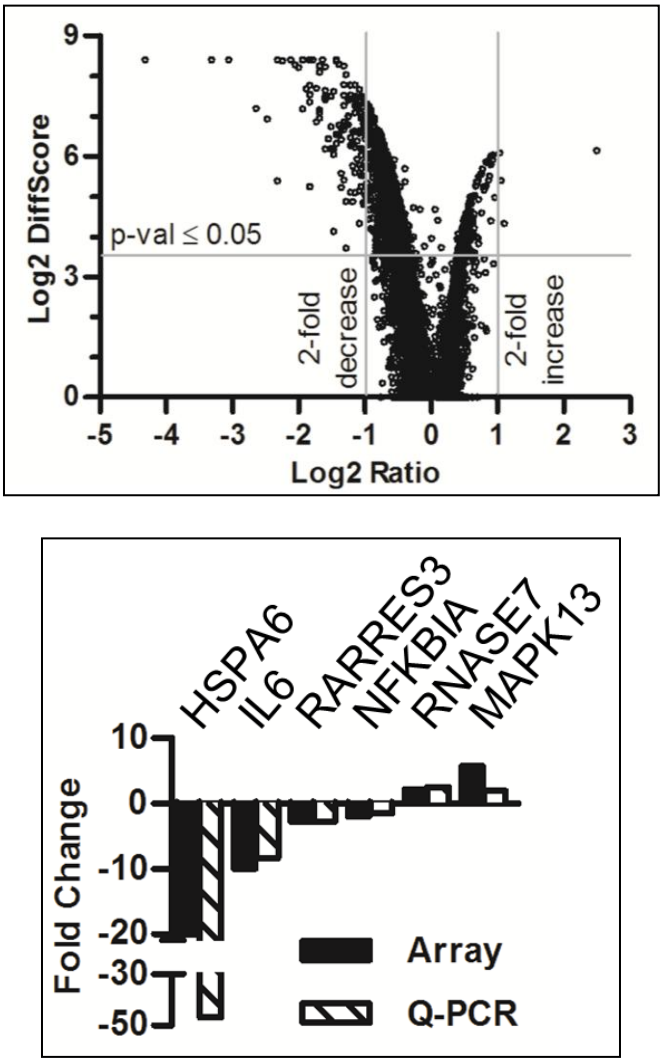

Figure 2.2. TNIP1 overexpression microarray results. Top panel. Volcano plot analysis of microarray results. Each point represents one gene. Bottom panel. Validation of microarray using qPCR. Note break in axis and change in scale.

Figure 2.3

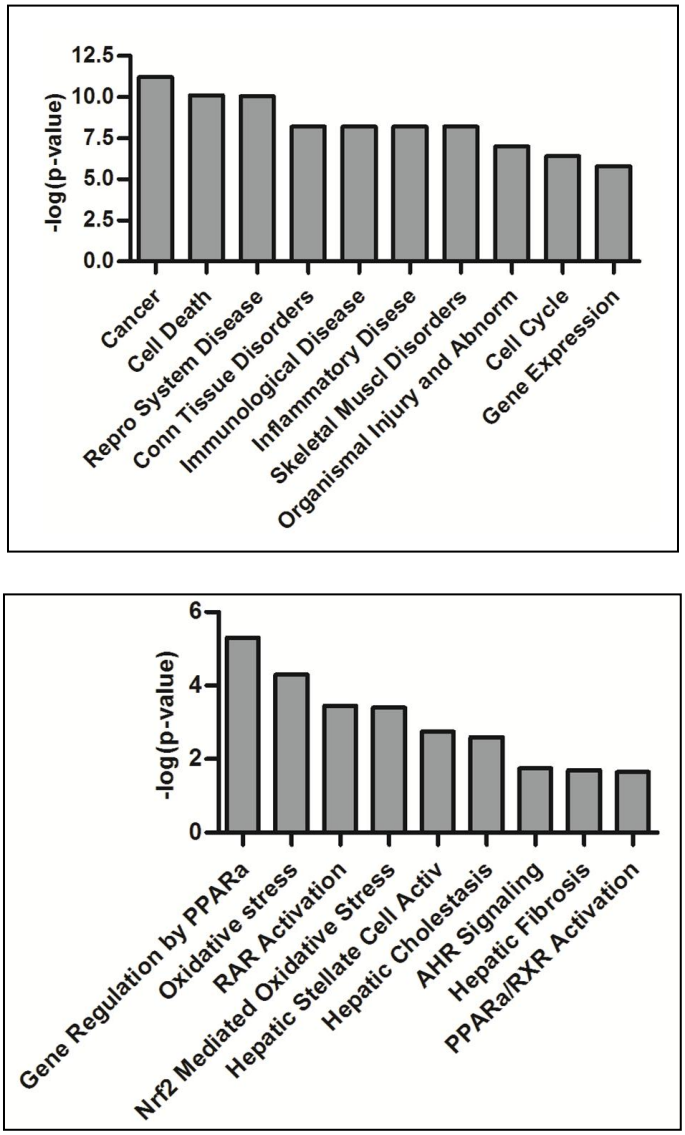

Figure 2.3. Ingenuity Pathway Analysis clustering of genes with significant expression change. Top panel. IPA biological function analysis of the top affected clusters. Bottom panel. IPA pathway cluster of the top affected pathways above the threshold.

To further confirm the pathways and functions observed using IPA, we also used the separate functional annotation software, DAVID. The top gene functional classifications observed were similar to the IPA clustering (Fig 2.4). From the DAVID analysis, the unexpected pathway affected by TNIP1 was the stress response pathway. To determine the potential TNIP1 effect on this novel TNIP1-associated pathway, we looked at the specific genes within this pathway altered by TNIP1.

Heat shock response genes' expression is repressed by TNIP1

The microarray results showed reduced expression of five HSP family members (HSPA6, DNAJB1, HSPA1B, HSPA1A and DNAJA1) by 20-, 5-, 3.2-, 3- and 2-fold, respectively. HSPA6 was the gene most repressed by TNIP1 in our analysis. Results from the microarray were validated via qPCR (Fig 2.5, top panel). Since the role of the HSPA family is better characterized in keratinocyte biology, we further assessed whether TNIP1's inhibitory effect on these genes extend to altered protein expression. We observed reduced protein expression of both HSPA1A and HSPA6 in response to enhanced TNIP1 protein expression (Fig 2.5, bottom panel).

In addition to using the HaCaT keratinocytes, we also examined the transcript expression levels of HSPA1A and HSPA6 in cultured normal human skin keratinocytes (NHEK). A well characterized and used method to induce NHEK differentiation from an undifferentiated population is to switch the media calcium concentration from low to high amounts. To test if the calcium switch

induced KC differentiation, we examined the mRNA levels of two KC differentiation markers observed in the spinous and granular layers, keratin 1 and involucrin, respectively (Fig 2.6). Control infected cells show 38- and 13-fold increased expression of keratin 1 and involucrin, respectively, suggesting KC differentiation is occurring. Interestingly, HSPA1A and HSPA6 expression was increased in differentiating KC compared to the undifferentiated KC (Fig 2.7). The TNIP1-mediated repression of these genes was only observed in differentiating keratinocytes. TNIP1 had no effect on HSPA1A and HSPA6 in low calcium cultured cells.

Figure 2.4

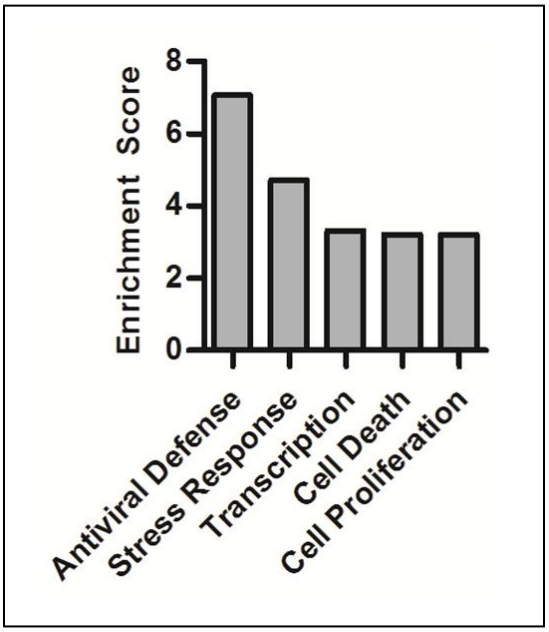

Figure 2.4. DAVID clustering of genes with significant expression change.

DAVID biological function analysis of the top affected clusters.

Figure 2.5

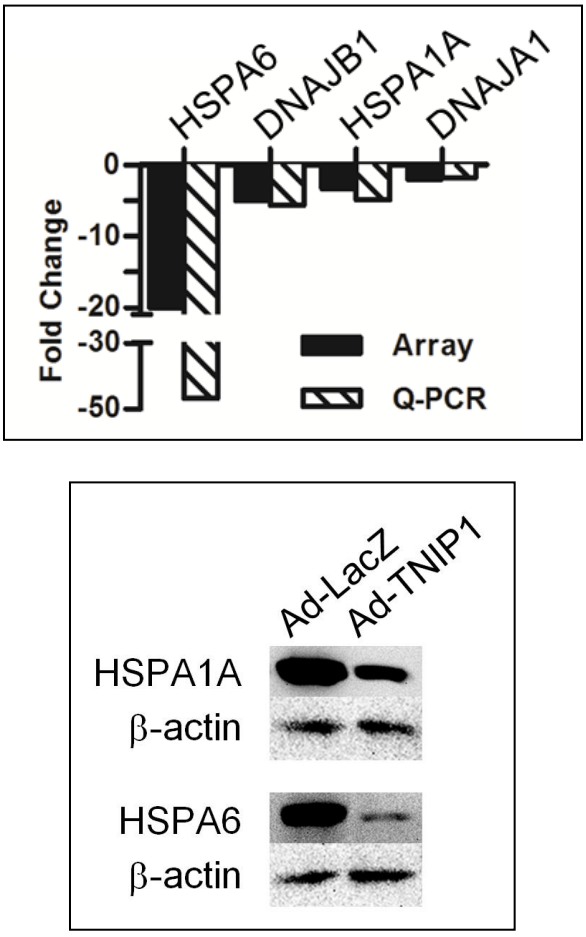

Figure 2.5. Effect of TNIP1 overexpression on HSPs in HaCaT KCs. Top panel. Microarray and qPCR analysis of HSPA6, DNAJB1, HSPA1A and DNAJA1 in HaCaT KCs. Bottom panel. Western blot analysis of HSPA1A and HSPA6 in HaCaT KCs. β-actin is used as a loading control.

Figure 2.6

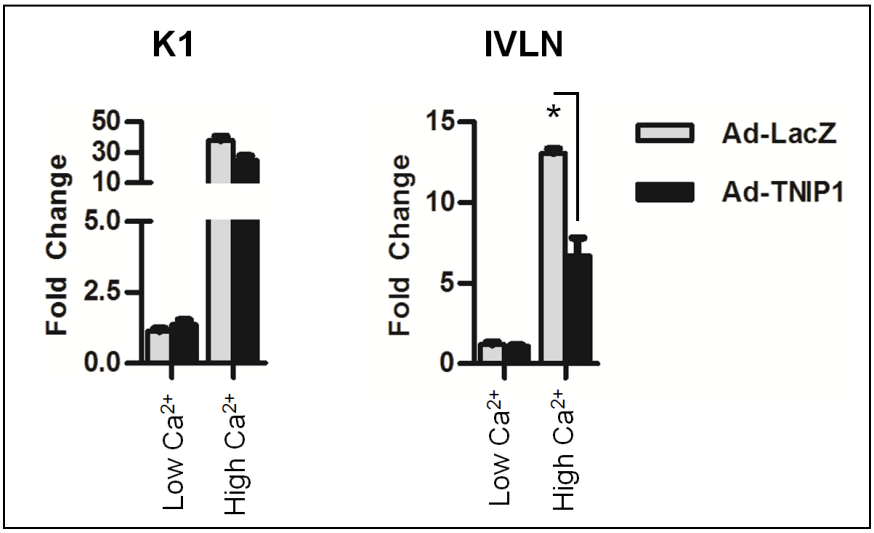

Figure 2.6. Effect of TNIP1 overexpression on KC differentiation markers in NHEKs. Quantitative PCR analysis of keratin 1 (left graph) and involucrin (right graph) in undifferentiated (low calcium) or differentiated (high calcium) NHEKs infected with Ad-LacZ (control) or Ad-TNIP1. Statistical significance was determined using Student's t-test, * $p < 0.05$. Bars are mean + SEM from experimental triplicates.

Figure 2.7

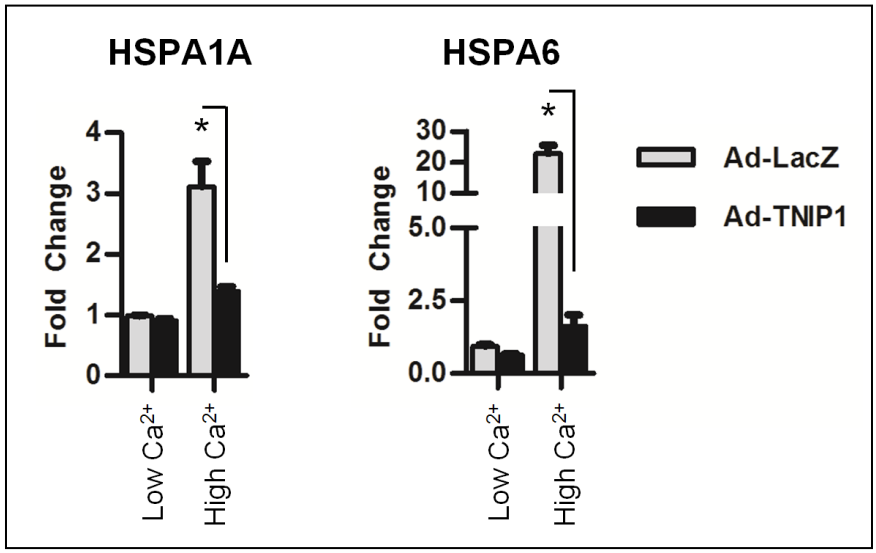

Figure 2.7. Effect of TNIP1 overexpression on HSPs in NHEKs. Quantitative PCR analysis of HSPA1A (left graph) and HSPA6 (right graph) in undifferentiated (low calcium) or differentiated (high calcium) NHEKs infected with Ad-LacZ (control) or Ad-TNIP1. Statistical significance was determined using Student's t-test, * $p < 0.05$. Bars are mean + SEM from experimental triplicates.

Discussion

The expression and roles of TNIP1 in cells and tissues are still being determined. Through several genome wide association studies and gene expression analysis, TNIP1 has been linked to various inflammatory diseases *(34, 38, 39, 87)*. Additionally, TNIP1's repressive effects have been observed experimentally in several receptor-mediated pathways, including TNFR and nuclear receptors, using promoter-responsive reporter constructs *(24, 25, 28, 31, 69, 88)* (refer to *(41)* for review). Consistent with TNIP1's repression of these pathways, our microarray results using cells overexpressing TNIP1 resulted in reduced expression of 136 of 139 genes, validating TNIP1's repressive effect. Decreased expression of TNFα and nuclear receptor target genes, including interleukin 6 (IL6), NFkB inhibitor alpha (NFKBIA) and retinoic acid receptor responder 3 (RARRES3), were observed, confirming TNIP1's role in repressing these pathways.

Pathway clustering analysis showed functions related to cancer, cell death and immunological diseases were affected using IPA, while DAVID *(97, 98)* analysis showed functions related to antiviral defense, transcription and cell death. The classification for cancer, immunological diseases and antiviral defense could be related because each of these functions have similar altered genes that are associated with inflammation. The specific functional grouping could be annotated differently within these clustering programs. However, since the gene lists altered are the similar, this could make the association between TNIP1 and these pathways stronger. A previously unknown TNIP1-associated

function affected from the TNIP1 overexpression in HaCaT KCs was the stress response pathway, indicating TNIP1 could play a role in modulating the cell stress response in skin KCs.

Expression levels of several stress-responsive genes from two HSP families, HSPA and DNAJ (also named HSP70 and HSP40, respectively), were decreased after TNIP1 overexpression in HaCaT KCs. HSPA1A/B, HSPA6, DNAJA1, and DNAJB1 levels were reduced as much as 20-fold in the microarray. In addition to their key roles in protecting the cell from various stressors, they play equally important functions in unstressed cells as molecular chaperones. Protein expression analysis for HSPA1A and HSPA6 further showed reduced protein expression, suggesting HaCaT KCs may have a reduced capacity to tolerate exposure to cell stressors with increased TNIP1 levels. In unstressed cells, TNIP1 could affect new protein synthesis and shuttling through reduced expression of HSPs, possibly affecting KC proliferation and differentiation.

TNIP1 appears to play important roles in regulating multiple receptor mediated signal pathways— from the membrane bound TNFR *(28, 67, 100)* signaling cascades to modulating the transcriptional activity of nuclear PPAR *(24)* and RAR *(23)*. Additionally, increased expression of TNIP1 has been implicated in several disease states, including psoriasis *(34, 52)*. Though TNIP1's specific role has not been identified in these diseases, our results observed TNIP1 overexpression reduced expression of several HSPs, a group of proteins whose expression also increases during psoriasis. These results show a discord in

these findings because increased levels of both TNIP1 and HSPs were observed. A potential explanation could be that, while increased TNIP1 levels result in reduced HSP expression, the inflammation-induced levels of HSPs could be greater than that found if TNIP1 expression was not increased. If TNIP1 levels were reduced in psoriasis, more HSPs could be observed in psoriatic lesions, which would protect the cell from further inflammation-induced damage.

Using NHEK cells, we were able to determine whether TNIP1 has an effect on HSPs in undifferentiating (low Ca^{2+} in the media) or a mixed population of undifferentiated and differentiated (high Ca^{2+} in the media) KCs *(101)*. To generate a greater change in the cell population, the high calcium cultured NHEKs were grown an extra 3 days after collecting the low calcium cultured cells. The extra time allowed to grow in addition to the increased calcium concentration further induces KC differentiation. Using undifferentiating vs. differentiating cultured NHEK cells, we observed the TNIP1-mediated reduction of HSPA1A and HSPA6 only in the mixed population with differentiating keratinocytes. These results are consistent with the HaCaT KC data because the cell culture conditions for the HaCaTs are also grown using high calcium media (1.45 mM Ca^{2+}). Thus, the HaCaT cells contain a mixed population of KCs. Interestingly, when we examined two markers of KC differentiation, involucrin and keratin 1, we observed a TNIP1-repressive effect on involucrin, but not keratin 1. These results suggest TNIP1 reduces the expression of specific genes and is not a general repressor of all genes.

In this chapter, we used a gene microarray to examine the specific genes and functions altered by increased TNIP1 levels in KCs. Results show that TNIP1-associated pathways and diseases were altered in response to enhanced TNIP1 protein levels. A novel pathway, the cell stress response, was also altered, in which HSP mRNA levels were reduced, possibly indicating TNIP1 could transcriptionally regulate these genes. The TNIP1-mediated repression of HSPA1A and HSPA6 extended to a decrease in protein expression further suggesting that TNIP1 may alter the cell stress response by inhibiting the production of these proteins.

Chapter 3

Transcriptional Regulation of HSPA6 in Basal and Stressed Conditions

Abstract

Epidermal KCs serve as the primary barrier between the body and environmental stressors. They are subjected to numerous stress events and are likely to respond with a repertoire of heat shock proteins (HSP). HSPA6 (HSP70B') is described in other cell types with characteristically low to undetectable basal expression, but is highly stress-induced. Despite this response in other cells, little is known about its control in keratinocytes (KC). We examined endogenous human KC HSPA6 expression and defined some responsible transcription factor sites in a cloned HSPA6 3kb promoter. Using promoter 5' truncations and deletions, negative and positive regulatory regions were found throughout the 3kb promoter. A region between -346 to -217 bp was found to be crucial to HSPA6 basal expression and stress inducibility. Site-specific mutations and DNA-binding studies show a previously uncharacterized AP1 site contributes to the basal expression and maximal stress induction of HSPA6. Additionally, a new heat shock element (HSE) within this region was defined. While this element mediates increased transcriptional response in thermally stressed KCs, it preferentially binds a stress inducible KC factor, other than HSF1 or HSF2. Intriguingly, this new HSPA6 HSE competes HSF1 binding a consensus HSE and binds both HSF1 and HSF2 from other epithelial cells. Taken together, our results demonstrate that the HSPA6 promoter contains essential negative and positive promoter regions and newly identified transcription factor targets, which

are key to the basal and stress inducible expression of HSPA6. Furthermore, these results suggest an HSF-like factor may preferentially bind this newly identified HSPA6 HSE in HaCaT KCs.

Introduction

Properly controlled heat shock protein (HSP) gene expression is integral to maintaining and restoring cell homeostasis under basal and stressed conditions, respectively. Although initially known by their transcription induction from thermal stress, HSP expression is also increased in response to toxic chemical and UV light assaults *(71)*. Additionally, the characterization of dozens of HSP genes across multiple families established that several members are constitutively expressed, accounting for their availability in "house-keeping" chaperone function *(73)*. As might be expected, within and across HSP families there are some coding sequence similarities, common substrate targets, and shared transcriptional control by HSF (heat shock factor) *(102, 103)*. However, these shared qualities belie the non-redundant role of several HSP identified in recent reports *(77-79, 104)*. HSPA1A (HSP70) is an important protein chaperone in unstressed conditions and is crucial to prevent stress-induced cell death. While closely related to HSPA1A, HSPA6 (HSP70B') has similar yet distinct functions and its expression patterns *(79, 105)* vary between cell types and cell densities *(83)*.

Like HSPA1A, HSPA6 expression is essential to increasing survival of cells exposed to increased temperatures or chemicals. Single or double siRNA-mediated knockdown of HSPA1A and/or HSPA6 suggest that while both HSPs are important to increasing cell survival, HSPA6 may be a secondary regulator of stress compared to HSPA1A *(79)*. Decreased expression of HSPA6 did reduce the cell viability after a 42°C heat stress or proteasome inhibitor MG-132

treatment, suggesting its importance in cell survival. HSPA6 likely forms complexes with HSPA1A and DNAJB1 (HSP40) *(82, 106)* to confer its protective function. Despite some HSPA6/HSPA1A overlap in facilitating cell survival, further work showed they have distinct protein substrates. Compared to HSPA1A, HSPA6 has higher affinity for unfolded p53 but has no effect in refolding the luciferase enzyme and peroxisomal proteins *(77, 78)*. Better definition of HSPA6 gene expression levels and the protein factors/promoter elements contributing to it would improve our understanding as to its availability or inducibility to meet these specific protective chaperone/refolding functions.

HSPA6 production under non-stressed conditions is variable, from not detected, to low expression levels, possibly dependent on cell type *(81, 82)* and growth condition differences *(83)*. Its capacity for significant induction under stressed conditions has been well-documented but what controls this or basal expression has mostly been elucidated using a ~287 bp minimal promoter *(84-86)*. To enhance our understanding of HSPA6 production in other cell types and control over its basal and inducible transcription, we examined HSPA6 expression in epidermal KCs and what might contribute to control of inducible and any basal expression. Various HSPs in KCs serve as a cadre of molecular chaperones and stress response proteins both for protein folding during cell differentiation and epidermal response to topical assaults. Insufficient HSP expression in KCs has detrimental consequences including i) inadequate integration of cytoskeletal and non-cytoskeletal proteins to generate the skin's barrier and ii) failure to cope with or recover from stresses as evidenced by poor

or absent wound healing *(107, 108)*. In brief, we found human KCs have significant capacity for HSPA6 induction at both mRNA and protein levels compared to the related HSPA1A. Additionally with computational analysis, cloning, and functional assessment of ~3kb of the HSPA6 promoter we found previously unidentified regions exerting negative or positive effects over basal expression as well as a novel (heat shock element) HSE upstream of those previously known *(85)*. Constitutive and strikingly inducible HSPA6 expression in combination with complex transcriptional regulation suggest it may be positioned to contribute significant chaperoning as well as stress-protective functions to epidermal KCs.

Materials and Methods

Cell culture

HaCaT, SCC13, MCF7, HeLa, HepG2 and dermal fibroblasts were cultured in a 3:1 DMEM/F12 media containing 10% FBS (Thermo Scientific HyClone, Logan, UT), 100U/ml penicillin, and 100 mg/ml streptomycin. HT29 cells were cultured in McCoy's 5a modified media containing 10% FBS, supplemented with 1% non-essential amino acids (NEAA), 100U/ml penicillin, and 100 mg/ml streptomycin. Caco2 cells were cultured in MEM media containing 20% FBS and supplemented with 1% NEAA, 1% pyruvate, 100U/ml penicillin, and 100 mg/ml streptomycin. All cells were grown in a 37°C with 5% CO_2 humidified incubator. For mRNA and protein analyses, cells were plated at 1.5 x 10^5 and 6.8 x 10^5 cells per well in 24- or 6-well plates, respectively. Twenty-four hours later, cells were stressed for 1 hour in a 42°C water bath (control cells were immersed in a 37°C water bath) and returned to a 37°C incubator for the indicated recovery time. Cells were collected for total RNA using the RNeasy kit (Qiagen, Valencia, CA) or protein using RIPA lysis buffer (10 mM Tris, 150 mM NaCl, 1% deoxycholic acid, 1% Triton, 0.1% SDS) supplemented with Halt Protease Inhibitor (Thermo Scientific, Waltham, MA). For transfection analysis, cells were plated to 70% confluency in 24-well plates. Twenty-four hours later, cells were transfected as described below.

Real-Time quantitative PCR analysis

Reverse transcription was performed using aliquots from the total RNA used for the microarray using the iScript reverse transcriptase (BioRad, Hercules, CA).

Gene expression changes were analyzed using POWER SYBR green master mix (Life Technologies, Grand Island, NY). Real-time PCR was performed using Applied Biosystems 7500 Fast Real-Time PCR system. Data analysis was carried out on ABI 7500 software using the ΔΔCT method. The primer sequences used and reaction conditions are listed on Table 2.1. All data were normalized to the ribosomal proten L13a (RPL13a) *(99)*.

Immunoblot analysis

Whole-cell lysates were prepared in RIPA buffer and the protein concentration was determined using the 660 nm Protein Assay (Thermo Pierce). Ten micrograms of protein were separated by SDS/PAGE, transferred to nitrocellulose membranes, rinsed with nanopure water and treated with Qentix (Thermo Scientific Pierce). Blots were incubated in blocking buffer consisting of 5% (w/v) non-fat dried milk, phosphate-buffered saline, and 0.1% Tween 20, then probed with HSP70B' antibody (ADI-SPA-754) at 1:1000 dilution (Enzo Life Sciences, Farmingdale, NY) or anti-HSPA1A antibody (ADI-SPA-810) at 1:1000 dilution (Enzo Life Sciences) *(82, 83)* followed by HRP (horseradish peroxidase)-conjugated secondary goat anti-mouse antibody at 1:10,000 dilution (PerkinElmer, Branford, CT). Blots were subsequently probed with β-actin antibody (ab8227) at 1:5,000 dilution (Abcam, Cambridge, MA) followed by HRP-conjugated secondary goat anti-rabbit antibody at 1:20,000 dilution (PerkinElmer). Between probing steps, blots were washed with 0.2% Tween20 in phosphate-buffered saline. Detection of binding was determined with enhanced

chemiluminescence reagents (Thermo Scientific Pierce). Band signals were digitally captured and analyzed using the Kodak image station CCF and Carestream molecular imaging software.

Generation of luciferase constructs

The HSPA6 promoter containing the -2963 to +48 bp sequence (herein referred to as -3 kb-luc) was PCR amplified from human genomic DNA (cat# 636401) (BD Biosciences, San Jose, CA) using forward: 5'-GAT GGG TAC CTC ATC TTG AAT TCC CAC AAC ACA TGG-3' and reverse: 5'-GGC TGA AGC TTA GTG AGG CTC TCC CTG CGG TTT CTC T-3' with added *KpnI* and *HindIII* sites (underlined), respectively for insertion into the promoterless vector pGL4.10 (Promega, Madison, WI) using the restriction sites indicated. 5'-promoter truncations (-1230, -647 and -70 -luc) were performed by using the upstream *KpnI* site and native restriction enzyme sites *BglII*, *EcoRI* and *NruI*, respectively. Digested sites were blunted and ligated. Internal promoter deletions were performed using the Quikchange Lightning site-directed mutagenesis kit (Agilent, Santa Clara, CA). Constructs ΔA, ΔB, ΔC, and ΔD were generated using the -1230 luc; constructs ΔE, ΔF, ΔG, and ΔH were generated using the -647 luc. Fragment G site specific mutants were generated using the Quikchange Lightning site-directed mutagenesis kit. The WHN, HSE, MZF1, C/EBP, AP1 and Zfx sites were mutated as indicated (Table 1). Sites were determined using NHR Scan *(109)*, Nubiscan *(110)* and MatInspector *(111)* web-based software. To generate the wild type (WT)-G-tk-luc, AP1 mutant (mt)-G-tk-luc, and HSEmt-G-

tk-luc construct, the HSPA6 G region was amplified via PCR using primers flanked by *KpnI* sites. The pGL4.10 construct containing the thymidine kinase (tk-luc) minimal promoter was used to insert the HSPA6 WT, AP1mt or HSEmt fragment G. All HSPA6 3kb isolate, all site-directed mutants, and deletion constructs were confirmed by sequencing (UConn Biotech Center).

Plasmid transfections

HaCaT cells were plated to 70% confluency 24 hours prior to transfections using 24-well plates. Eight hours prior to transfection, media was replaced with 0.5 mL serum-containing 3:1 DMEM/F12 media. The appropriate HSPA6 promoter pGL4.10 plasmid (200 ng) and pCMV-β Galactosidase (100 ng) was transfected using Fugene6 (Promega) using 100 µL serum-free media. Twenty-four hours later, cells were stressed for 1 hour in a 42°C water bath (control cells in a 37°C bath) and returned to a 37°C incubator for 4 hours. Cells were then collected and assayed for the luciferase activity (Promega), protein concentration (Pierce), and β-galactosidase activity *(96)*.

Electrophoretic mobility shift assay (EMSA)

Nuclear extracts were prepared from HaCaT or HeLa cells as previously described *(44)*. Protein concentrations were determined by BCA protein assay (Pierce, Rockford, IL). Oligomers (Integrated DNA Technology, IDT, Coralville, IA) were annealed and end-labeled with ^{32}P-ATP (Perkin Elmer). EMSA oligonucleotide probe sequences are shown on Table 2. Fifteen or ten

micrograms of nuclear extracts were incubated with radiolabeled HSE or AP1 oligomers, respectively. For AP1 EMSAs, nuclear extracts were preincubated with the appropriate antibodies or unlabeled competition oligomers 1 hour or 15 minutes, respectively, at room temperature prior to the addition of the radiolabeled oligonucleotide probes. The mixture was incubated at room temperature for 30 minutes and then loaded into a 6% polyacrylamide gel. Gels were electrophoresed at 3.5mA/gel in 0.5X TBE buffer for 10 hours at 4°C. For HSE EMSAs, nuclear extracts were preincubated with unlabeled competition oligomers 15 minutes at room temperature prior to the addition of the radiolabeled oligonucleotide probes. Antibodies were added and the mixture was incubated at room temperature for 20 minutes, then on ice for 10 minutes. Samples were loaded on a 4% polyacrylamide gel and electrophoresed at 3.5mA/gel in 0.5X TBE buffer for 8 hours at 4°C. Anti- c-Jun (SC-45X), c-Fos (SC-52X), HSF1 (SC-9144x) and HSF2 (SC-13056X) antibodies were obtained from Santa Cruz Biotechnology (Santa Cruz, CA). Gels were dried and exposed to Amersham Hyperfilm MP (GE, Buckinghamshire, UK) for at least 16 h at -80°C with intensifying screens. Films were developed using a Kodak X-Omat 2000.

Statistical analysis

All data were analyzed using Prism Software version 5 (GraphPad) (La Jolla, CA). Student's t-test was used to compare between paired results. ANOVA with Newman Keuls *post hoc* was used to compare between grouped results, when necessary. Statistical significance was defined as $p \leq 0.05$.

Table 3.1. Site-directed mutagenesis primer sequences. Underlined sequences denote mutations within the binding site.

Site name	**Sequence within HSPA6**	**Mutated sequence**
WHN	ACGC	A<u>TA</u>C
HSE	GGGAGGAGCTAGAACCTTCC	GGGAGGAGCTA<u>ATT</u>CCTTCC
MZF1	GCGGGGAAGGT	GCG<u>TAG</u>A<u>G</u>GGT
C/EBP	CTCAGGCTGCTGAAA	CTCA<u>T</u>GC<u>ACT</u>TG<u>TC</u>A
AP1	TGAGTCA	T<u>T</u>AGT<u>T</u>A
ZFX	CTGGCCTGGCG	CT<u>AAGA</u>TGGCG

Table 3.2. Oligomers used for EMSA probes. Underlined sequences denote mutations within the binding site. The predicted HSE mutation encompasses one HSE repeat, whereas the double mutant encompasses two HSE inverted repeats.

Oligomer name	**Primer sequence**
Predicted AP1 top	CTAGCAGCAGCCTGAGTCAGAGGCGGG
Predicted AP1 bottom	CTAGCCCGCCTCTGACTCAGGCTGCTG
AP1 consensus top	CTAGCGCTTGATGACTCAGCCGGAA
AP1 consensus bottom	CTAGTTCCGGCTGAGTCATCAAGCG
Predicted AP1 mutant top	CTAGCAGCAGCCTTAGTTAGAGGCGGG
Predicted AP1 mutant bottom	CTAGCCCGCCTCTAACTAAGGCTGCTG
Predicted HSE top	CTAGGGGAGGAGCTAGAACCTTCCCCGCA
Predicted HSE bottom	CTAGTGCGGGGAAGGTTCTAGCTCCTCCC
HSE consensus top	CTAGCGAAACCCCTGGAATATTCCCGACC
HSE consensus bottom	CTAGGGTCGGGAATATTCCAGGGGTTTCG
Predicted HSE mutant top	CTAGGGGAGGAGCTAATTCCTTCCCCGCA
Predicted HSE mutant bottom	CTAGTGCGGGGAAGGAATTAGCTCCTCCC
Predicted HSE double mutant top	CTAGGGGAGGAGCCCATTATAGTAGCGCA
Predicted HSE double mutant bottom	CTAGTGCGCTACTATAATGGGCTCCTCCC

Results

Constitutive and inducible expression of HSPA6 in KCs

Basal and induced levels of HSPA6 were determined in HaCaT KCs under standard culture and thermal stress conditions. Basal expression of HSPA6 was detected in unstressed cells with several fold increase in protein levels observed at 8- and 24-hours post heat shock (Fig 3.1, top panel). HSPA6 mRNA was highly upregulated immediately following heat stress, then gradually decreased over 8-12 hours after the stress period to levels similar to basal expression (Fig 3.1, bottom panel). To validate the heat shock, HSPA1A protein and mRNA expression was also examined. The induction pattern of HSPA1A protein and mRNA was similar to HSPA6, but to a lesser fold induction than HSPA6 (Fig 3.2). Variable levels of HSPA6 and HSPA1A were also detected in other epithelial (HT29, MCF-7, Caco2, HepG2) and epidermis-derived (SCC13), cells with relatively little detected in dermal fibroblast cells (Fig 3.3) under standard (non-stressed) culture conditions. HSPA6 cell-type range of expression and induction suggested a combination of ubiquitous and stress-specific factors may control its gene expression.

Determining specific transcription factor binding sites within the HSPA6 promoter

To guide physical isolation of the human HSPA6 promoter, we started with an *in silico* examination of sequences upstream of the referenced transcription start site *(112)* and 5'UTR of the NCBI mRNA reference sequence *(113)* NM_002155.3. NHR Scan *(109)*, NubiScan *(110)* and MatInspector *(111)*

Figure 3.1

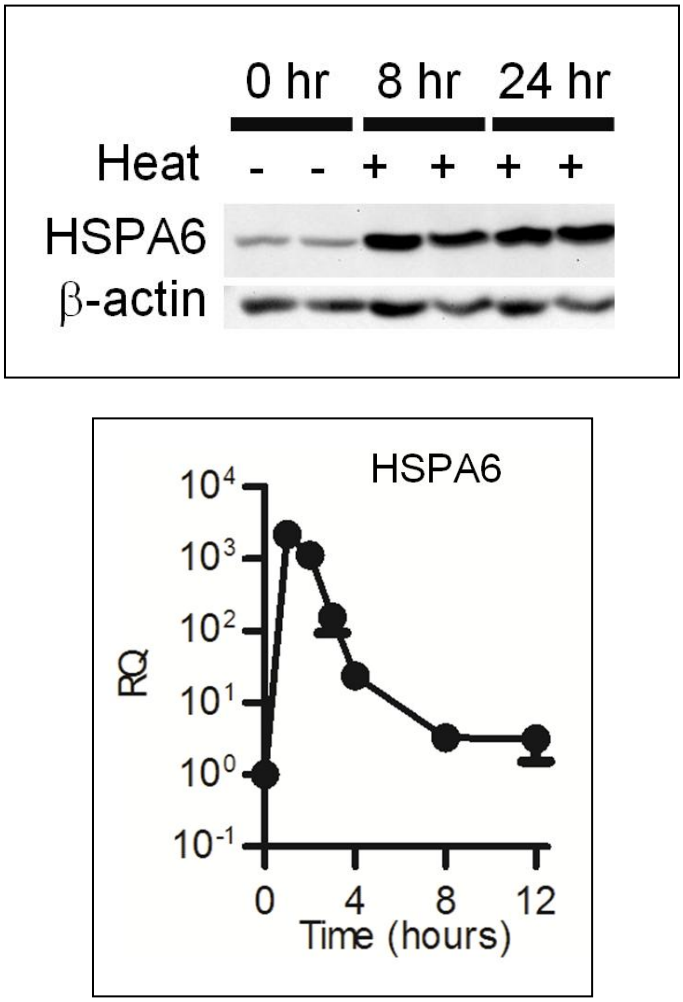

Figure 3.1. Basal and heat-inducible expression of HSPA6 in HaCaT KCs. Top panel. HSPA6 protein expression before (0 hr) and post-heat shock (8 and 24 hr). Samples shown from duplicate cultures. Bottom panel. HSPA6 mRNA expression before (0 hr) and post-heat shock (1, 2, 3, 4, 8 and 12 hr). Unless otherwise indicated, all cells are unstressed. β-actin used as western blot loading control.

Figure 3.2

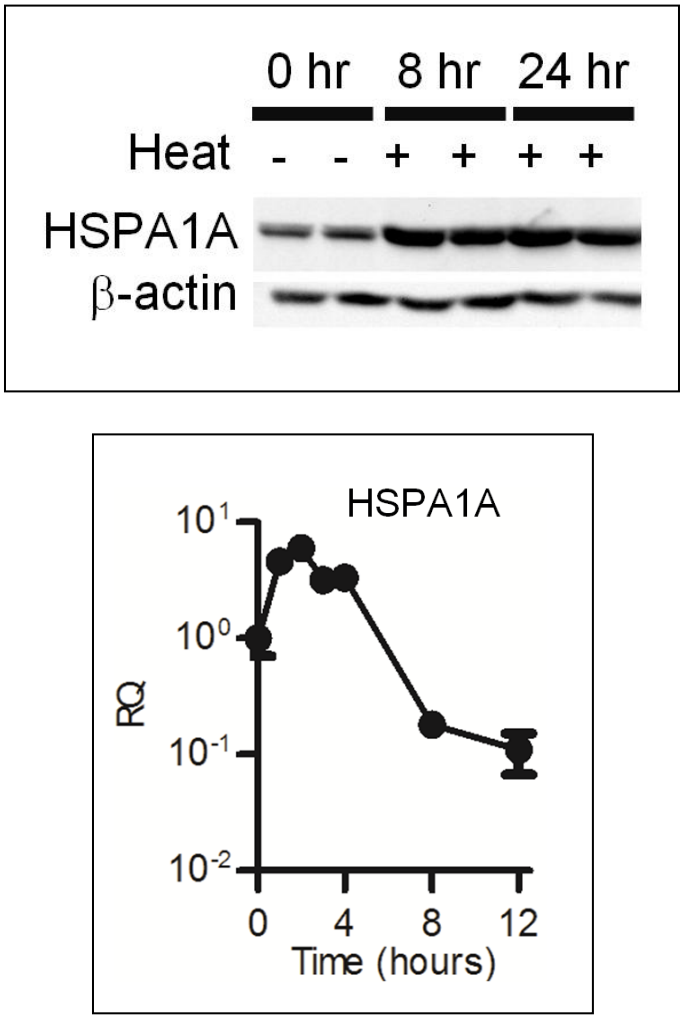

Figure 3.2. Basal and heat-inducible expression of HSPA1A in HaCaT KCs. Top panel. HSPA1A protein expression before (0 hr) and post-heat shock (8 and 24 hr). Samples shown from duplicate cultures. Bottom panel. HSPA1A mRNA expression before (0 hr) and post-heat shock (1, 2, 3, 4, 8 and 12 hr).

Figure 3.3

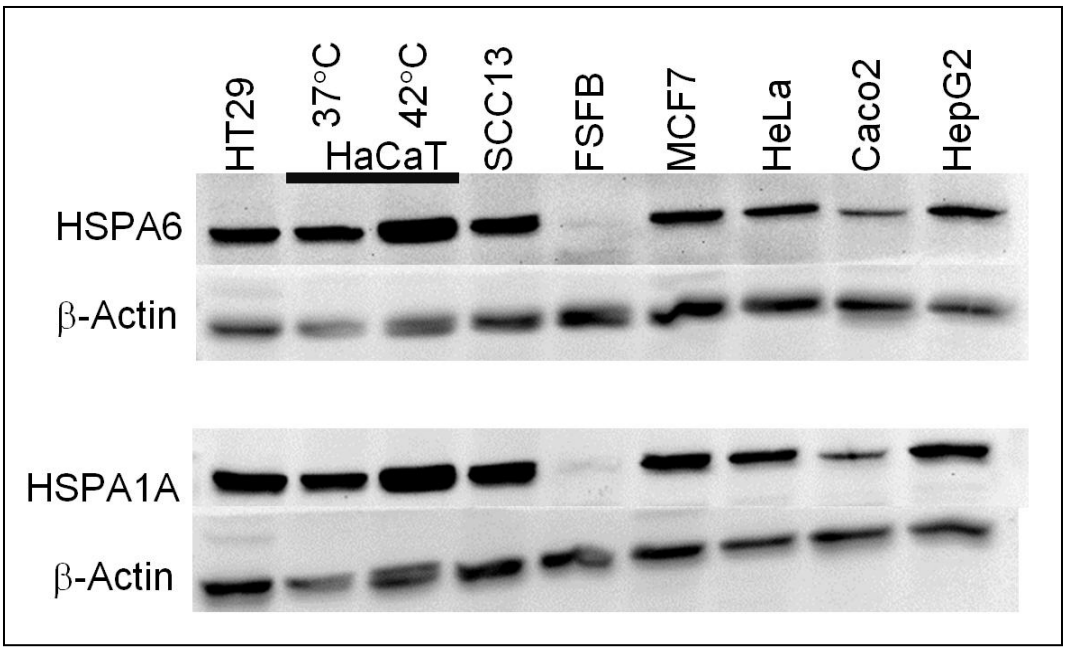

Figure 3.3. Expression of HSPs in various cell types. HSPA6 (top panel) and HSPA1A (bottom panel) protein expression in various cells. Unless otherwise indicated, all cells are unstressed. β-actin used as western blot loading control.

analysis suggested high scoring hits for diverse transcription factors up through the first few thousand base pairs of DNA. Germane to our laboratory's interest in nuclear receptors, putative peroxisome proliferator activated receptor (PPAR) and retinoic acid receptor (RAR) response elements were located between ~ -3000 to -1200 bp upstream of the transcriptional start site. To determine HSPA6 expression responsiveness to these and other transcription factors, we isolated and cloned its promoter region from -2962 to +48 bp (-3 kb) into a pGL4.10 luciferase reporter gene construct (Fig 3.4). Endogenous HSPA6 expression and HSPA6 -3 kb-luc promoter activation marginally increased only in presence of high concentration of PPARγ ligand or overexpressed PPARγ receptor and high concentration of ligand, respectively (data not shown). Since PPARγ has low expression in KCs, we hypothesized that other transcription factor(s) may be responsible for the expression of HSPA6.

Searching the promoter for other predicted sites, further *in silico* promoter analysis was performed. In addition to searching for factors that contribute to HSPA6's basal expression, we searched for heat shock elements (HSE) that may contribute to the stress inducibility of HSPA6. Our analysis found previously recognized sites such as two HSEs at -181 to -161 bp and -100 to -60 bp, an AP1 site at -139 to -132 bp, and a predicted TATA box within the proximal HSPA6 promoter, -283 to +110 bp (Wada 2007, Leung 1990). Importantly, previously unrecognized potential transcription factor binding sites (such as AP1 and upstream HSEs) (Fig 3.5) were identified suggesting additional control possibilities for basal and inducible HSPA6 promoter activity.

Figure 3.4

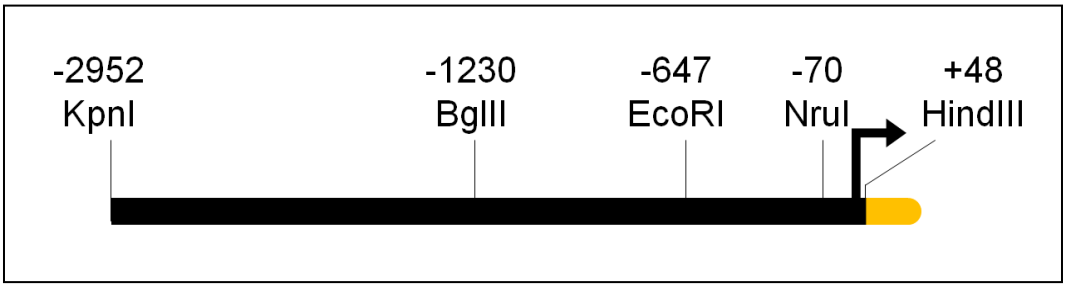

Figure 3.4. Native restriction enzyme sites within the HSPA6 3kb promoter. Diagram of the HSPA6 promoter from -2952 to +48 bp. Restriction enzyme sites shown and used for generating promoter truncation constructs. Yellow region indicates start of the luciferase reporter gene.

Figure 3.5

Figure 3.5. *In silico* analysis of the HSPA6 3kb promoter. Top panel. HSPA6 promoter sequence between -1300 to -1100 bp. Red sequences denote putative HSE. Bottom panel. HSPA6 promoter sequence between -700 to +48 bp. Red sequences denote putative HSE. Blue sequences denote putative AP1 sites. Nucleotides in boldface denote predicted TATA box. Underlined sections denote previously identified HSEs. Italicized section denotes previously identified AP1 site.

HSPA6 promoter contains negative and positive basal regulatory regions

To narrow down the responsive regions involved in HSPA6 regulation, we generated a series of 5' truncation constructs using naturally occurring restriction enzyme sites (Fig 3.4). Transfection results from the truncated HSPA6 promoter constructs from unstressed cells showed the -647-luc had increased luciferase activity compared to the "minimal" -70-luc. Interestingly, extending the 5' promoter to -1230 bp and further led to a reduction of luciferase activity back to the minimal promoter levels (Fig 3.6, left panel). These results suggest the regulation of unstressed HSPA6 includes both negative (between -1230 to -648 bp) and positive (between -647 to -70 bp) elements. Heat-induced expression (Fig 3.6, right panel) was observed with promoter regions inclusive of sequence upstream of the previously described -181 and -100 bp HSEs. Notably however, the fold induction of the -1230 bp and -3 kb were significantly greater than the fold induction of the -647 bp reporter suggesting other proactive elements involved in maximal stress response.

To further guide our search for HSPA6 promoter regions contributing to its overall basal activity and stress response, we generated several constructs deleting ~150 bp lengths within the -1230-luc or -647-luc constructs. Deletions within the -1230-luc, ΔA-, ΔB-, ΔC- and ΔD-luc, (Fig 3.7, left panel) showed removal of fragment D (-806 to -648) increased the promoter activity 76%, suggesting possible negative regulatory element(s) within this region (Fig 3.7, middle panel). The stress responsiveness of ΔA-, ΔB-, ΔC- and ΔD-luc were also

compromised as a decrease in fold induction was observed with these constructs compared to full-length -1230-

luc (Fig 3.7, right panel). Internal promoter deletions within the -647-luc, ΔE-, ΔF-, ΔG- and ΔH-luc (Fig 3.8, left panel), suggested fragments F, G and H each contribute to the activation of the HSPA6 promoter. Removal of fragments F or H reduced the promoter activity to ~35% compared to the full-length -647-luc. Deletion of fragment G (-346 to -217 bp) (Fig 3.8, middle and right panels) led to the complete loss of the HSPA6 promoter activity. While deletion of each individual fragment reduced the heat inducibility of the promoter, the induction of ΔG-luc was significantly reduced back to basal levels of -647-luc. Because removal of fragment G lost all promoter activation we focused on determining the possible site(s) within this region that are crucial for the activation of the HSPA6 promoter.

A novel AP1 site within -346 to -217 bp contributes to the activation of the HSPA6 promoter

A transcription factor binding site search within fragment G (-346 to -217 bp) determined 6 top-scoring predicted elements: WHN, HSE, MZF1, C/EBP, AP1 and ZFX (Fig 3.9). We generated site-specific mutants within the -647-luc constructs to determine which binding site may contribute to the unstressed (37°C) expression of HSPA6. Of these candidate sites, mutation of WHN, HSE and MZF1 had no significant effect on the basal HSPA6 promoter activation,

Figure 3.6

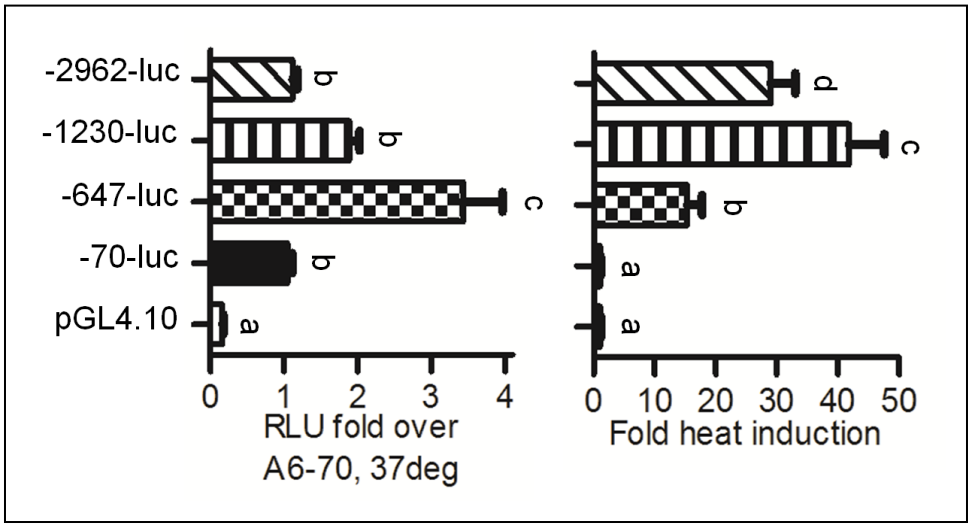

Fig 3.6. Determining the transcriptionally regulated regions within the HSPA6 promoter. Left panel. Promoter activation at basal, 37°C conditions. The graph is normalized to the -70-luc. Right panel. Promoter induction due to a 1 hour, 42°C heat stress. Graph shown as fold inducibility compared to 37°C condition. Letters denote statistical significance using ANOVA with Newman Keuls post-hoc, $p < 0.05$. Bars are mean + SEM from n=3, triplicate experiments.

Figure 3.7

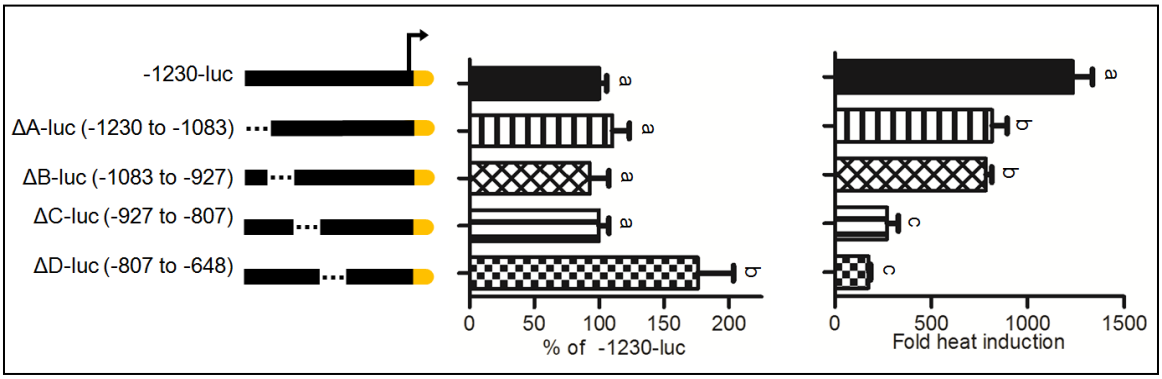

Figure 3.7. Localizing the repressible region within the HSPA6 promoter. Left panel. Internal deletions A, B, C, and D between -1230 to -648 denoted as the dotted line. Middle panel. Promoter activation at basal, 37°C conditions. Graph shown as percent of -1230-luc. Right panel. Promoter induction due to a 1 hour, 42°C heat stress. Graph shown as fold inducibility compared to 37°C condition. Letters denote statistical significance using ANOVA with Newman Keuls post-hoc, $p < 0.05$. Bars are mean + SEM from n=3, triplicate experiments.

Figure 3.8

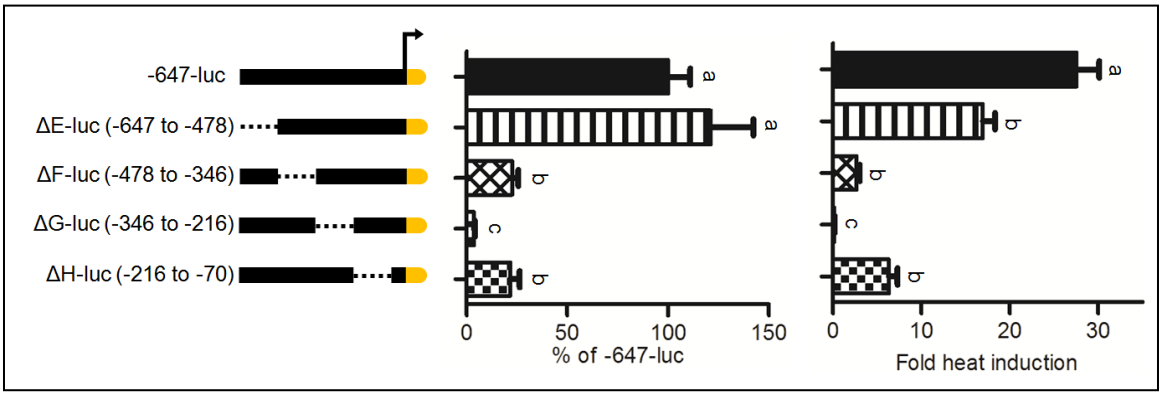

Figure 3.8. Localizing the basal and inducible regions within the HSPA6 promoter. Left panel. Internal deletions E, F, G, and H between -647 to -70 denoted as the dotted line. Middle panel. Promoter activation at basal, 37°C conditions. Graph shown as percent of -647-luc. Right panel. Promoter induction due to a 1 hour, 42°C heat stress. Graph shown as fold inducibility compared to 37°C condition. Letters denote statistical significance using ANOVA with Newman Keuls post-hoc, $p < 0.05$. Bars are mean + SEM from n=3, triplicate experiments.

whereas C/EBP and ZFX specific mutants resulted in an ~50% increase in the -647-luc promoter activity. Only mutation of AP1 resulted in activity loss. This local length of the HSPA6 promoter seems to share the trait of positive and negative control we saw upstream with -1230 bp and -3 kb lengths. Thus the -346 to -217 bp region is likely crucial for proper positive and negative promoter regulation of within the HSPA6 native promoter.

To independently assess regulation conferred by region G, we fused the -346 to -217 bp region to the minimal tk- promoter (Fig 3.10). This G-tk-luc construct did not significantly change the luciferase activity compared to the tk-luc construct. When the AP1 site was mutated, a ~54% reduction was observed compared to wild type fragment G tk-luc (G-WT tk-luc). These results suggest fragment G activation potential is promoter context dependent, contributing to the native HSPA6 promoter but not a heterologous (tk) promoter. These results are consistent with the predicted -244 bp AP1 site contributing to the promoter activation of HSPA6.

To test for physical association of AP1 to the predicted binding site, electrophoretic mobility shift assays (EMSAs) were performed. Using the predicted HSPA6 -244 bp AP1 site as the ^{32}P-labeled oligomers, our EMSA results show an AP1 specific band competed by an unlabeled HSPA6 AP1 site and consensus AP1 site, but not by the mutated AP1 site. Addition of AP1 subunit (cJun, cFos, or combined) specific antibody disrupted the band species in the cFos and the combined cJun/cFos lanes (Fig 3.11). Based on reporter

Figure 3.9

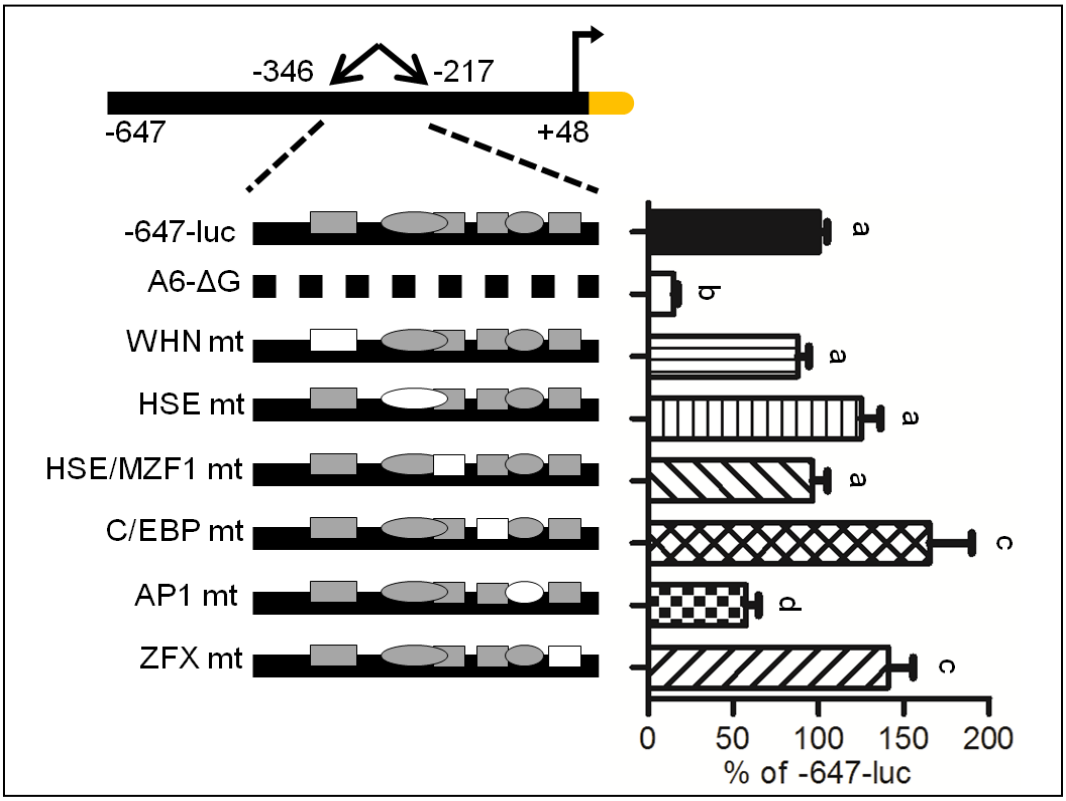

Figure 3.9. Searching for transcription factor binding sites between the -346 to -216 bp region of HSPA6. Site specific mutations within the -647-luc construct. Filled shapes indicate wild-type elements. Specific site mutants are shown as empty shapes. Graph shown as percent of -647-luc. Letters denote statistical significance using ANOVA with Newman Keuls post-hoc, $p < 0.05$. Bars are mean + SEM from n=3, replicate experiments.

Figure 3.10

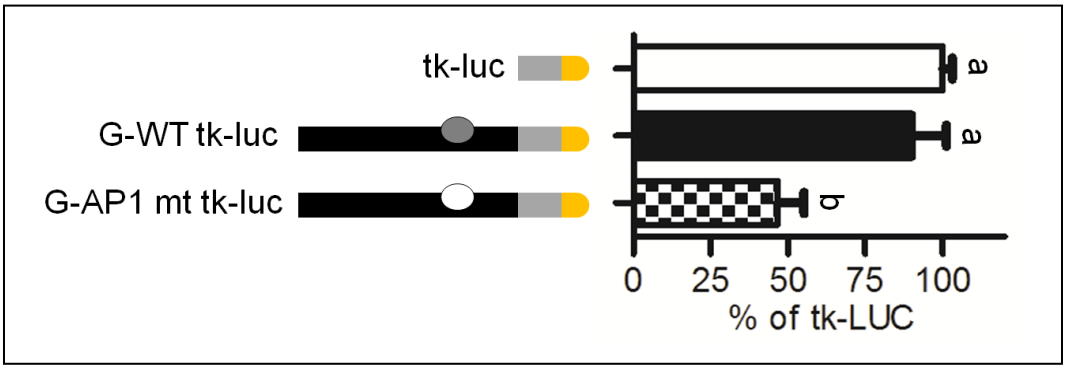

Figure 3.10. Characterization of the -244 bp AP1 site. AP1 specific mutant within the fragment G-tk-luc construct. Graph shown as percent of tk-luc. Letters denote statistical significance using ANOVA with Newman Keuls post-hoc, $p < 0.05$. Bars are mean + SEM from n=3, replicate experiments.

Figure 3.11

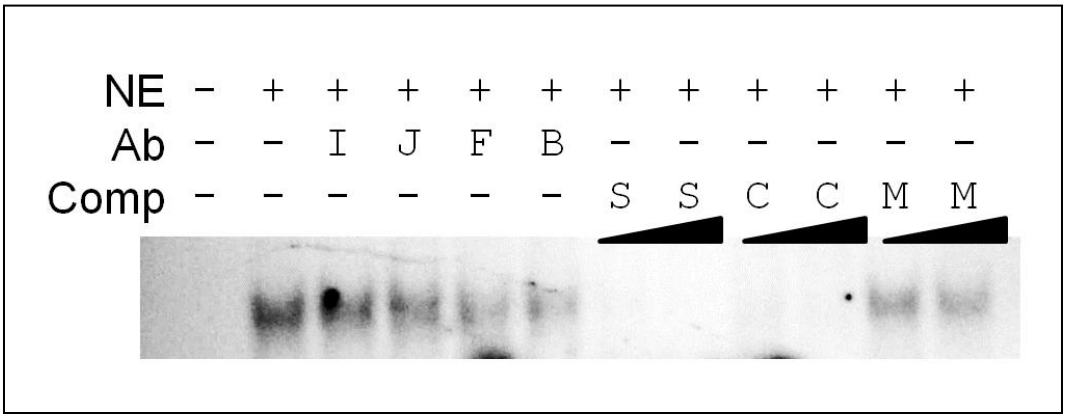

Figure 3.11. EMSA binding analysis of AP1 proteins c-Jun and c-Fos to the -244 bp AP1 site. Antibodies include non-specific IgG (I), anti-c-Jun (J), anti-c-Fos (F) or both anti-c-Jun and anti-c-Fos (B). Non-radiolabeled competitor oligomers include self HSPA6 AP1 site (S), consensus oligomer (C) or mutated AP1 (M) at 5 or 50-fold excess.

construct and the protein-DNA interaction experiments, HSPA6 -244 to -237 is a newly identified, functional AP1 site contributing to transcriptional activity of the HSPA6 promoter in unstressed conditions.

A novel heat shock element within -346 to -217 bp contributes to the activation and thermal induction of the HSPA6 promoter

In addition to promoter elements that might contribute to control of basal activity, our transcription factor search predicted a previously unreported heat shock element within region G. To test its contribution, or how other sites might affect overall stress response, we tested 6 site-specific mutants (Fig 3.12) under basal versus stressed conditions to determine fold induction. Mutations within the WHN, HSE, HSE/MZF1, and AP1 sites significantly reduced the stress inducibility of -647-luc, whereas C/EBP and ZFX specific mutations had no significant effect on stress inducibility. Taken together, these separate binding sites each contribute to the heat inducibility of the promoter and likely have an additive effect in order to gain maximal stress inducibility.

To address the heat stress inducibility of the fragment G HSE, we fused the -346 to -217 bp region to the tk-luc construct. This specific construct is advantageous as it tests the fragment G candidate HSE independent of the previously described HSEs more proximal to the transcriptional start site. The G-WT-tk-luc was heat induced ~20-fold compared to the tk-luc. In contrast, the G-HSEmt tk-luc abolished all stress induction (Fig 3.13). These results show that the -284 bp HSE contributes to the increased expression of HSPA6 due to stress induction.

Using the functionally defined HSPA6 -284 bp HSE as EMSA probe, a band pattern observed from unstressed HaCaT KC nuclear extracts increases in intensity with heat shock. The binding species could be competed with unlabeled wild type, mutant, and double mutant HSPA6 HSE site, but not unlabeled consensus HSE oligomers (Fig 3.14, top panel). Additionally, HSF1 or HSF2 specific antibodies did not affect the band pattern (Fig 3.14, bottom panel). Using ^{32}P-labeled consensus HSE oligomers as EMSA probe, our unlabeled HSPA6 HSE was able to compete the HSF1 specific band, suggesting that the -284 bp HSE can compete for HSF1 under these circumstances (Fig 3.15).

In an attempt to resolve these disparate results (HSE -284 transcriptionally active in mediating thermal stress response but not performing as a classic HSF-binding HSE *in vitro*) we compared the HSPA6 -284 bp HSE binding with that of a consensus HSE (derived from the HSPA1A promoter) *(114)* with an alternate nuclear protein source, HeLa cells. Using HeLa nuclear extracts, the HSPA6 -284 bp HSE generated a binding complex recognized by HSF1 antibody from unstressed and stressed cells, while a HSF2 complex was recognized from stressed cells (Fig 3.16). As a control, we confirmed that the same extracts were generating a HSF1-containing complex on the A1A consensus HSE (Fig 3.17). Together, these transcription activation and EMSA results suggest a stress-associated transcription factor, other than HSF1 or HSF2, binds the -284 bp HSE in HaCaT KCs to activate the HSPA6 promoter. Intriguingly, when HeLa cells are used, HSF1 and HSF2 can bind this site suggesting a cell specific transcription factor binding of this HSE.

Figure 3.12

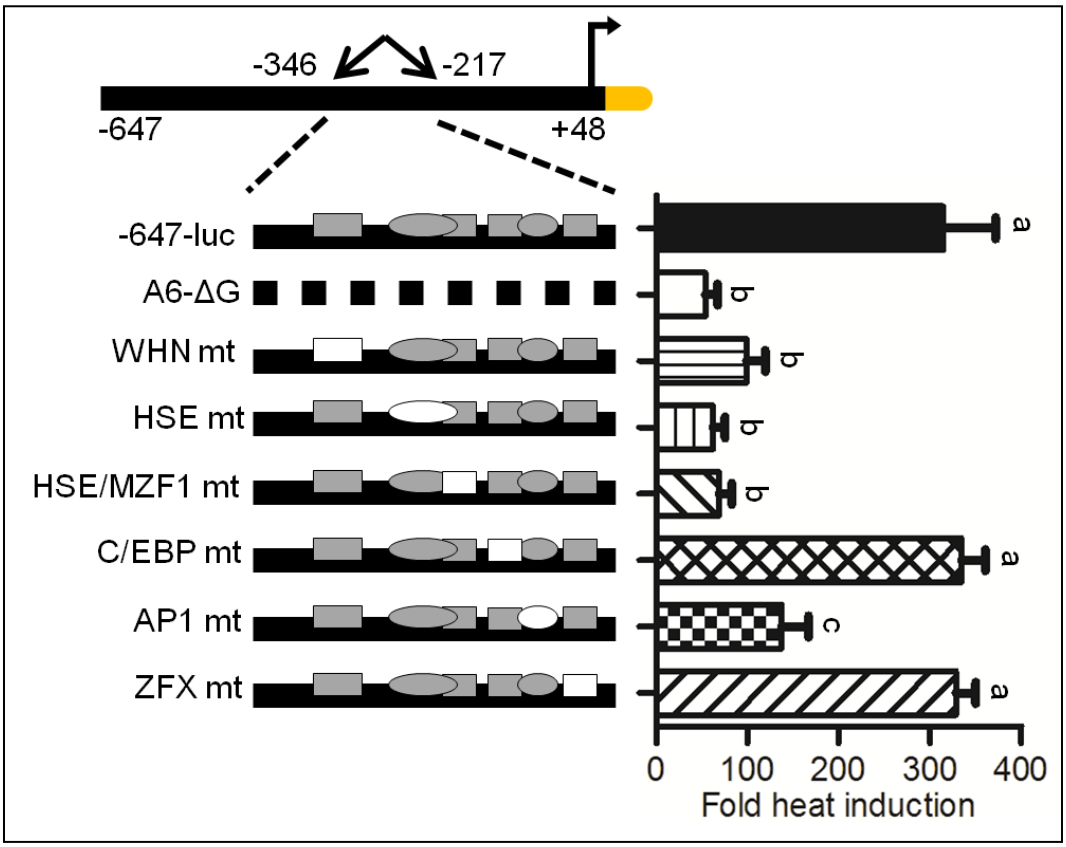

Figure 3.12. Searching for heat responsive elements between -346 to -216 bp region of HSPA6. Site specific mutations within the -647-luc construct. Specific Filled shapes indicate wild-type elements. Specific site mutants are shown as empty shapes. Graph shown as fold heat induction. Letters denote statistical significance using ANOVA with Newman Keuls post-hoc, $p < 0.05$. Bars are mean + SEM from n=3, replicate experiments.

Figure 3.13

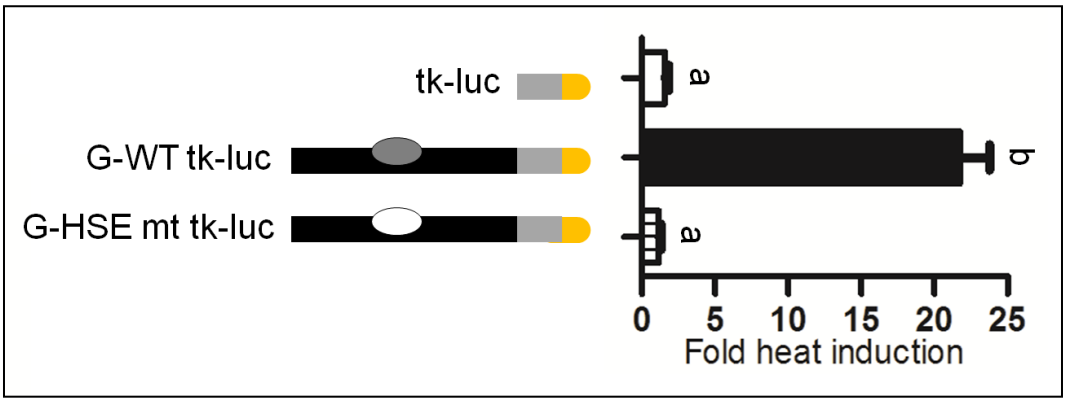

Figure 3.13. Characterization of the -284 bp HSE. HSE specific mutant within the fragment G-tk-luc construct. Graph shown as fold heat induction. Letters denote statistical significance using ANOVA with Newman Keuls post-hoc, $p < 0.05$. Bars are mean + SEM from n=3, replicate experiments.

Figure 3.14

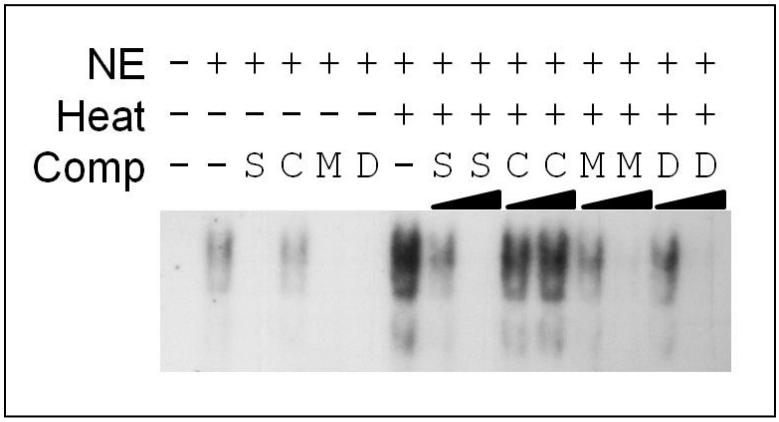

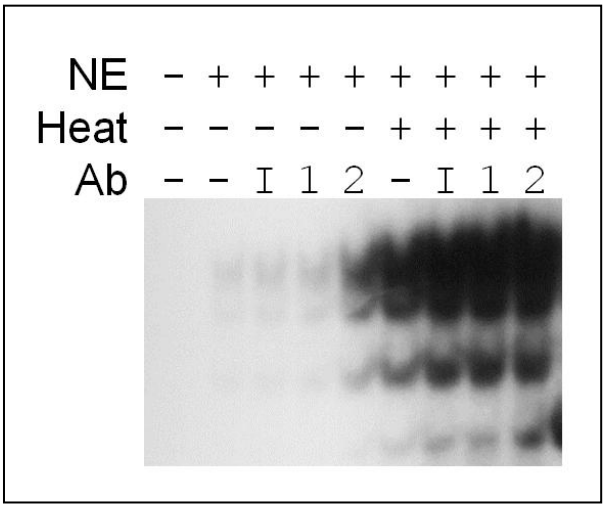

Figure 3.14. EMSA binding analysis of HaCaT HSF proteins to the -284 bp HSE. EMSA of HSPA6 HSE with HaCaT KC nuclear extracts incubated with unlabeled competitor oligomers. **d.** As in c with IgG, HSF1 or HSF2 specific antibodies. Antibodies include non-specific IgG (I), anti-HSF1 (1), or anti-HSF2 (2) . Non-radiolabeled competitor oligomers include self HSPA6 HSE site (S), consensus HSE (C), mutated HSE (M) or double mutated HSE (D) at 10 or 100-fold excess.

Figure 3.15

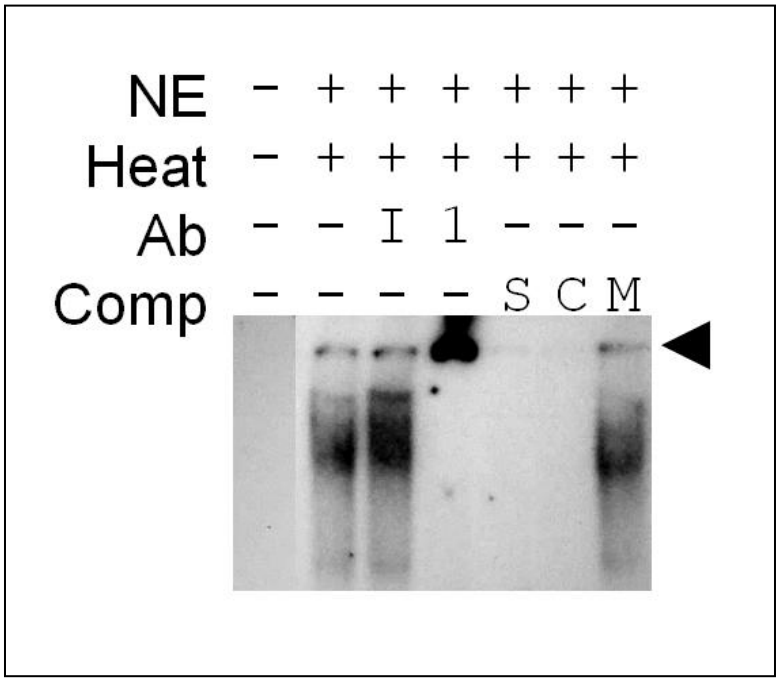

Figure 3.15. EMSA binding analysis of HaCaT HSF proteins to a consensus HSE. EMSA of consensus HSE with HaCaT KC nuclear extracts. Antibodies include non-specific IgG (I), anti-HSF1 (1), or anti-HSF2 (2). Non-radiolabeled competitor oligomers include self HSPA6 HSE site (S), consensus HSE (C) or mutated HSE (M) at 10 or 100-fold excess. Arrowhead denotes supershift.

Figure 3.16

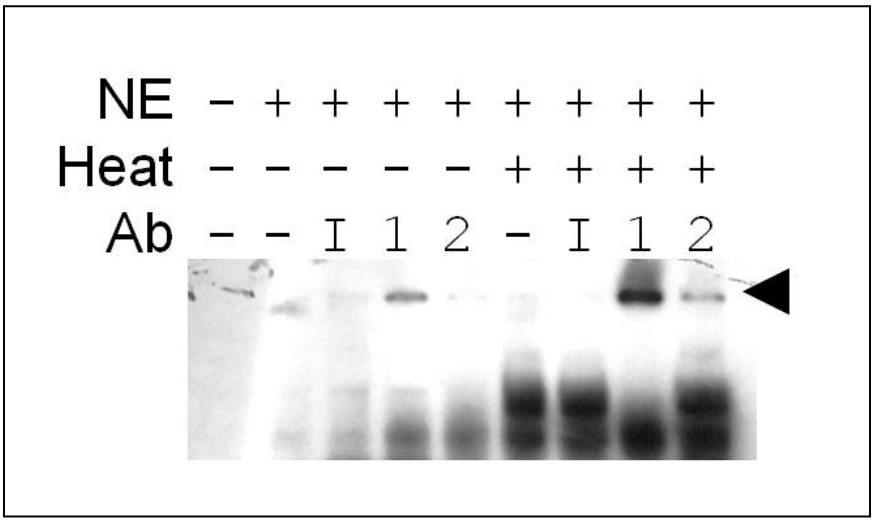

Figure 3.16. EMSA binding analysis of HeLa HSF proteins to the -284 bp HSE. EMSA of HSPA6 HSE with HeLa nuclear extracts. Antibodies include non-specific IgG (I), anti-HSF1 (1), or anti-HSF2 (2). Arrowheads denote supershift.

Figure 3.17

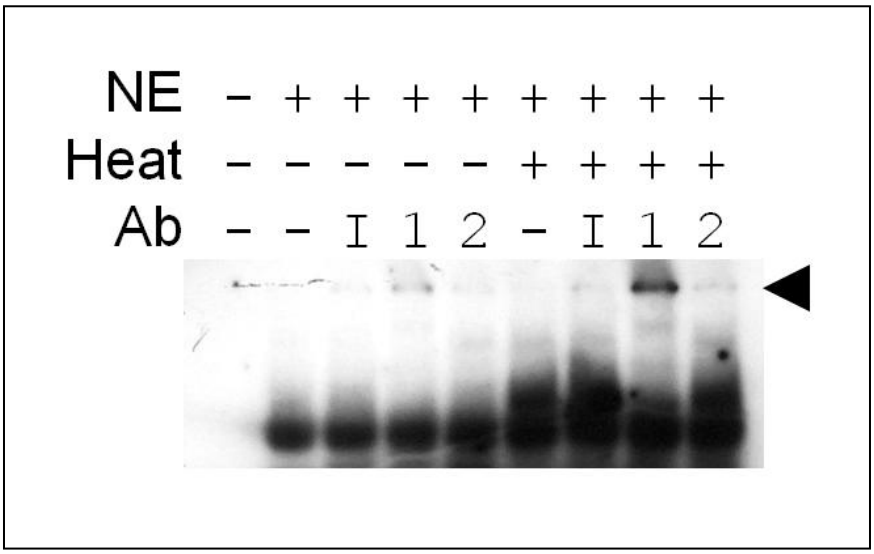

Figure 3.17. EMSA binding analysis of HeLa HSF proteins to a consensus HSE. EMSA of consensus HSE oligomer with HeLa nuclear extracts. Antibodies include non-specific IgG (I), anti-HSF1 (1), or anti-HSF2 (2). Arrowhead denotes supershift.

Discussion

Although discovered over 20 years ago *(112)*, HSPA6's role as a chaperone and stress-responding protein have only been recently studied *(79, 82, 105, 115)*. Relative to other members of its HSP70 family, little is known about HSPA6 transcriptional regulation in stressed and unstressed cells *(85, 86)*. Basal expression of HSPA6 was not detected in basal, unstressed cells using a range cell types; however highly stress inducible expression was noted with a wide range of expression *(82, 83, 116)*.

Using a previously characterized, highly specific HSPA6 antibody *(82)*, our studies were consistent with a recent report *(81)* demonstrating detectable but variable levels of constitutive HSPA6 protein and mRNA in all cell types examined. Basal expression of HSPA6 could be dependent on different cell growth conditions and may address the HSPA6 detection here but not in prior analysis of HaCaT KCs *(74)*. The majority of the cells grown in our lab (HaCaT, SCC13, MCF7, HeLa, HepG2 and dermal fibroblasts) are grown in a 3:1 ratio of DMEM:Ham's F12 or are grown in DMEM supplemented with non-essential amino acids (HT29 and Caco2). Modifying the ingredients of the cell culture media has led to increased expression of HSPs *(117, 118)*. Gomez-Sucerquia and colleagues used cell culture media supplemented with non-essential amino acids, which could contribute to the basal expression of HSPA6 *(81)*. In addition to the media composition, the cell density also affects the expression of HSPA6. Noonan and colleagues observed that HT-29 cells plated at a low cell density had increased expression of HSPA6 compared to cells cultured at a high cell

density *(83)*. Upon thermal stress, HaCaT KCs responded with induction of both HSPA1A and HSPA6, although the latter to many more fold at the mRNA level. Given its detection in non-stress conditions (*(81)* and our report), its capacity for significant fold induction *(82, 119)*, and its likely contribution to post-stress cell survival *(83)* we sought to better define control of its basal and stress-inducible expression in KCs, a cell type with wide dependence on chaperone function and likely to encounter diverse stress conditions. We found novel elements contributing to its basal expression and importantly an upstream HSE likely contributing to its maximal induction during a stress response.

An *in silico* promoter analysis indicated several candidate regulatory elements throughout the first several thousand base pair of the promoter guiding our cloning of a 3kb region (-2962 to +48 bp). Prior to our work, Wada and colleagues examined the contribution of an AP1 site and 2 HSEs within the proximal region (-287 to +110 bp) of the HSPA6 promoter to develop a reporter construct sensitive to cadmium chloride exposure *(84, 85)*. Taking advantage of longer promoter regions we isolated, we found that a region further upstream (-807 to -648 bp; here named fragment D) confers negative regulation and contributes to heat stress inducibility on HSPA6. The presence of repressive regions is consistent not only in the transfection results, but may also explain the reduced endogenous expression in several cell types, such as dermal fibroblasts and Caco2 cells. If these repressive factors are highly expressed in dermal fibroblasts and Caco2 cells, the expression of HSPA6 would be greatly reduced. Despite this region's overall limiting effect on promoter activity, we established a

novel HSE in this region (-807 to -648 bp) that contributes to the HSPA6 maximal stress inducibility. Furthermore, we observed that a region (-346 to -216 bp, fragment G) in our extended promoter, directly upstream of previously identified AP1 (-139 bp) and HSEs (-181 and -100 bp) sites, is crucial for the basal and heat inducibility of HSPA6 likely by its provision of an additional AP1 site and another HSE. To test the activating potential of this region, fragment G was fused to a (tk) promoter where it could confer stress responsiveness to this heterologous promoter but not raise its basal activity. Interesting, when the AP1 site was mutated in this fragment, basal activity was reduced suggesting that fragment G was a combination of both positive (like AP1) and negative elements (as yet to be identified) and that loss of AP1 favored the remaining negative control from this region. Nevertheless, given that under basal, unstressed conditions, this fragment G region can confer promoter activation in the context of the HSPA6 promoter, we sought to determine possible factors contributing to this region's basal and stress inducibility.

Within fragment G (-346 to -216 bp), six top-scoring transcription factor binding sites were predicted: WHN, HSE, HSE/MZF1, C/EBP, AP1 and ZFX. In unstressed conditions, site specific mutants within fragment G showed that an AP1 site at -240 bp contributes to the HSPA6 promoter activation. Surprisingly, our mutation analysis discovered two presumptive repressive elements, C/EBP and ZFX *(120, 121)*, within this region. Similar to the full HSPA6 3kb promoter, this shorter fragment also contains both positive and negative elements which contribute to the overall basal transcription of HSPA6. Consistent with this AP1

site contributing to the basal activation of HSPA6, we found that cFos, a typical subunit of the AP1 protein dimer, but not cJun binds the AP1 site within fragment G. We expect that since the AP1 heterodimer can be made from several subunits (cJun, junB, junC, Fra-1, Fra-2, cFos or fosB), the dominant AP1 dimer bound to the -240 AP1 binding site could be cFos and another subunit other than cJun. Results from the promoter mutation and EMSA analyses confirm that a new AP1 site within fragment G contributes to the basal and inducible expression of HSPA6. Other non-HSF proteins have also been recently shown to contribute control over basal and stress-induced HSP expression. Ataxin-3, possibly through DNA binding but more likely through its interaction with transcription factors, augments the full capacity of the HSP70 (HSPA1A) promoter to thermal and chemical stress *(122)*.

In addition to its basal regulation, we characterized the functional elements within -346 to -216 that contribute to its stress inducibility. The predicted HSE at -284 bp (gGGAg gAGCt aGAAc cTTCc) contains one imperfect site (site 1) and two perfect sites (sites 3 and 4). The HSE specific mutation of site 3 prevented the stress inducibility to a similar effect of the deletion of entire fragment G, indicating these nucleotides contribute to the only HSE in this region. Sites other than the HSE (WHN, HSE/MZF1 and AP1) also appear to contribute to the maximal heat induction of HSPA6. The HSE/MZF1 site is labeled as such due to the overlap between key nucleotides within these two sites. The mutations within MZF1 also affect HSE site 4. We believe that the decrease in stress inducibility due to the MZF1 mutation is due to the loss of a core HSE repeat.

Mutating the AP1 site, which plays a role in basal activation of HSPA6, also reduced the induction compared to the full length, wild type -647-luc. Similar to HSPA1A, multiple HSEs *(123)* and the elements conferring basal activation *(124)* of HSPA6 may be necessary to obtain the maximal stress inducibility. The HSE within fragment G may be working in concert with other factors to achieve the maximal stress inducibility of HSPA6. Our results show that this HSE is necessary for the stress inducibility within -346 to -216 bp region of the HSPA6 promoter.

The new HSPA6 HSE we demonstrated at -284 bp provided thermal responsiveness both in the context of the HSPA6 promoter and when transferred to the heterologous tk promoter. While this sequence was able to bind HaCaT KC stress-associated nuclear protein(s) in vitro, it was surprising that these binding factors were not recognized by either HSF1 or HSF2 antibodies. Intriguingly, when this site was used as a competitor for the ^{32}P-labeled consensus HSE, again with HaCaT KC nuclear extracts, it competed HSF1 from the consensus probe. To test the binding of our site to HSF, we performed the EMSA analysis using nuclear extracts from a different cell type, HeLa cells. Data from the HeLa EMSAs suggest our site binds HSF1 under unstressed and stressed conditions, and HSF2 primarily in stressed nuclear extracts. It is possible that a different HSF family member may bind this HSE, HSF4. This transcription factor can compete for HSF1 binding *(125)*, however expression of HSF4 has not been tested in KCs. Thus our site may bind one of these HSFs, or possibly a different stress-inducible factor. To date, HSF4's function and

expression have mainly been characterized in eye development, playing a role in the lens development *(126)*. Altogether, the results from the promoter reports and DNA-binding assays show our site as a functional HSE which can bind HSF1 and HSF2, but preferentially binds another, yet characterized stress inducible factor when presented with HaCaT KC nuclear proteins.

In the present study, we performed an analysis of HSPA6 promoter to search for core basal and inducible transcriptional elements, finding both positive and negative regulatory regions. Two factors, AP1 and HSF, contribute to the expression of HSPA6. AP1 regulates HSPA6 transcription under both unstressed and stressed conditions, whereas a HSF-like factor HSF contributes to the heat inducibility of HSPA6. In addition to characterizing these regions, our HSE EMSA results suggest an HSF-like factor from HaCaT KCs may preferentially bind the HSPA6 promoter warranting further investigation of this possibly novel factor.

Chapter 4

TNIP1-HSP Mechanism of Repression and Overall Keratinocyte Consequences

Abstract

The increased expression of TNFα-induced protein 3-interacting protein 1 (TNIP1), a repressor of transcription factor activation or activity, was shown to affect the cell stress response through a reduction in HSP expression. HSPs are not only important in protecting cells from the harmful effects of various stressors, they play key roles as molecular chaperones during basal, unstressed conditions. These results suggest TNIP1 could regulate the cell stress response. However, its exact role in this process and the mechanism of the TNIP1-mediated transcriptional repression is not yet characterized. We hypothesized that TNIP1 acts on PPAR, RAR or NF-kB, the TNIP1-repressed factors, to reduce the expression of HSPs. Using HSPA6 to model the repression on all HSPs, we observed TNIP1 does not act through these transcription factors. We further localized a ~150 bp region within the HSPA6 promoter and determined several predicted transcription factor binding sites, suggesting TNIP1 modulates HSP repression through a novel, yet uncharacterized pathway. Additionally, we assessed the effect of TNIP1 on keratinocyte proliferation and differentiation. We found that a chronic, but not acute, overexpression of TNIP1 blocks keratinocyte cell growth to possibly through decreasing the HSP chaperone function.

Introduction

The TNFα-induced protein 3 interacting protein 1 (TNIP1) is a regulator of various receptor-mediated signaling pathways, including those initiated by TNFα receptor TNFR *(28, 31, 88)* and nuclear receptors (NR) peroxisome proliferator activated receptors (PPAR) and retinoic acid receptors (RAR) *(23, 24)* (Fig 1.3 TNIP1 pathway figure). This repressive effect results in downstream or direct inhibition of transcription factor activation or activity. Typically, a resulting outcome of TNFR signaling is the activation of NFκB, a transcription factor involved in modulating the immune and stress responses. Through interactions with upstream signaling proteins, TNIP1 blocks the nuclear translocation of NFκB, therefore preventing the transcription of its target genes. In a separate mechanism, TNIP1 directly binds with NRs PPAR or RAR, but not their heterodimer parter retinoid X receptor (RXR), in presence of receptor agonist. Overall, TNIP1 can be thought of as a direct or indirect repressor of transcription factor activation or activity, possibly having an effect on cellular processes or diseases (for a recent review on TNIP1, refer to *(41)*).

A biological association with inflammatory diseases has also been determined for TNIP1 observed at the genetic, transcript, protein or expression levels. Through genome wide association scans, TNIP1 promoter and intronic single nucleotide polymorphisms (SNPs) were found in inflammatory diseases including but not limited to psoriasis, systemic lupus erythematosus and rheumatoid arthritis *(34, 38, 39, 87)*. Specific nucleotide or amino acid mutations were found at the mRNA and protein level *(43, 51)*. Furthermore, increased

TNIP1 levels were linked to psoriasis and rheumatoid arthritis *(33, 34)*. The altered expression of TNIP1 in these diseases could lead to aberrant signaling of these pathways. While TNIP1 has been associated to these pathways and diseases, the specific role and target genes affected by TNIP1 have yet been characterized.

To search for specific genes and possibly novel pathways affected by TNIP1, we overexpressed recombinant TNIP1 using an adenoviral construct in HaCaT KCs and performed a gene microarray (Figs 2.1 & 2.2). The results not only confirmed TNIP1's role in these pathways and biological functions, but discovered a novel TNIP1-regulated function: regulation of the cell stress response (Figs 2.3 & 2.4). Increased expression of TNIP1 in HaCaT keratinocytes (KC) repressed the expression levels of heat shock protein (HSP) mRNA and protein expression, specifically HSPA6 and HSPA1A by 20- and 3.3-fold, respectively (Figs 2.5 & 2.6). While best characterized for their role in preventing protein unfolding and aggregation during times of cellular stress *(71, 73, 78)*, expression of these proteins is crucial in unstressed conditions as well. They have chaperone functions in aiding proper folding of newly synthesized proteins and shuttling of many molecules.

Expression of both HSPA1A and HSPA6 is essential to increasing survival of cells exposed to increased temperatures or chemicals. Pharmacologic repression of HSPA1A expression in keratinocytes resulted in reduced resistance to UV treatment *(93)*. Furthermore, HSPA1A and HSPA6 specific siRNA-mediated knockdown suggest that expression of either HSPs are important to

increasing cell survival. A reduction of both HSPs led to a greater loss of thermotolerance, resulting in reduced cell viability *(79)*. Decreased expression of HSPA6 did reduce the cell viability after a 42°C heat stress or proteasome inhibitor MG-132 treatment, suggesting its importance in cell survival. HSPA6 likely forms complexes with HSPA1A and DNAJB1 (HSP40) *(82, 106)* to confer its protective function. Despite some HSPA6 and HSPA1A overlap in facilitating cell survival, further work showed they have distinct protein substrates. Compared to HSPA1A, HSPA6 has higher affinity for unfolded p53 but had no effect in refolding the luciferase enzyme and peroxisomal proteins *(77, 78)*.

In this chapter, we examined the potential mechanism for the TNIP1-mediated repression of HSPs. We chose HSPA6 because this gene was reduced 20-fold by increased TNIP1 compared to the 3.3-fold reduction of HSPA1A. We isolated and cloned the HSPA6 3 kb promoter to the pGL4.1 luciferase reporter gene construct. Surprisingly, our results indicate that TNIP1 does not repress HSPA6 through known TNIP1-mediated transcription factors, PPAR, RAR and NFκB. This suggests that a novel TNIP1-repressible pathway could inhibit HSP expression. Additionally, this work suggests chronic TNIP1 overexpression, but not acute, prevents the growth of cultured keratinocytes, suggesting TNIP1 may play a role in the keratinocyte proliferation and differentiation process.

Materials and Methods

Cell Culture

HaCaT KCs *(95)* were cultured in 37°C with 5% CO_2 humidified incubator in a 3:1 DMEM/F12 media containing 10% FBS (Thermo Scientific HyClone, Logan, UT), 100U/ml penicillin, and 100 mg/ml streptomycin. The cells were plated on 6- or 24-well plates at a density of 6.8 x 10^5 or 1.5 x 10^5 cells per well, respectively. Twenty-four hours after, cells were infected with an adenovirus construct expressing TNIP1 (Ad-TNIP1) or LacZ as a control (Ad-LacZ) at an multiplicity of infection (MOI) of 500 using Polybrene infection reagent (Millipore, Billerica, MA) *(96)*. Sixteen hours post-infection, the viral mixture was aspirated and media replaced. Twenty-four hours post-infection, cells were collected for total RNA using the RNeasy kit (Qiagen, Valencia, CA) or protein using RIPA lysis buffer (10 mM Tris, 150 mM NaCl, 1% deoxycholic acid, 1% Triton, 0.1% SDS), or were used for further stress assays.

Cells underwent thermal stress in a 42°C water bath for 1 hour; unstressed cells were immersed in a 37°C water bath for 1 hour (control). Cells were allowed various recovery times in a 37°C humidified incubator, as indicated.

Real-Time quantitative PCR analysis

Reverse transcription was performed using aliquots from the total RNA used for the microarray using the iScript reverse transcriptase (BioRad, Hercules, CA). Gene expression changes were analyzed using POWER SYBR green master mix (Life Technologies, Grand Island, NY). Real-time PCR was

performed using Applied Biosystems 7500 Fast Real-Time PCR system. Data analysis was carried out on ABI 7500 software using the ΔΔCT method. The primer sequences used and reaction conditions are listed on Table 2.1. All data was normalized to the ribosomal proten L13a (RPL13a) *(99)*.

Generation of luciferase constructs

The HSPA6 promoter containing the -2963 to +48 bp sequence (herein referred to as -3 kb-luc) was PCR amplified from human genomic DNA (cat# 636401) (BD Biosciences, San Jose, CA) using forward: 5'-GAT GGG TAC CTC ATC TTG AAT TCC CAC AAC ACA TGG-3' and reverse: 5'-GGC TGA AGC TTA GTG AGG CTC TCC CTG CGG TTT CTC T-3' with added *KpnI* and *HindIII* sites (underlined), respectively for insertion into the promoterless vector pGL4.10 (Promega, Madison, WI) using the restriction sites indicated. 5'-promoter truncations (-1230, -647 and -70 -luc) were performed by using the upstream *KpnI* site and native restriction enzyme sites *BglII*, *EcoRI* and *NruI*, respectively. Digested sites were blunted and ligated. Internal promoter deletions were performed using the Quikchange Lightning site-directed mutagenesis kit (Agilent). Constructs ΔE, ΔF, ΔG, and ΔH were generated using the -647 luc. Fragment G site specific mutants were generated using the Quikchange Lightning site-directed mutagenesis kit. Sites were determined using NHR Scan *(109)*, Nubiscan *(110)* and MatInspector *(111)* web-based software. All HSPA6 3kb isolate and truncation constructs were confirmed by sequencing (University of Connecticut Biotech Center).

Plasmid transfections

HaCaT KCs were plated to 70% confluency 24 hours prior to transfections using 24-well plates. Eight hours prior to transfection, media was replaced with 0.5 mL serum-containing 3:1 DMEM/F12 media. The appropriate HSPA6 promoter pGL4.10 plasmid (200 ng) and pCMV-β Galactosidase (100 ng) was transfected using Fugene6 (Promega) using 100 µL serum-free media. Twenty-four hours later, cells were stressed for 1 hour in a 42°C water bath (control cells in a 37°C bath) and returned to a 37°C incubator for 4 hours. Cells were then collected and assayed for the luciferase activity (Promega), protein concentration (Pierce), and β-galactosidase activity *(96)*.

Cell Survival Assay

Cell viability was determined using the MTS assay (Promega). HaCaT KCs were cultured in 24-well plates and adeno-infected as described previously. Twenty-four hours after infection, cells were stressed in a 42°C or 37°C water bath (control) for 1 hour.

HaCaT colony growth transient assay

HaCaT KCs were seeded in triplicate into 6-well plates (4,500 cells/well) and transfected the following day with Effectene (Qiagen; Valencia, CA). Each well received 300 ng pCMV-β-gal and either 216 ng of empty pcDNA3.1+ (Invitrogen; Carlsbad, CA) and 840 ng pBluescript KS^+ or 3000 ng pcDNA3.1+TNIP1 sense insert for at least a 20:1 molar difference of pcDNA3.1+

construct to β-gal marker plasmid to provide that any β-gal positive colony subsequently counted had derived from a pcDNA-transfected cell. Differences in pcDNA3.1+ expression vector amounts standardized copy number of expression constructs. Cells were fed 18hrs post-transfection and 3 days later. Seven days post-transfection cells were fixed in 2% paraformaldehyde and histochemically stained for β-gal. Counting protocols for b-gal positive cells, total cell number, and colony number were as described [Zhao JBC 276, p27907] for another NR-interacting protein.

Constitutive expression of TNIP1 in HaCaT cells

HaCaT KCs were seeded and transfected with either empty pcDNA3.1+ (Invitrogen; Carlsbad, CA) and 840 ng pBluescript KS^+ or 3000 ng pcDNA3.1+TNIP1 sense or antisense insert containing a neomycin resistant cassette at equal copy numbers. Forty-eight hours after transfection, all cultures were put under G418 neomycin selection (600 ug/mL) and was replaced during every cell feeding days. Cell growth was observed daily.

Statistical analysis

All data were analyzed using Prism Software version 5 (GraphPad) (La Jolla, CA). Student's t-test was used to compare between paired results. ANOVA with Newman Keuls *post hoc* was used to compare between grouped results, when necessary. Statistical significance was defined as $p \leq 0.05$.

Results

HSPA6 promoter contains known TNIP1-responsive transcription factor binding sites

Since TNIP1 expression results in the reduced activation or activity of various transcription factors, we assessed whether the mechanism of TNIP1's repression could be through these factors. As a model for the TNIP1-repression of these HSP familes, we further characterized one HSP, HSPA6. We isolated and cloned the promoter of HSPA6 3 kb promoter region (-2952 to +48 bp relative to the transcriptional start site) to a luciferase reporter gene construct. In silico promoter analysis found predicted binding sites for TNIP1-regulated transcription factors (Fig 4.1). Between the -647 to +48 bp promoter, no putative sites were located. Lengthening the promoter to -1230 bp, two predicted NFκB sites were found at -665, and -939 bp. Extending further to -2952 bp, two NFκB site (-2830 and -2985bp), two retinoic acid response elements (RARE) (-1625 and -2419 bp) and five peroxisome proliferator response elements (PPRE) (-1580, -1643, -1986, -2604 and -2768 bp).

TNIP1 does not repress HSPA6 through previously characterized pathways

To localize the TNIP1-responsive region, we generated several 5'-promoter truncations using naturally occurring restriction enzyme sites. Transfection results show that the "minimal" -70 bp promoter was unaffected by TNIP1. Extending the promoter to -647 bp resulted in a ~60% reduction in promoter activation. Further lengthening the promoter to -1230 and beyond had Figure 4.1

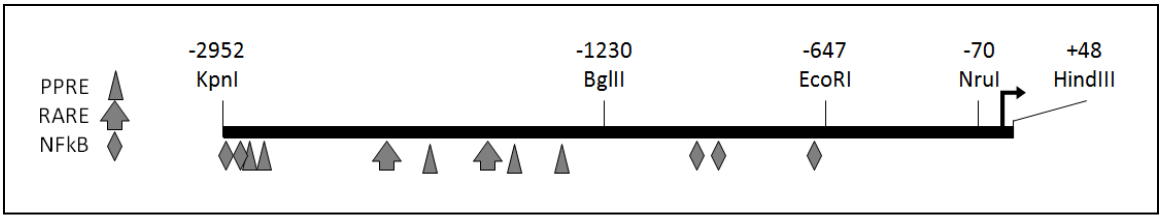

Figure 4.1. *In silico* analysis of the HSPA6 3 kb promoter searching for TNIP1-repressed transcription factors. The promoter isolate was from -2952 to +48 bp. KpnI and HindIII were generated using the primers to amplify the promoter. BglII, EcoRI and NruI are naturally occurring restriction enzyme sites and were use to generate promoter truncation constructs. The triangles, arrows and diamonds denote predicted PPRE, RARE and NFκB binding sites, respectively.

Figure 4.2

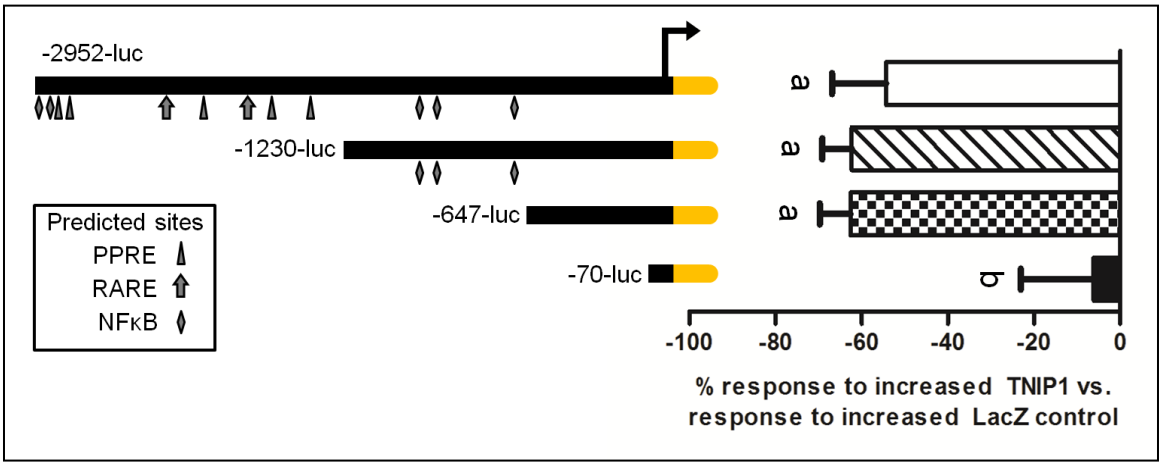

Figure 4.2. Analysis of the HSPA6 promoter truncation constructs. Diagram of the HSPA6 5' promoter truncation constructs. The triangles, arrows and diamonds denote predicted PPRE, RARE and NFκB binding sites, respectively. Yellow region indicates the start of the luciferase reporter gene. Graph shown as percent response to increased TNIP1 compared to LacZ control. Letters denote statistical significance between unstressed cells $p<0.05$. using ANOVA with Newman Keul's post-hoc. Bars are mean + SEM from n=3, experimental triplicates.

no change in TNIP1 repression compared to the -647 bp promoter, suggesting the -647 to -70 bp fragment of the HSPA6 promoter contains a TNIP1-repressible element (Fig 4.2).

The TNIP1-repressive region within the HSPA6 promoter is between -216 to -70 bp

To narrow down the fragment repressed by TNIP1 within -647 to -70 bp, a series of internal promoter deletions was generated deleting ~150 bp regions within the -647-luc construct. Four internal deletion constructs were generated: ΔA- (-647 to -478 bp), ΔB- (-478 to -346 bp), ΔC- (-346 to -216 bp) and ΔD-luc (-216 to -70 bp). Only deletion of fragment D (-216 to -70 bp) resulted in significant increases in promoter activation (~330%) (Fig 4.3), suggesting TNIP1 sensitive regions are within this fragment. Deletion of fragments A, B and C had no significant changes in HSPA6 promoter activation. *In silico* promoter analysis of region D (Table 4.2, respectively) showed 6 predicted transcription factor binding sites, respectively. More importantly, this region contain no known TNIP1-repressible transcription factors, indicating that TNIP1 may repress HSPs through a novel, possibly not yet characterized TNIP1-repressible factor.

HSPA6 and HSPA1A expression is repressed by TNIP1 in heat stressed conditions

Since we found that TNIP1 represses HSPA6 in unstressed conditions, we tested whether TNIP1 can repress the levels of HSPA6 under heat-stressed conditions. We extended our analysis to determine whether HSPA1A is also

affected by TNIP1 in stressed conditions. In the control, Ad-LacZ infected cells, the stress-induction pattern was similar for both HSPs, however, HSPA6 had a greater fold induction. As expected, TNIP1 overexpression reduced basal (t=0) expression of both HSPs. The repression under stressed conditions was different for HSPA6 and HSPA1A. HSPA6 expression was decreased immediately after cell stress and up to 8 hours post heat shock (Fig 4.4, top panel). Interestingly, at each timepoint tested, the expression of HSPA6 was ~10-fold less in TNIP1 overexpressed cells compared to the control infected cells; however, the pattern of stress induction and decrease to basal levels was similar, regardless of TNIP1 overexpression. HSPA1A did not show TNIP1-responsiveness after heat stress (Fig 4.4, bottom panel). The differential regulation of these two HSPs could suggest a different mechanism for TNIP1 repression. Although TNIP1 represses HSPs in basal, unstressed conditions, its control over these HSPs varies under stressed conditions.

TNIP1 does not affect cell survival following a short term overexpression

To assess the consequence of reduced HSPA6 in stressed conditions in response to increased TNIP1, we assessed whether the cell survival of HaCaT KCs are compromised after thermal stress. In a similar timeline, TNIP1 or control LacZ was increased 24 hours prior to thermal stress, modeling a “short-term” overexpression. Adeno-infected cells were heat stressed for 1 hour at 42°C, then given a 23 hour recovery period at 37°C; unstressed cells were incubated for 1 hour at 42°C then given the same recovery conditions. Using the MTS assay to

determine the cell viability, we observed that under these conditions increased TNIP1 expression had no effect on both unstressed and heat-stressed KCs (Fig 4.5).

Long term increased TNIP1 expression hinders cell growth

To determine the effects of altered TNIP1 levels past 24 hours, we examined the effect of TNIP1 7-days post overexpression. Using a method different than the adenovirus, we transiently co-transfected single cell HaCaT keratinocytes with a limiting amount of a β-gal construct as indicator of transfection and either an empty vector or one containing the TNIP1 cDNA insert. Keratinocytes transfected with TNIP1 yielded more small colonies and fewer large colonies compared to those receiving the control vector (Fig 4.6). This overall growth reduction is reflected in a significant decrease of the median cells per colony for TNIP1 transfected cells (TNIP1, 15/colony; empty vector, 21/colony).

To address consequences stemming from chronic altered TNIP1 levels, we attempted to generate a HaCaT keratinocyte line stably over-expressing TNIP1. Control neo^r clones were successfully generated from transfection with the empty and TNIP1 antisense vector 14-days later. However, HaCaT keratinocytes transfected with the TNIP1 cDNA insert did not yield any lines. These “long-term” assays demonstrate a negative TNIP1 effect on colony expansion and suggest why the long-term growth required for cell line generation may not have been possible from TNIP1 over-expressing cells.

Figure 4.3

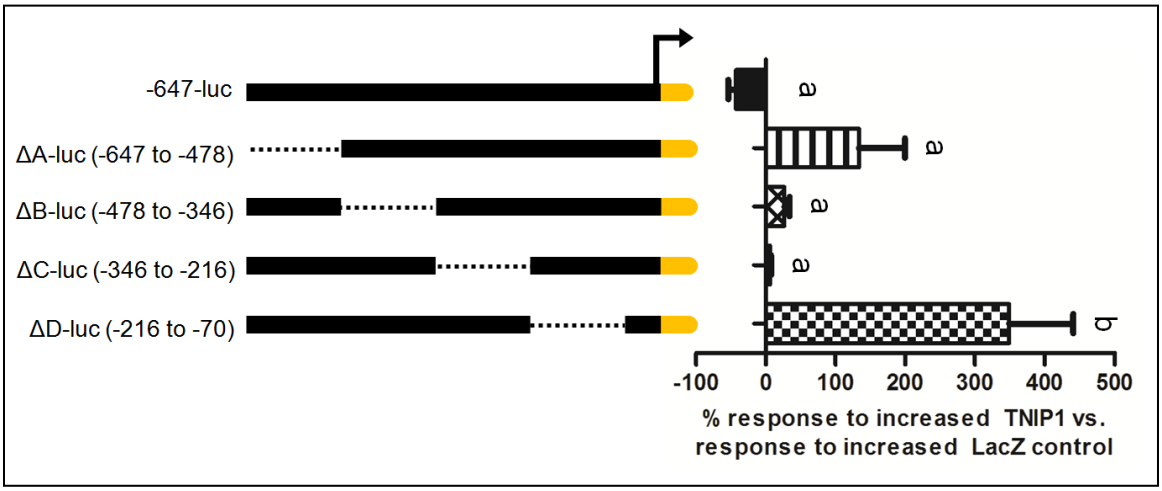

Figure 4.3. Analysis of the HSPA6 promoter deletion constructs. Diagram of the HSPA6 internal promoter deletions within -647-luc construct. Deletions are shown as the dotted line. Graph shown as percent response to increased TNIP1 compared to LacZ control. Letters denote statistical significance between unstressed cells $p<0.05$. using ANOVA with Newman Keul's post-hoc. Bars are mean + SEM from n=3, experimental triplicates.

Table 4.1. List of predicted transcription factor binding sites within the -216 to -70 bp region of the HSPA6 promoter.

TF Binding Site	**Location**	**Score**
p53 tumor suppressor	-200	0.933
Heat shock factors	-171	0.97
Estrogen response elements	-160	0.924
RNA polymerase II transcription factor II B	-154	1
ZF5 POZ domain zinc finger	-152	0.92
E-box binding factors	-144	0.935
AP1, Activating protein 1	-135	1
MAF and AP1 related factors	-134	0.961
GC-Box factors SP1/GC	-124	0.924
EGR/nerve growth factor induced protein C & related factors	-123	0.93
Pleomorphic adenoma gene	-108	0.935
GC-Box factors SP1/GC	-101	0.931
Heat shock factors	-89	0.905
Mouse Krueppel like factor	-71	0.986

Figure 4.4

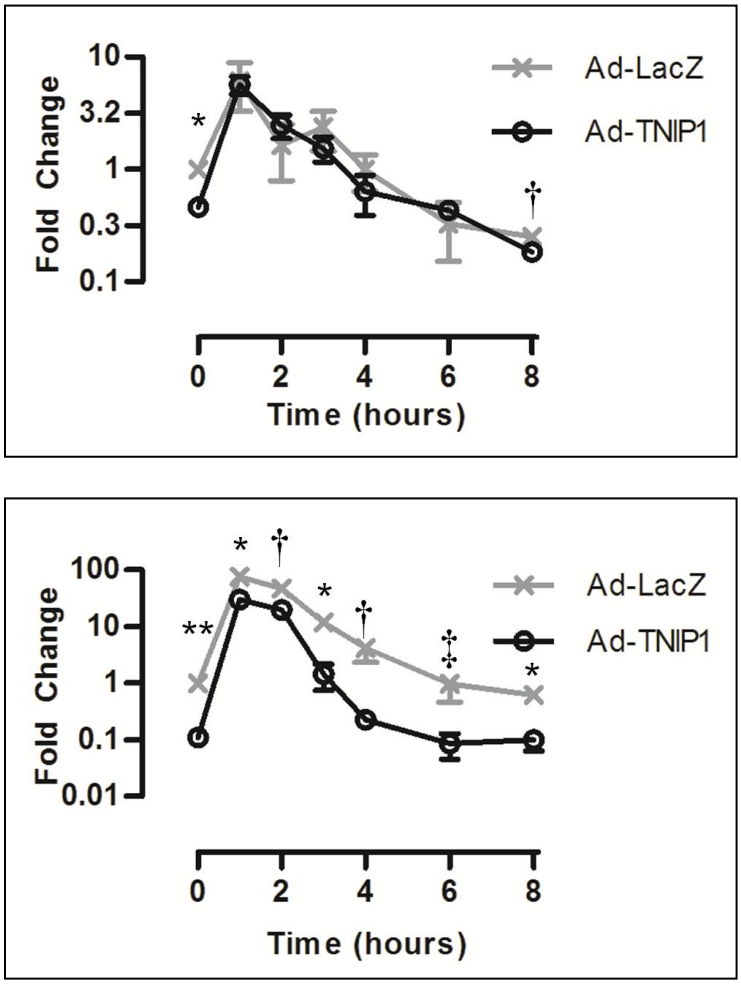

Figure 4.4. Effect of TNIP1 overexpression on HSPs in heat stressed HaCaT KCs. Quantitative PCR of HSPA1A (top panel) and HSPA6 (bottom panel) before (t = 0 hour) or after (t = 1, 2, 3, 4, 6 and 8 hours) a 1 hour heat stress at 42°C. Statistical significance was determined using Student's t-test, LacZ vs. TNIP1: **=p<0.01; *=p<0.05; †=p<0.1; ‡=p<0.15. Bars are mean + SEM from experimental triplicates.

Figure 4.5

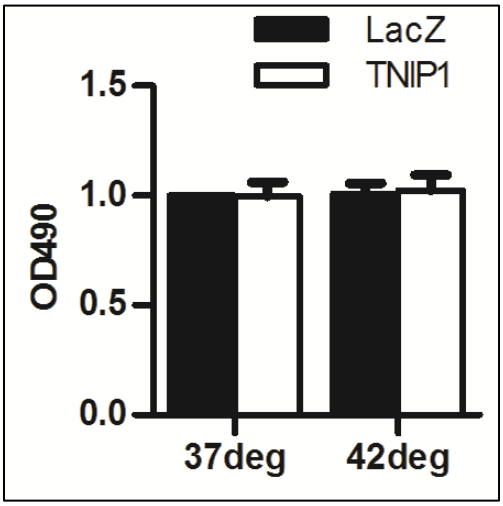

Figure 4.5. Effect of "short term" increased TNIP1 levels on HaCaT KCs viability and growth. Cell viability analysis of HaCaTs overexpressing LacZ (control) or TNIP1 using an adenoviral vector. Cell viability was assessed using the MTS assay after a 1 hour heat shock at 42°C, then given a 23 hour recovery period at 37°C.

Figure 4.6

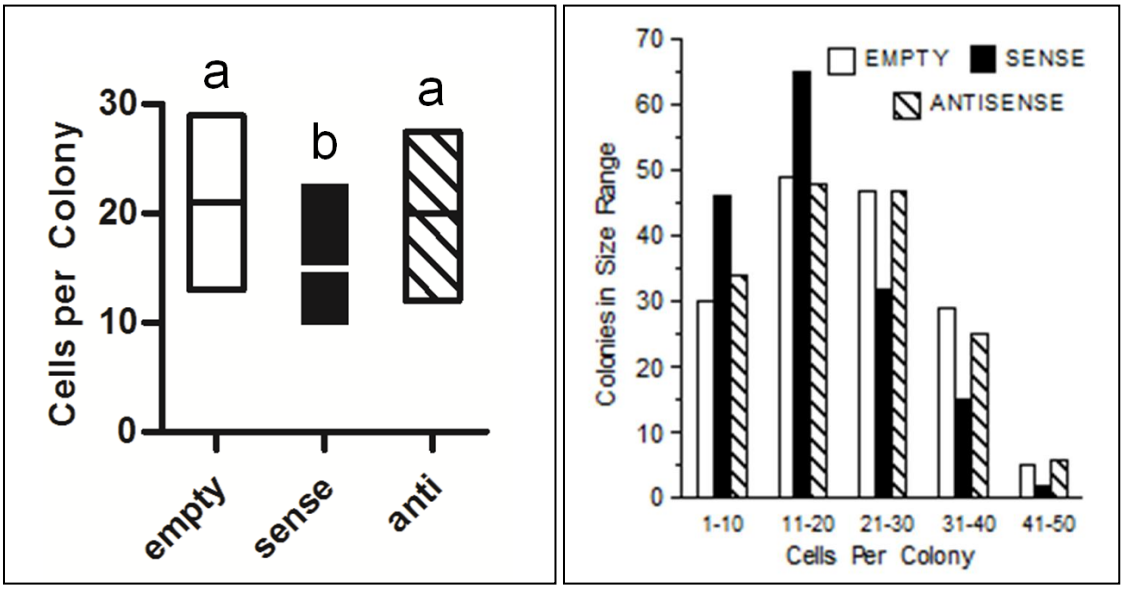

Figure 4.6. Effect of "long term" increased TNIP1 levels on HaCaT KCs viability and growth. (Left panel) Long term effect of increased sense TNIP1, or control empty vector or antisense TNIP1. Cells per colony were determined 7 days after TNIP1 overexpression. The box-plot bottom and top edges border the 25th to 75th percentile, respectively, of colony sizes for each construct; the horizontal line across box is at the 50th percentile, the colony median (not the mean). Colony sizes for Naf transfection are significantly depressed (*, $p<0.05$, Student's t-test) compared to empty vector controls. (Right panel) Size comparison of early HaCaT keratinocyte colonies developed following single-cell transfection with a β-gal marker and empty expression vector (open bars) or expression vector with Naf sense cDNA (solid bars).

Discussion

As observed from results presented in Chapter 2, TNIP1 overexpression in HaCaT KCs resulted in reduced expression of several HSP family members, including HSPA1A and HSPA6. While TNIP1's repressive roles in the TNFR and NR pathways have been elucidated, these pathways have not been known to result in the transcriptional regulation of HSPs. Using HSPA6 as a model for other TNIP1-regulated HSP repression, several putative NFκB binding sites, PPREs and RAREs were located between the -2952 to -647 bp fragment of the HSPA6 promoter. We determined the TNIP1-sensitive region within the promoter between -647 to -478 bp and -216 to -70 bp, suggesting the TNFR and NR pathways do not play a role in regulating these HSPs. This region lacked any known TNIP1-repressed transcription factors even after extending our search to include Elk2 *(89)* and C/EBP *(68)*, the known TNIP1-inhibited downstream targets of EGFR and TLR, respectively. These results suggest that the TNIP1-mediated repression of HSPA6, and likely other HSPs, could be through a novel, not yet determined TNIP1-repressible transcription factor.

To test the TNIP1-repression of HSPA6 under heat stressed conditions, we observed TNIP1 could reduce HSPA6 heat inducibility in addition to its basal expression. These results could suggest the mechanism of TNIP1's repression, while not yet fully characterized, could be independent of the thermal stress induction. Interestingly, HSPA1A expression was only decreased in unstressed conditions. The differential repression of HSPA6 and HSPA1A may suggest that TNIP1 regulates these HSPs through different mechanisms under stressed and

unstressed conditions. However, a possible mechanism could be that the TNIP1-repressible transcription factor binds a site next to a heat shock element. When HSF is activated, it could displace the TNIP1-repressible transcription factor binding the promoter, facilitating the HSF binding the HSE. A similar effect is observed in the Ga_{i2} promoter, where SP1 binding is disrupted by activation of C/EBP binding an adjacent site *(127)*. Determining any predicted binding site(s) near a heat shock element within HSPA1A and matching it with the predicted site(s) within the -216 to -70 bp promoter region of HSPA6 could be an avenue to determine the specific mechanism of the TNIP1-mediated HSP repression.

Since HSPA6 is affected under both unstressed and stressed conditions, we tested whether repression of this HSP can affect the cell survival of HaCaT cells after a 1 hour, 42°C heat shock. The short term cell viability was not affected by increased TNIP1 in basal or stressed conditions, suggesting that under these conditions, TNIP1 has no overall effect on KC's stress response. Under stressed conditions, however, TNIP1 only reduced HSPA6 expression, not HSPA1A, directly after thermal stress and up to an 8 hour time period. Since these proteins have similar functions in cell protection, it is possible that the redundancy in function between these two HSPs is sufficient to protect HaCaT KCs under heat stressed conditions 24 hours post TNIP1 overexpression. The effect of increased TNIP1 may affect the HSPs chaperone function, since multiple HSPs are decreased. We assessed whether a long term TNIP1 overexpression could affect the KCs growth under basal conditions. Transient overexpression of TNIP1 resulted in a reduction in cell number per colony after 7-

days. Stably overexpressing TNIP1 resulted in no colony growth after 2 weeks. The decrease in HSP expression levels could have led to the increase in KC cell death. Prior work where the HSPA1A gene was deleted in a mouse model shows a change in tissue physiology and function in unstressed cells *(128)*, indicating its importance not only in stress protection, but as a molecular chaperone. The decrease of various HSPs by TNIP1 could affect the normal structure and proliferation of keratinocytes, possibly resulting in the observed decrease in cell growth. Taken together, these results suggest that the chronic overexposure to TNIP1 negatively affects cell growth under basal, unstressed conditions. The decreased levels of HSPs and the resulting reduced chaperone ability may impair these cells to properly synthesize new proteins required for cell growth and proliferation.

In this chapter, we found that the TNIP1-mediated repression of HSPA6 is not through known TNIP1-repressed transcription factors, but likely a novel, not yet characterized mechanism. Additionally, the effect of TNIP1 on HSPs varies in heat stressed conditions, where only HSPA6, not HSPA1A, expression was reduced. The overall cell consequences of increased TNIP1 were observed in a chronic overexpression of TNIP1, resulting in decreased KC growth and proliferation.

Chapter 5

Summary, conclusions and future directions

Summary and conclusions

Initial work on the TNFα-induced protein 3 (TNFAIP3)-interacting protein 1 (TNIP1) started in our laboratory while searching for novel NR coregulators in the skin. Previous efforts characterized TNIP1's role as an agonist-bound NR corepressor, specifically of PPAR and RARs *(24, 25)*, and determined TNIP1's transcriptional regulation and start sites (see Appendix 1 for TSS results) *(44, 129)*. Researchers from other laboratories found TNIP1 to reduce the activation and nuclear translocation of several transcription factors, including NF-kB (see *(41)* for a current review). Overall, the resulting effect of TNIP1 can be generalized as the direct or indirect repression of transcription factor activity or activation.

These factors and their associated pathways, in part, regulate several biological processes, including inflammatory diseases and KC growth. Indeed, TNIP1 has been implicated in several diseases, including psoriasis, a disease characterized by KC hyperproliferation and incomplete differentiation *(34, 52)*. Altered TNIP1 sequence and increased expression levels were observed in this disease, suggesting it may play a role in regulating KC function. Although TNIP1's transcriptional regulation, repressive role in several pathways, and association in various biological processes have been established, the specific genes regulated by TNIP1 and the overall cellular outcomes of increased TNIP1 expression have not yet been determined.

The work in this thesis aimed to determine the genes and pathways regulated by TNIP1 as well as characterize the consequences of transient increased expression of TNIP1 in KCs. The studies described validated TNIP1's role in regulating the NR pathways, inflammatory diseases, and cell death. Several novel TNIP1-regulated pathways and genes were also found, including the cell stress response and repression of several HSPs. Proteins within this family, which have been implicated in psoriasis and cell death, were reduced as much as 20-fold in response to increased TNIP1. The reduced expression of these HSPs in the HaCaT KCs, which are an immortalized, but non-tumorigenic KC cell line, was validated by using normal human epidermal KCs. Interestingly, in addition to reducing HSP expression in differentiated KCs, TNIP1 overexpression in the normal human epidermal KCs resulted in blocking the induction of involucrin, a KC differentiation marker, indicating that TNIP1 could modulate KC differentiation.

To examine TNIP1's effect on cultured KCs, we assessed the overall the growth of KCs following increased TNIP1 levels. TNIP1 had no effect on cell growth in normal or heat stressed conditions 24 hours after transient overexpression; long term (7 day) transient overexpression of TNIP1 led to decreased cell colony size and number. Attempting to generate a chronic, stably overexpressing TNIP1 KC line resulted in complete loss of cell growth, suggesting that TNIP1 may play key roles in KC biology, possibly through repression of HSP chaperone expression.

HSPA6 was used as a model to determine the possible mechanism of how TNIP1 reduces HSP expression. HSPA6 was the gene reduced the most after TNIP1 overexpression. We hypothesized that the TNIP1-mediated repression was through the known, well characterized TNIP1-repressed transcription factors PPAR, RAR or NF-kB. While several predicted binding sites were found within the -3 kb promoter, the specific region responsive to TNIP1 (-216 to -70 bp) lacked these predicted binding sites. In addition to these transcription factors, two others have been described to be repressed by TNIP1 through upstream regulatory proteins, Elk-2 and C/EBP. Unfortunately, this promoter region also lacks predicted binding sites for these factors. A possible pathway involved in the HSP repression could be the EGFR-ERK2 pathway. The repression of Elk-2 by TNIP1 is mediated by blocking EGFR-induced ERK2 nuclear translocation. *In silico* promoter analysis of the -216 to -70 bp region suggests some of the top predicted sites could be ERK2 activated, such as EGR1, KLF and E-box binding transcription factors. However, these sites and their associated transcription factors are not known regulators HSPs expression. An in depth analysis to examine if these factors regulate HSPA6 could be assessed for future experiments.

A second possibility is that TNIP1 may reduce the expression of the transcription factor(s) regulating the transcription of HSPA6. Searching the list of predicted transcription factor sites within this fragment (Table 4.2), four genes encoding transcription factors whose expression was reduced by TNIP1 overexpression were found. AP1 heterodimer protein subunits (fosB, c-fos and c-

jun) and early growth response 1 (EGR1) mRNA expression was decreased. It is unlikely that AP1 is involved in the TNIP1 repression because a separate region of the promoter, which is also contains an AP1 site, is not responsive to TNIP1. It is possible that EGR1 protein expression is reduced after TNIP1 overexpression, causing a reduction in HSPA6 transcription. This presupposes that EGR1 transcriptionally regulates the expression of HSPs, which has not yet been characterized.

To determine if an ERK2-mediated transcription factor (EGR1, KLF or E-box binding transcription factors) repressed by TNIP1 could be contributing to the reduced HSP expression, an extensive examination would need to be done to (1) establish if ERK2 activation results in increased endogenous HSP expression, (2) determine whether ERK2 stimulation can activate the -216 to -70 bp promoter region of HSPA6, (3) test if these factors bind the promoter, and (4) characterize if TNIP1 can repress this factor. Since the aims of this research were to determine the pathways affected by and cellular outcomes due to increased TNIP1, the work presented in this thesis met this goal.

Along with Gomez-Sucerquia *(81)*, a novel finding from this research was the observation that HSPA6 protein was readily found in unstressed all cell types examined (Ramirez et al submitted), whereas other laboratories noted little to no basal expression in varying cell types including HaCaT KCs *(74, 82, 83, 112, 115, 130, 131)*. The antibody (ADI-SPA-754) used was previously characterized by *(82)* to be highly specific to HSPA6, suggesting that the band observed was HSPA6. A possible explanation for this discrepancy could be the DMEM/F12

media used to grow the cells. The media used to culture all the cells contains a 3:1 ratio of DMEM to Ham's F12 (HaCaT, SCC13, MCF7, HeLa, HepG2 and dermal fibroblasts) or were supplemented with non-essential amino acids (HT29 and Caco2). Modifying the ingredients of the cell culture media has led to increased expression of HSPs *(117, 118)*. Additionally, *(81)* supplemented the culture media with non-essential amino acids. HSPA6 protein expression was observed in untreated cells. The basal expression of HSPA6 could be sensitive not only to changes in cell density *(83)*, but also cell culture media components. The additional supplement to our HaCaT media could explain the difference in basal HSPA6 expression level compared to *(74)*.

Future directions

The studies described in this thesis open up a number of possibilities in characterizing the role TNIP1 plays not only in regulating HSPs, but in normal and diseased KC biology. With respect to the TNIP1-mediated repression of HSPs, this work suggests TNIP1 could alter the chaperone function, but not the immediate stress-protective role, of HSPs. Interestingly, the reduction in KC cell growth was only observed in long-term TNIP1 overexpression. It would be interesting to examine the expression levels of these HSPs after chronic TNIP1 exposure to assess whether the reduced levels of HSPs could contribute to the reduced cell viability.

Further work to elucidate the mechanism of the HSP repression by TNIP1 is necessary. To date, the work described examined whether transcription factors PPAR, RAR or NF-kB were involved in the repression of HSPs. Our work indicates that these factors were not responsible for the reduced expression of HSPs. This may suggest a new factor, and possibly pathway, is repressed by TNIP1 to block the transcription of these genes. While a TNIP1-responsive fragment within the HSPA6 promoter was localized, the specific element within it was not determined. Site-directed mutagenesis of the top-scoring sites could be done to elucidate the specific transcription factor involved in the repression of HSPA6 and possibly other HSPs. In addition to the TNIP1-mediated repression of HSPA6, putative transcription factor binding sites and a ~150 bp region within the central region of the promoter was responsive to a yet uncharacterized repressive factor(s) in normal, basal conditions. Further investigation is needed

to determine the factor(s) contributing to the reduced expression of HSPA6 in unstressed conditions.

While the association between TNIP1 and KCs proliferation and differentiation was characterized in this research, the specific role it could play in inflammatory diseases, such as psoriasis, has not yet been determined. In the TNIP1 microarray, expression of a number of inflammatory cytokines was reduced; most notably IL-6 was decreased 10-fold. This result was only determined at one timepoint, 24 hours post TNIP1 overexpression. To determine TNIP1's role in regulating these cytokines, a time-course study examining the varied expression level of these, and other proteins, is necessary. Studying the changes of these genes' expression could determine a mechanism for how TNIP1 affects these diseases.

A shortcoming to the research presented here was most the work presented was performed in cultured normal or immortalized monolayer of KCs. While these cell lines retain the differentiation properties, they are still not stratified KCs such as found in skin. A possible avenue for research to mimic the stratification of KCs into layers is to generate a KC organotypic model *(132)*. These organotypic cultures recapitulate the biochemical markers of differentiating KCs resulting in cornification of the cultured cells. In these cultures, TNIP1 expression can be increased and the thickness of the organotypic layer quantified. In this approach, a direct effect of KC proliferation and differentiation can be examined in a manner where the level of TNIP1 overexpression could be controlled. More importantly, the effect of increasing TNIP1 could be assessed in

a “dose-dependent” fashion. Conversely, to assess the impact of TNIP1 in whole animal models, an adenoviral gene transfer can be performed in normal mice *(65, 66)*. Although this method was previously performed by the Beyaert laboratory to exogenously express TNIP1, the effect on KC homeostasis was not assessed.

Appendix 1

TNIP1 protein expression up to 96 hours post adeno-infection

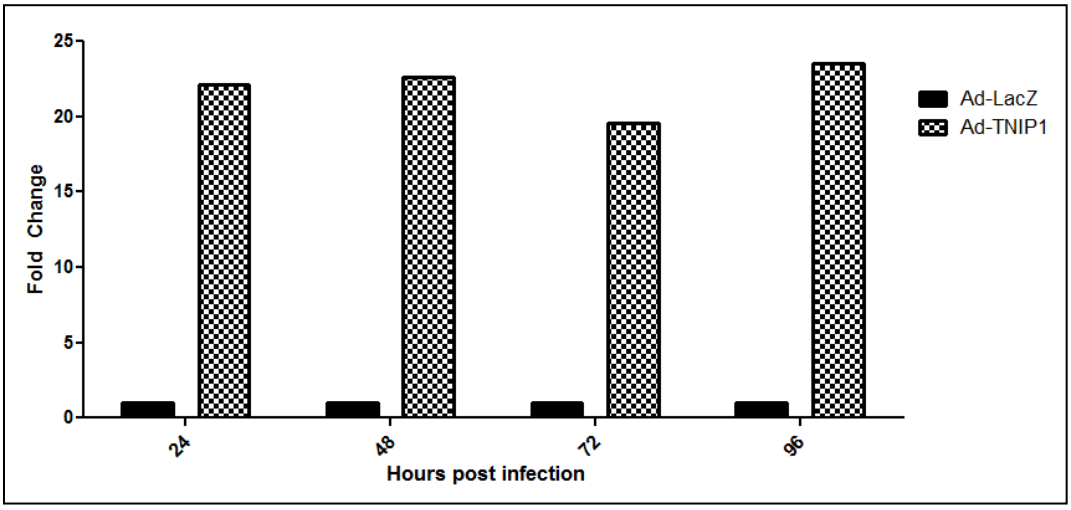

This experiment was performed by Carmen Zhang (experiment # 158) before the microarray was performed. TNIP1 -overexpressed HaCaT cells were collected at 24-, 48-, 72-, or 96-hours post infection. TNIP1 expression was increased up to the 96-hour timepoint.

APPENDIX 2

Microarray data from TNIP1 overexpression in HaCaT KCs

SYMBOL	ratio t/w	ILMN_GENE	DEFINITION
HSPA6	0.05	HSPA6	Homo sapiens heat shock 70kDa protein 6 (HSP70B') (HSPA6), mRNA.
IL6	0.1	IL6	Homo sapiens interleukin 6 (interferon, beta 2) (IL6), mRNA.
FOSB	0.12	FOSB	Homo sapiens FBJ murine osteosarcoma viral oncogene homolog B (FOSB), mRNA.
ZC3HAV1	0.16	ZC3HAV1	Homo sapiens zinc finger CCCH-type, antiviral 1 (ZC3HAV1), transcript variant 2, mRNA.
EGR1	0.18	EGR1	Homo sapiens early growth response 1 (EGR1), mRNA.
DNAJB1	0.2	DNAJB1	Homo sapiens DnaJ (Hsp40) homolog, subfamily B, member 1 (DNAJB1), mRNA.
LOC652878	0.2	LOC652878	PREDICTED: Homo sapiens similar to heat shock 70kDa protein 6 (HSP70B) (LOC652878), mRNA.
ARID5B	0.21	ARID5B	Homo sapiens AT rich interactive domain 5B (MRF1-like) (ARID5B), mRNA.
HERC5	0.23	HERC5	Homo sapiens hect domain and RLD 5 (HERC5), mRNA.
MX1	0.24	MX1	Homo sapiens myxovirus (influenza virus) resistance 1, interferon-inducible protein p78 (mouse) (MX1), mRNA.
ISG20	0.25	ISG20	Homo sapiens interferon stimulated exonuclease gene 20kDa (ISG20), mRNA.
ACTR10	0.26	ACTR10	Homo sapiens actin-related protein 10 homolog (S. cerevisiae) (ACTR10), mRNA.
MYH3	0.26	MYH3	Homo sapiens myosin, heavy polypeptide 3, skeletal muscle, embryonic (MYH3), mRNA.
IFI27	0.27	IFI27	Homo sapiens interferon, alpha-inducible protein 27 (IFI27), mRNA.
AXUD1	0.28	AXUD1	Homo sapiens AXIN1 up-regulated 1 (AXUD1), mRNA.
DUSP1	0.28	DUSP1	Homo sapiens dual specificity phosphatase 1 (DUSP1), mRNA.
IFIT2	0.28	IFIT2	Homo sapiens interferon-induced protein with tetratricopeptide repeats 2 (IFIT2), mRNA.
SGK	0.28	SGK	Homo sapiens serum/glucocorticoid regulated kinase (SGK), mRNA.

	0.28	HS.579631	AGENCOURT_10229596 NIH_MGC_141 Homo sapiens cDNA clone IMAGE:6563923 5, mRNA sequence
CYR61	0.29	CYR61	Homo sapiens cysteine-rich, angiogenic inducer, 61 (CYR61), mRNA.
CLCF1	0.3	CLCF1	Homo sapiens cardiotrophin-like cytokine factor 1 (CLCF1), mRNA.
IFIT3	0.3	IFIT3	Homo sapiens interferon-induced protein with tetratricopeptide repeats 3 (IFIT3), mRNA.
FLJ31875	0.31	FLJ31875	Homo sapiens hypothetical protein FLJ31875 (FLJ31875), mRNA.
HSPA1B	0.31	HSPA1B	Homo sapiens heat shock 70kDa protein 1B (HSPA1B), mRNA.
JUN	0.31	JUN	Homo sapiens jun oncogene (JUN), mRNA.
OASL	0.31	OASL	Homo sapiens 2'-5'-oligoadenylate synthetase-like (OASL), transcript variant 1, mRNA.
PPP1R15A	0.31	PPP1R15A	Homo sapiens protein phosphatase 1, regulatory (inhibitor) subunit 15A (PPP1R15A), mRNA.
ARID3B	0.32	ARID3B	Homo sapiens AT rich interactive domain 3B (BRIGHT- like) (ARID3B), mRNA.
CPEB3	0.33	CPEB3	Homo sapiens cytoplasmic polyadenylation element binding protein 3 (CPEB3), mRNA.
FOS	0.33	FOS	Homo sapiens v-fos FBJ murine osteosarcoma viral oncogene homolog (FOS), mRNA.
HSPA1A	0.33	HSPA1A	Homo sapiens heat shock 70kDa protein 1A (HSPA1A), mRNA.
MX2	0.33	MX2	Homo sapiens myxovirus (influenza virus) resistance 2 (mouse) (MX2), mRNA.
TRIB1	0.33	TRIB1	Homo sapiens tribbles homolog 1 (Drosophila) (TRIB1), mRNA.
ZFP36	0.33	ZFP36	Homo sapiens zinc finger protein 36, C3H type, homolog (mouse) (ZFP36), mRNA.
USP36	0.34	USP36	Homo sapiens ubiquitin specific peptidase 36 (USP36), mRNA.
DUSP5	0.35	DUSP5	Homo sapiens dual specificity phosphatase 5 (DUSP5), mRNA.
ERRFI1	0.35	ERRFI1	Homo sapiens ERBB receptor feedback inhibitor 1 (ERRFI1), mRNA.
IFIT1	0.35	IFIT1	Homo sapiens interferon-induced protein with tetratricopeptide repeats 1 (IFIT1), transcript variant 2, mRNA.
EDN1	0.36	EDN1	Homo sapiens endothelin 1 (EDN1), mRNA.

G1P3	0.36	G1P3	Homo sapiens interferon, alpha-inducible protein (clone IFI-6-16) (G1P3), transcript variant 1, mRNA.
RARRES3	0.36	RARRES3	Homo sapiens retinoic acid receptor responder (tazarotene induced) 3 (RARRES3), mRNA.
RGC32	0.36	RGC32	Homo sapiens response gene to complement 32 (RGC32), mRNA.
BCL3	0.37	BCL3	Homo sapiens B-cell CLL/lymphoma 3 (BCL3), mRNA.
HERC6	0.37	HERC6	Homo sapiens hect domain and RLD 6 (HERC6), transcript variant 4, mRNA.
IFIH1	0.37	IFIH1	Homo sapiens interferon induced with helicase C domain 1 (IFIH1), mRNA.
PIM1	0.37	PIM1	Homo sapiens pim-1 oncogene (PIM1), mRNA.
WARS	0.37	WARS	Homo sapiens tryptophanyl-tRNA synthetase (WARS), transcript variant 1, mRNA.
ABTB2	0.38	ABTB2	Homo sapiens ankyrin repeat and BTB (POZ) domain containing 2 (ABTB2), mRNA.
PTGS2	0.38	PTGS2	Homo sapiens prostaglandin-endoperoxide synthase 2 (prostaglandin G/H synthase and cyclooxygenase) (PTGS2), mRNA.
	0.38	HS.263832	BX096516 Soares_NhHMPu_S1 Homo sapiens cDNA clone IMAGp998J135216, mRNA sequence
BHLHB2	0.39	BHLHB2	Homo sapiens basic helix-loop-helix domain containing, class B, 2 (BHLHB2), mRNA.
ISG15	0.39	ISG15	Homo sapiens ISG15 ubiquitin-like modifier (ISG15), mRNA.
OAS2	0.39	OAS2	Homo sapiens 2'-5'-oligoadenylate synthetase 2, 69/71kDa (OAS2), transcript variant 3, mRNA.
RN7SK	0.39	RN7SK	Homo sapiens RNA, 7SK, nuclear (RN7SK) on chromosome 6.
ATF3	0.4	ATF3	Homo sapiens activating transcription factor 3 (ATF3), transcript variant 4, mRNA.
CTGF	0.4	CTGF	Homo sapiens connective tissue growth factor (CTGF), mRNA.
ELF3	0.4	ELF3	Homo sapiens E74-like factor 3 (ets domain transcription factor, epithelial-specific) (ELF3), mRNA.
HMFN0839	0.4	HMFN0839	Homo sapiens lung cancer metastasis-associated protein (MAG1), mRNA.
MIDN	0.4	MIDN	Homo sapiens midnolin (MIDN), mRNA.

PRICKLE1	0.4	PRICKLE1	Homo sapiens prickle homolog 1 (Drosophila) (PRICKLE1), mRNA.
STX3A	0.4	STX3A	Homo sapiens syntaxin 3 (STX3), mRNA.
TMEM2	0.4	TMEM2	Homo sapiens transmembrane protein 2 (TMEM2), mRNA.
CITED2	0.41	CITED2	Homo sapiens Cbp/p300-interacting transactivator, with Glu/Asp-rich carboxy-terminal domain, 2 (CITED2), mRNA.
LATS2	0.41	LATS2	Homo sapiens LATS, large tumor suppressor, homolog 2 (Drosophila) (LATS2), mRNA.
UGCG	0.41	UGCG	Homo sapiens UDP-glucose ceramide glucosyltransferase (UGCG), mRNA.
	0.41	HS.543887	AGENCOURT_14535501 NIH_MGC_191 Homo sapiens cDNA clone IMAGE:30415823 5, mRNA sequence
BAG3	0.42	BAG3	Homo sapiens BCL2-associated athanogene 3 (BAG3), mRNA.
CCL5	0.42	CCL5	Homo sapiens chemokine (C-C motif) ligand 5 (CCL5), mRNA.
SP110	0.42	SP110	Homo sapiens SP110 nuclear body protein (SP110), transcript variant c, mRNA.
XAF1	0.42	XAF1	Homo sapiens XIAP associated factor-1 (XAF1), transcript variant 2, mRNA.
CD55	0.43	CD55	Homo sapiens CD55 molecule, decay accelerating factor for complement (Cromer blood group) (CD55), mRNA.
DCUN1D3	0.43	DCUN1D3	Homo sapiens DCN1, defective in cullin neddylation 1, domain containing 3 (S. cerevisiae) (DCUN1D3), mRNA.
EPSTI1	0.43	EPSTI1	Homo sapiens epithelial stromal interaction 1 (breast) (EPSTI1), transcript variant 2, mRNA.
FOXO3A	0.43	FOXO3A	Homo sapiens forkhead box O3A (FOXO3A), transcript variant 2, mRNA.
GLTSCR1	0.43	GLTSCR1	Homo sapiens glioma tumor suppressor candidate region gene 1 (GLTSCR1), mRNA.
LGP2	0.43	LGP2	Homo sapiens likely ortholog of mouse D11lgp2 (LGP2), mRNA.
LOC387841	0.43	LOC387841	PREDICTED: Homo sapiens similar to ribosomal protein L13a, transcript variant 2 (LOC387841), mRNA.
CCRN4L	0.44	CCRN4L	Homo sapiens CCR4 carbon catabolite repression 4-like (S. cerevisiae) (CCRN4L), mRNA.

FHL2	0.44	FHL2	Homo sapiens four and a half LIM domains 2 (FHL2), transcript variant 1, mRNA.
IFI6	0.44	IFI6	Homo sapiens interferon, alpha-inducible protein 6 (IFI6), transcript variant 2, mRNA.
PARP14	0.44	PARP14	Homo sapiens poly (ADP-ribose) polymerase family, member 14 (PARP14), mRNA.
BCL6	0.45	BCL6	Homo sapiens B-cell CLL/lymphoma 6 (zinc finger protein 51) (BCL6), transcript variant 2, mRNA.
BTG1	0.45	BTG1	Homo sapiens B-cell translocation gene 1, anti-proliferative (BTG1), mRNA.
DKK4	0.45	DKK4	Homo sapiens dickkopf homolog 4 (Xenopus laevis) (DKK4), mRNA.
FOXA1	0.45	FOXA1	Homo sapiens forkhead box A1 (FOXA1), mRNA.
IFITM1	0.45	IFITM1	Homo sapiens interferon induced transmembrane protein 1 (9-27) (IFITM1), mRNA.
RAB30	0.45	RAB30	Homo sapiens RAB30, member RAS oncogene family (RAB30), mRNA.
SAMD9L	0.45	SAMD9L	Homo sapiens sterile alpha motif domain containing 9-like (SAMD9L), mRNA.
TXNRD1	0.45	TXNRD1	Homo sapiens thioredoxin reductase 1 (TXNRD1), transcript variant 4, mRNA.
YTHDC1	0.45	YTHDC1	Homo sapiens YTH domain containing 1 (YTHDC1), transcript variant 1, mRNA.
C6orf128	0.46	C6ORF128	Homo sapiens chromosome 6 open reading frame 128 (C6orf128), mRNA.
IFI44	0.46	IFI44	Homo sapiens interferon-induced protein 44 (IFI44), mRNA.
IL29	0.46	IL29	Homo sapiens interleukin 29 (interferon, lambda 1) (IL29), mRNA.
PRKCH	0.46	PRKCH	Homo sapiens protein kinase C, eta (PRKCH), mRNA.
STX11	0.46	STX11	Homo sapiens syntaxin 11 (STX11), mRNA.
TRIM26	0.46	TRIM26	Homo sapiens tripartite motif-containing 26 (TRIM26), mRNA.
DUSP19	0.47	DUSP19	Homo sapiens dual specificity phosphatase 19 (DUSP19), mRNA.
FAM46A	0.47	FAM46A	Homo sapiens family with sequence similarity 46, member A (FAM46A), mRNA.
IRF7	0.47	IRF7	Homo sapiens interferon regulatory factor 7 (IRF7), transcript variant d, mRNA.

KLF6	0.47	KLF6	Homo sapiens Kruppel-like factor 6 (KLF6), transcript variant 2, mRNA.
S100A2	0.47	S100A2	Homo sapiens S100 calcium binding protein A2 (S100A2), mRNA.
TMEM27	0.47	TMEM27	Homo sapiens transmembrane protein 27 (TMEM27), mRNA.
TSC22D1	0.47	TSC22D1	Homo sapiens TSC22 domain family, member 1 (TSC22D1), transcript variant 1, mRNA.
ZNF342	0.47	ZNF342	Homo sapiens zinc finger protein 342 (ZNF342), mRNA.
ADM	0.48	ADM	Homo sapiens adrenomedullin (ADM), mRNA.
ANTXR2	0.48	ANTXR2	Homo sapiens anthrax toxin receptor 2 (ANTXR2), mRNA.
CCNL1	0.48	CCNL1	Homo sapiens cyclin L1 (CCNL1), mRNA.
EFNB2	0.48	EFNB2	Homo sapiens ephrin-B2 (EFNB2), mRNA.
GPRC5A	0.48	GPRC5A	Homo sapiens G protein-coupled receptor, family C, group 5, member A (GPRC5A), mRNA.
HS3ST2	0.48	HS3ST2	Homo sapiens heparan sulfate (glucosamine) 3-O-sulfotransferase 2 (HS3ST2), mRNA.
MAF	0.48	MAF	Homo sapiens v-maf musculoaponeurotic fibrosarcoma oncogene homolog (avian) (MAF), transcript variant 1, mRNA.
SPEN	0.48	SPEN	Homo sapiens spen homolog, transcriptional regulator (Drosophila) (SPEN), mRNA.
	0.48	HS.572444	Homo sapiens cDNA: FLJ21679 fis, clone COL09221
AHR	0.49	AHR	Homo sapiens aryl hydrocarbon receptor (AHR), mRNA.
C18orf8	0.49	C18ORF8	Homo sapiens chromosome 18 open reading frame 8 (C18orf8), mRNA.
CPEB2	0.49	CPEB2	PREDICTED: Homo sapiens cytoplasmic polyadenylation element binding protein 2, transcript variant 2 (CPEB2), mRNA.
DDX58	0.49	DDX58	Homo sapiens DEAD (Asp-Glu-Ala-Asp) box polypeptide 58 (DDX58), mRNA.
EIF2C2	0.49	EIF2C2	Homo sapiens eukaryotic translation initiation factor 2C, 2 (EIF2C2), mRNA.
F2RL1	0.49	F2RL1	Homo sapiens coagulation factor II (thrombin) receptor-like 1 (F2RL1), mRNA.
IFITM2	0.49	IFITM2	Homo sapiens interferon induced transmembrane protein 2 (1-8D) (IFITM2), mRNA.
LDLR	0.49	LDLR	Homo sapiens low density lipoprotein receptor

			(familial hypercholesterolemia) (LDLR), mRNA.
PLEKHC1	0.49	PLEKHC1	Homo sapiens pleckstrin homology domain containing, family C (with FERM domain) member 1 (PLEKHC1), mRNA.
RNMT	0.49	RNMT	Homo sapiens RNA (guanine-7-) methyltransferase (RNMT), mRNA.
SP100	0.49	SP100	Homo sapiens SP100 nuclear antigen (SP100), transcript variant 1, mRNA.
TRIM21	0.49	TRIM21	Homo sapiens tripartite motif-containing 21 (TRIM21), mRNA.
C15orf39	0.5	C15ORF39	Homo sapiens chromosome 15 open reading frame 39 (C15orf39), mRNA.
C1orf77	0.5	C1ORF77	Homo sapiens chromosome 1 open reading frame 77 (C1orf77), mRNA.
CDKN1A	0.5	CDKN1A	Homo sapiens cyclin-dependent kinase inhibitor 1A (p21, Cip1) (CDKN1A), transcript variant 2, mRNA.
DDIT3	0.5	DDIT3	Homo sapiens DNA-damage-inducible transcript 3 (DDIT3), mRNA.
DNAJA1	0.5	DNAJA1	Homo sapiens DnaJ (Hsp40) homolog, subfamily A, member 1 (DNAJA1), mRNA.
FBXO32	0.5	FBXO32	Homo sapiens F-box protein 32 (FBXO32), transcript variant 2, mRNA.
IRS2	0.5	IRS2	Homo sapiens insulin receptor substrate 2 (IRS2), mRNA.
NFKBIA	0.5	NFKBIA	Homo sapiens nuclear factor of kappa light polypeptide gene enhancer in B-cells inhibitor, alpha (NFKBIA), mRNA.
PARP12	0.5	PARP12	Homo sapiens poly (ADP-ribose) polymerase family, member 12 (PARP12), mRNA.
	0.5	HS.495542	PREDICTED: Homo sapiens hypothetical gene supported by BC027323 (LOC441477), mRNA
LTB4R2	2.04	LTB4R2	Homo sapiens leukotriene B4 receptor 2 (LTB4R2), mRNA.
RNASE7	2.07	RNASE7	Homo sapiens ribonuclease, RNase A family, 7 (RNASE7), mRNA.
UAP1L1	2.14	UAP1L1	Homo sapiens UDP-N-acteylglucosamine pyrophosphorylase 1-like 1 (UAP1L1), mRNA.
MAPK13	5.63	MAPK13	Homo sapiens mitogen-activated protein kinase 13 (MAPK13), mRNA.

Appendix 3

Protocol for making pGL4.1 HSPA6 <u>5' truncation</u> constructs

- The HSPA6 -2962 to +48 (herein called 3kb) promoter fragment was PCR'ed from human genomic placental DNA (BD Biosciences cat# 636401)
- PCR primers sequences
  - Forward: gatg***<u>CTCGAG</u>***tttggctgtgtccccacccgaatatca (KpnI underlined)
  - Reverse: GGCTG***<u>AAGCTT</u>***CTTGTCGGATGCTGGA (HindIII underlined)
- PCR conditions using Roche High Fidelity PCR master kit
  - 94°C for 3 minutes
  - 94°C for 30 seconds
  - 62°C for 30 seconds
  - 68°C for 3.5 minutes
  - 68°C for 5 minutes

  } 32x
- HSPA6 3kb promoter was inserted using KpnI and HindIII sites into the pGL4.10 vector.
- To generate HSPA6 5'-truncation constructs, pGL4.1 HSPA6 3kb construct was digested with KpnI (left) and a second restriction site (BglII for -1230; EcoRI for -647; NruI for -70) to remove the upstream DNA fragments. DNA was blunt ended, gel extracted, and ligated.
- HSPA6 3kb sequence restriction enzyme sites

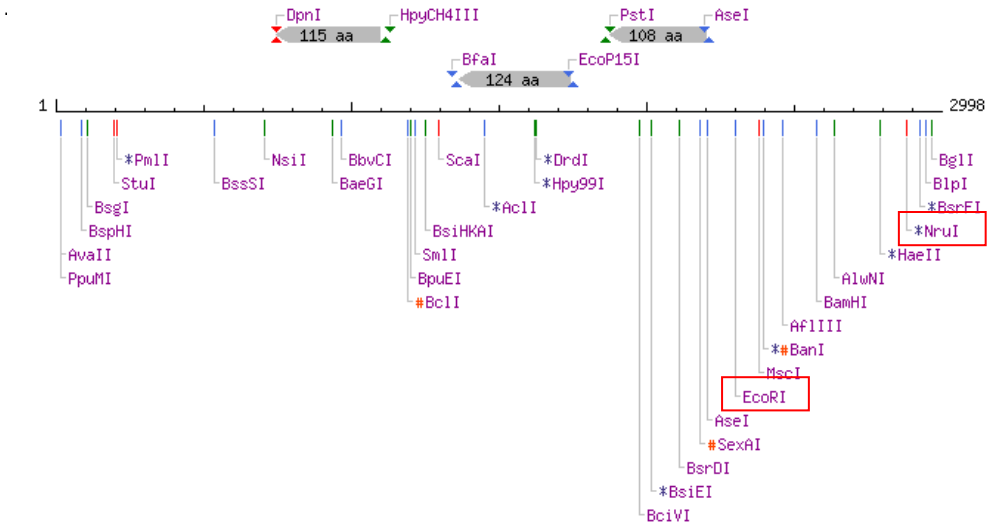
DpnI
HpyCH4III
115 aa
PstI
AseI
108 aa
BfaI
EcoP15I
124 aa
1
2998
*PmlI
StuI
BsgI
BspHI
AvaII
PpuMI
NsiI
BssSI
BbvCI
BaeGI
ScaI
*DrdI
*Hpy99I
*AclI
BsiHKAI
SmlI
BpuEI
#BclI
BglI
BlpI
*BsrFI
*NruI
*HaeII
AlwNI
BamHI
AflIII
*#BanI
MscI
EcoRI
AseI
#SexAI
BsrDI
*BsiEI
BciVI

2 sites only

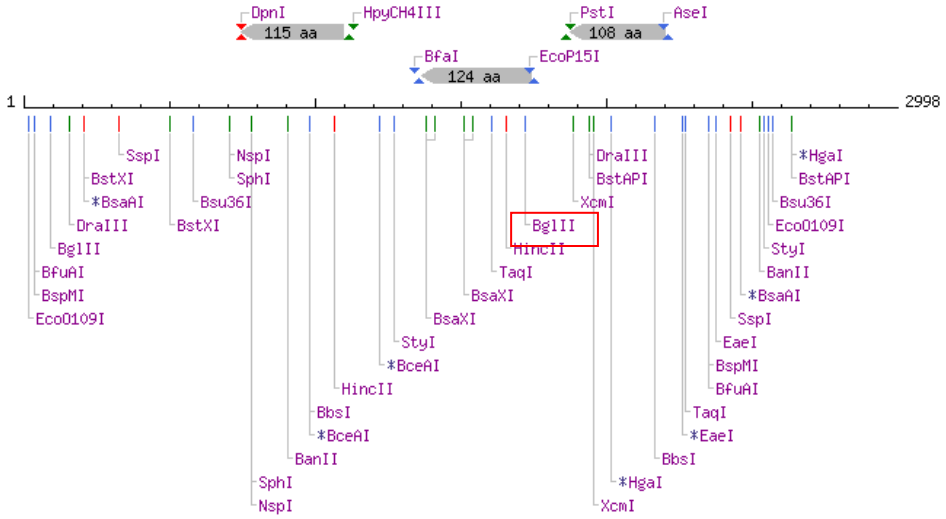
DpnI
HpyCH4III
115 aa
PstI
AseI
108 aa
BfaI
EcoP15I
124 aa
1
2998
SspI
BstXI
*BsaAI
DraIII
BglII
BfuAI
BspMI
Eco0109I
NspI
SphI
Bsu36I
BstXI
BglII
HincII
TaqI
BsaXI
StyI
*BceAI
HincII
BbsI
*BceAI
BanII
SphI
NspI
DraIII
BstAPI
XcmI
*HgaI
XcmI
BbsI
TaqI
*EaeI
BspMI
BfuAI
EaeI
SspI
*BsaAI
BanII
StyI
Eco0109I
Bsu36I
BstAPI
*HgaI

Biotech center sequenced HSPA6 promoter (-2962 to +48)

- -2962 (introduced KpnI site) to -1231 bp
  - TCATCTTGAATTCCCACAACACATGGGAGGGACCCAGTGGAAGGTAACTGA
    ATCATGGGGCAGGTCTTTCCCATGCTGTTCTTGTGATAGTGAATAAGTCTCA
    TGAGATCTGATGGTTTTAAAAAGGGGAGTTTCCCTGCACAAGCTCTCTCTTC
    TCTTGTTTGCCACCATGTGAGACATGACTTTCACCTTTTGCCATGATTGTGA
    GGCCTCCCAGCCACGTGGAACTGTAAGTCCATTAAACCTCTTTCTTTTGTAA
    ATTGCCCCGTCTCAGGTATGTCTTTATTAGCAGTGTGAGAATGGGCTAACAC
    ATACAACTTGCTTTTTTTTTGTACTCAATATTGAGTCGTGAGCTTTGCACCAC
    ATTAGAATGTCTATTTAAGTCATTACTTTAAGGTCGGTTCTATTTTTAAAGCTA
    CTCAAACTAAGCTACTAAACATAAGTGGATATATTTAAGTGTATGTATAAAAT
    TTATACTAGGCCAGCTGCAGTGGCTCATGCCTGTAATCCCAAAGCTGTGGA
    AGGTAGAGGTGGGACTGATTGAGGCCACGAGTTCAAGGCTGCAGTGAGCT
    GTGATTGCATCACTGTACTCCAGCCTGAGGGACAGAGCAGGAACCAGAAAA
    AAATAAAATAAAAAGAAACAAACAAAAAAACCCCCAACAACCCTACAGTGGC
    TCTTTTAGAAAAAACAAACAAACAAAACCAAAACTGTACTGCATGCATAAGCT
    CCCCTATGCTATGTTTGAACCACTCTGAAGAGATCAATTAAAAAGAAGTGAG
    TGATATTGGAAGCATGCCTCTGTGATGCTGTGGTAACATTCATAGGCTGCGT
    TAGGGCTATGCCTGTAACTCTTGGAGATGAGTGGGTAAGTGGGGTTTTGAG
    GTGGCTGGGGGCTGGAAGAGAAGGTTGGAGGAGCCCACACAAGACAGCC
    CCTTAACACGCCGGGGCACAGAACCCCAGGCTGGGCCAACTTTTCCCTGCT
    GAGGTGAAGACCCGTCTCTTGCAGGCCGTTGGCAAATGTCTTGACTCTGGC
    ATCCAGGTGTGACCAGCTTAGACCCTGAGAGTGAGTGAATTTAAAGTTGAC
    AGCTTCTTTCCCTTTTGGAATTATGAAATAGGTTACTTCTTTTCAAGGACAGT
    TTGATTTTCCACTGTGTAAGTCATATATTGCACATTTCTTTAAACATTCCCTTT
    TTTCCTGAACTGATCACCTTACCAGTACGGCTGATCCTCTCAAGCAGCAAAC
    TCTACCAGCTGTCACTGGTGCTCTCGGAGAGACGATTAACCAAGGAACCCA
    GCCCGGGAACAGTACTGACCTCTACTTCTGGACTCCTGCCTCCCTCTTAAAA
    AGTCCCTTGAACTTCCTAGTGGGTTCTAACCTGTCAAAGGAGAAAATAGCCA
    TCTATGGAGTAAGGGTTTTTAGTTTCTCTTTTTACAAATGGAAGTTTCCTCTG
    AATCAGGCAAGTAACGTTAAATAGAAGCCAACTTTTAAGTTTCTCTAACACAC
    TGCTAAATTGTAACACCAGACTGTACCACATACTCTCCAGCTGCCAGCTATT
    GCAGTTGCCATCCTTGTTACTATAGTGGTGAGTATCTCTGCCTGTCATGCGT
    GAGAGAGGGGGTCGATTCCCCGACGGGGAGGTCACGGGAAATTGTGTGAG
    GATTTTGTCAACCTTCAGAAGTCTCAGAAATGTCTCCTTGTTTTGGCTTTCAG
    CGGAAATCCGAACGCCAGCA

- -1230 (Existing BglII site) to -648 bp
  - GATCTGAATGGAATGTTCTGGATTGAAGAAAGTGGGAAATGGCCTCAATTCA
    CAAAGTCACAACCTGATAAAAACCAGTGTGACTTTACTGCCCAGTGAACCCA
    TCTCGTCCTCCAGCCTTTAGGAGGTAGGTTGGACTGGAGCCTGCAGTAGTT
    TACTCTCCACCTGAGTCCTGGTCTCCAGCTGGGAACCCACTTAGGCCATA**G**
    AGAAAAACGCACACTGTGCCTCTCCACCGGGCCTCTGGAGACGAGGCTCC
    TCGGGGATACAAACAGTGGGGAGAACATGAGGGACATCCCGACCGTACTC
    TGCGTCCTCCTTTCCCAGGTGTTGCGTTCTCTCTTGGGCTGAGTGGCGAGG
    TCTCTCCCGAGTCCCAGGGCCACAGTGCAATGTCACATCTCCTTTGTGGAA
    AGTGACTGGTAAAGGAGAGAGAACAAAACTGGAGGAA**C**GTAAAGTCTTCAG
    CCACCTGGTTTAATTTATTCAAGAGTGATTAATCCTAGATGAGAAAAAGAATT
    GAAATGGATCGGAAAAAAATGAAAGTGCATTGGCCGGGAATCGAACCCGGG
    CCTCCCGCGTGGCAGGCGAG

- -647 (Existing EcoRI site) to -71 bp
  - AATTCTACCACTGAACCACCAATGCTACTGTCAGCTAAAGACCTGCAGTATT
    GTCTCTTAAAGCTCACTATCTCTGGCCATTC**G**CTAAGGAACCAGGCACCGTC
    TTAAATCGCGGTTTGGAAAATATTTTGTTCAAGATAAAACTGTTTTAAGATAT

ACGTGTATATATCTTATATATCTGTATTCGCATGGTAACATATCTTCGGCCTT
CCTGAGCCGCTGGGCTCTCAGCGGCCCTCCAAGGCAGCCCGCAGGCCCCT
GTGTGCCTCAGGGATCCGACCTCCCACAGCCCCGGGGAGACCTTGCCTCT
AAAGTTGCTGCTTTTGCAGCCTCTGCCACAACCGCGCGTCCTCAGAGCCAG
CC**G**GGAGGAGCTAGAACCTTCCCCGCATTTCTTTCAGCAGCCTGAGTCAGA
GGCGGGCTGGCCTGGCGTAGCCGCCCAGCCTCGCGGCTCATGCCCCGAT
CTGCCCGAACCTTCTCCCGGGGTCAGCGCCGCGCCGCGCCACCCGGCTGA
GTCAGCCCGGGCGGGCGAGAGGCTCTCAACTGGGCGGGAAGGTGCGGGA
AGGTGCGGAAAGGTTCG

- -70 (Existing NruI site) to +48
  - CGAAAGTTCGCGGCGGCGGGGGTCGGGTGAGGCGCAAAAGGATAAAAAG
    CC**C**GTGGAAGCGGAGCTGAGCAGATCCGAGCCGGGCTGGCTGCAGAGAA
    ACCGCAGGGAGAGCCTCACT

Protocol for making pGL4.1 HSPA6 internal deletion constructs

- The Agilent QuikChange Lightning Site Directed Mutagenesis kit (Cat #210518) was used to generate the HSP deletion constructs (HSPA6 B, C, D, W, X, Y, and Z). As per the manufacturer's instructions, ~100-150 bp can be accurately deleted from the sequence.
- Deletion A was generated through "normal" cloning procedure.
- pGL4.1 HSPA6 -647 deletion construct (B-D) primers.
    - B forward:
      CTGTTTTAAGATATACGTGTATATATCTTGCCTCTAAAGTTGCTGCTTTTGCAGCC
    - B Reverse:
      GGCTGCAAAAGCAGCAACTTTAGAGGCAAGATATATACACGTATATCTTAAAACAG
    - C Forward:
      ACAGCCCCGGGGAGACGCCGCCCAGCCTCG
    - C Reverse:
      CGAGGCTGGGCGGCGTCTCCCCGGGGCTGT
    - D Forward:
      CGGGCTGGCCTGGCGTACGAAAGTTCGCGGC
    - D Reverse:
      GCCGCGAACTTTCGTACGCCAGGCCAGCCCG
- pGL4.1 HSPA6 -647 deletion construct (A) primers.
    - A Forward:
      gatcGGTACCCTTATATATCTGTATTCGCATGGTAACATATC (KpnI site)
    - A Reverse:
      ttggAAGCTTAGTGAGGCTCTCCCTGCGG (HindIII site)
- pGL4.1 HSPA6 -1230 deletion construct (W-Z) primers.
    - W Forward:
      CTCTGGCCTAACTGGCCGCAGTAGTTTACTCTCCACCTGAGTCC
    - W Reverse:
      GGACTCAGGTGGAGAGTAAACTACTGCGGCCAGTTAGGCCAGAG
    - X Forward:
      GGAGGTAGGTTGGACTGGAGCCTGCTCTGCGTCCTCCTTTCCCAGG
    - X Reverse:
      CCTGGGAAAGGAGGACGCAGAGCAGGCTCCAGTCCAACCTACCTCC
    - Y Forward:
      GAACATGAGGGACATCCCGACCGAGAGAGAACAAAACTGGAGGAAcG
    - Y Reverse:
      CGTTCCTCCAGTTTTGTTCTCTCTCGGTCGGGATGTCCCTCATGTTC
    - Z Forward:
      CCTTTGTGGAAAGTGACTGGTAAAGGAATTCTACCACTGAACCACC
    - Z Reverse:
      GGTGGTTCAGTGGTAGAATTCCTTTACCAGTCACTTTCCACAAAGG

Biotech center sequenced HSPA6 promoter internal deletion sequence

- W deletion sequence (-1230 to -1084)
  - gatctgaatggaatGTTCTGGATTGAAGAAAGTGGGAAATGGCCTCAATTCACAAA GTCACAACCTGATAAAAACCAGTGTGACTTTACTGCCCAGTGAACCCATCTC GTCCTCCAGCCTTTAGGAGGTAGGTTGGACTGGAGCCTG
- X Deletion sequence (-1083 to -928)
  - CAGTAGTTTACTCTCCACCTGAGTCCTGGTCTCCAGCTGGGAACCCACTTA GGCCATAGAGAAAAACGCACACTGTGCCTCTCCACCGGGCCTCTGGAGAC GAGGCTCCTCGGGGATACAAACAGTGGGGAGAACATGAGGGACATCCCGA CCGTA
- Y Deletion sequence (-927 to -808)
  - CTCTGCGTCCTCCTTTCCCAGGTGTTGCGTTCTCTCTTGGGCTGAGTGGCG AGGTCTCTCCCGAGTCCCAGGGCCACAGTGCAATGTCACATCTCCTTTGTG GAAAGTGACTGGTAAAGG
- Z Deletion sequence (-807 to -648)
  - AGAGAGAACAAAACTGGAGGAACGTAAAGTCTTCAGCCACCTGGTTTAATTT ATTCAAGAGTGATTAATCCTAGATGAGAAAAAGAATTGAAATGGATCGGAAA AAAATGAAAGTGCATTGGCCGGGAATCGAACCCGGGCCTCCCGCGTGGCA GGCGAG
- A Deletion sequence (-647 to -479)
  - AATTCTACCACTGAACCACCAATGCTACTGTCAGCTAAAGACCTGCAGTATT GTCTCTTAAAGCTCACTATCTCTGGCCATTCGCTAAGGAACCAGGCACCGTC TTAAATCGCGGTTTGGAAAATATTTTGTTCAAGATAAAACTGTTTTAAGATAT ACGTGTATATAT
- B Deletion sequence (-478 to -347)
  - CTTATATATCTGTATTCGCATGGTAACATATCTTCGGCCTTCCTGAGCCGCT GGGCTCTCAGCGGCCCTCCAAGGCAGCCCGCAGGCCCCTGTGTGCCTCAG GGATCCGACCTCCCACAGCCCCGGGGAGAC
- C Deletion sequence (-346 to -217)
  - CTTGCCTCTAAAGTTGCTGCTTTTGCAGCCTCTGCCACAACCGCGCGTCCT CAGAGCCAGCCGGGAGGAGCTAGAACCTTCCCCGCATTTCTTTCAGCAGCC TGAGTCAGAGGCGGGCTGGCCTGGCGTA
- D Deletion sequence (-216 to -71)
  - GCCGCCCAGCCTCGCGGCTCATGCCCCGATCTGCCCGAACCTTCTCCCGG GGTCAGCGCCGCGCCGCGCCACCCGGCTGAGTCAGCCCGGGCGGGCGAG AGGCTCTCAACTGGGCGGGAAGGTGCGGGAAGGTGCGGAAAGGTTCG

APPENDIX 4

TNIP1 Transcriptional Start Site (TSS)

5' RNA ligase-mediated rapid amplification of cDNA ends (5' RLM-RACE)

Total RNA was extracted from human cell cultures Caco-2, HaCaT, HeLa, HepG2, Jurkat, MCF7, SCC13, SCC25, normal dermal foreskin fibroblasts (FSFB), and scleroderma explant (Sclero expl) fibroblasts using RNeasy (QIAgen, Valencia, CA). 5' RLM-RACE was performed with the GeneRacer system (Invitrogen). Briefly, 1-2 µg of total RNA was treated with calf intestinal phosphatase and then tobacco acid pyrophosphatase, ligated to the GeneRacer RNA oligonucleotide sequence, and then reverse transcribed using SuperScript III RT. PCR amplification of the resulting cDNA was performed using two sets of primers. PCR products were cloned into pCR4-TOPO vector and sequenced.

Mapping TNIP1's transcriptional start sites (TSS)

The TNIP1 gene sequence is increasingly GC rich and without a recognizable TATA box nearing the cluster of expected TSS defined by cap-analysis of gene expression (CAGE) database extractions [16,30]. These characteristics are consistent with this region being dispersed rather than focused type of promoter and furthermore predict multiple transcription start sites over a 50-100 nucleotide region [31]. Because of its reliance on 5' capped mRNA, the RLM-RACE approach is advantageous in determining bona fide TSS. Using it and RNA from human cell cultures, we mapped multiple TSS to the 5' region of the TNIP1 gene (Fig 1A). All but one of the TSS reside in either of two alternative first exons (Fig 1B & 1C) [32,33].

A TSS in exon 2 (Fig 1D) is previously unknown. Among the cell types examined it is characteristic for MCF-7 cells; no other cell's TSS mapped to this point in exon 2 nor did MCF-7 cells produce message from either of the two major TSS clusters. Within each TSS cluster, actual start sites spanned lengths of ~30 or ~90 nucleotides. Both of these clusters experimentally validate our CAGE-mapped TSS [16]. TSS in the 90 nucleotide span overlap the point previously used as +1 in numbering ~600bp [15] and ~6000bp [16] promoter clones and are associated with long exon 1. For consistency with these reports, we have retained such numbering in this study (+1, open arrow, Fig 1C). The other TSS cluster is ~6000 nucleotides upstream of this region suggestive of an alternative promoter. Interestingly, while TSS for some cells (normal dermal fibroblasts; immortalized, non-tumorigenic HaCaT keratinocytes; malignant keratinocyte lines SCC13 or SCC25; Caco2; and adenocarcinoma HeLa cells) mapped to both regions, for other cells, (HepG2 and Jurkat), the TSS cluster mapped to only the upstream region.

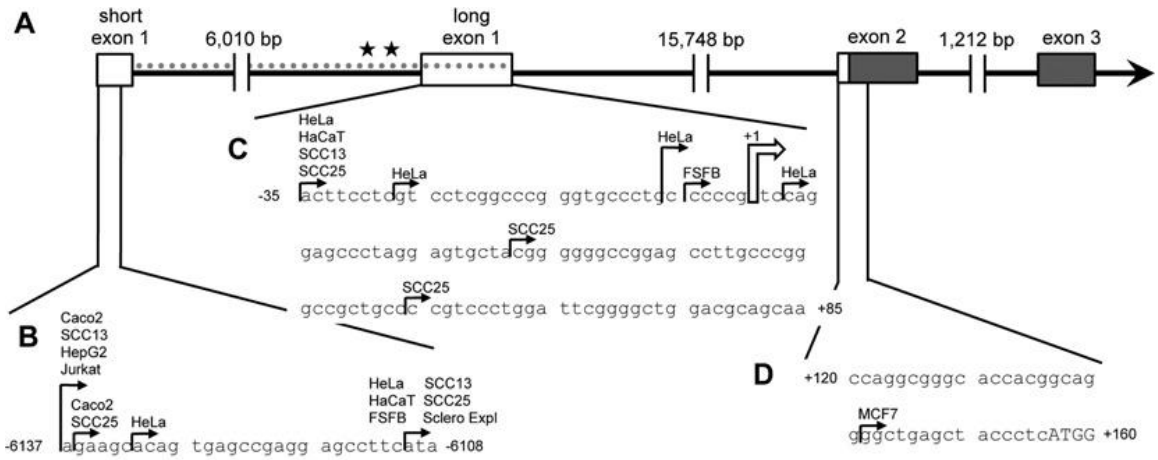

Mapping the TSS of TNIP1. *A.* Schematic illustration of the TNIP1 gene including alternative first exons. Gray dotted line denotes our 6 kb promoter. *B,C & D* partial sequences showing the multiple TSS for short exon 1, long exon 1 and exon 2 (resp.). Our +1 is denoted in long exon 1 by the open arrow. (All untranslated regions are in lower case, and coding regions in upper case.) Nucleotide numbers in *B,C & D* reflect positions in the relative genomic sequence based on the assigning +1 in long exon as denoted above. ★denotes the location of the -131 and -150 Sp sites.

Appendix 5

Experiment numbers for each figure

Figure #	Corresponding Experiment #	Type of experiment
2.1	76	Validation of TNIP1 overexpression
2.2 top	47	TNIP1 overexpression microarray results
2.2 bottom	68, 69, 71, 72, 73, 84	qPCR validation of the microarray
2.5	53	Effect of TNIP1 overexpression on HSPs in HaCaT KCs
2.6, 2.7	119	Effect of TNIP1 overexpression on KC in NHEKs
3.1, 3.2	121, 195	Basal and heat-inducible expression of HSPs in HaCaT KCs
3.3	197	Expression of HSPA6 in various cell types
3.6	150	Determining the transcriptionally regulated regions within the HSPA6 promoter
3.7	187, 202	Localizing the repressible region within the HSPA6 promoter
3.8	187, 188	Localizing the basal and inducible regions within the HSPA6 promoter
3.9	193, 196	Searching for transcription factor binding sites between -346 to -216 bp region of the HSPA6 promoter
3.10	199	Characterization of the -244 bp AP1 site
3.11	200	EMSA binding analysis of AP1 proteins c-Jun and c-Fos to the -244 AP1 site
3.12	193, 196	Searching for heat responsive elements between -346 to -216 bp region of HSPA6
3.13	207	Characterization of the -284 bp HSE
3.14, 3.16	201	EMSA binding analysis of HSF proteins to the -284 bp HSE
3.15, 3.17	203	EMSA binding analysis of HSF proteins to a consensus HSE
4.2	153, 162, 205	Analysis of the HSPA6 promoter truncation constructs + TNIP1
4.3	206	Analysis of the HSPA6 promoter deletion constructs + TNIP1
4.4	129	Effect of TNIP1 overexpression on HSPs in heat stressed HaCaT KCs
4.5	By Nora McHugh	Effect of “short term” increased TNIP1 levels on HaCaT KCs viability and growth
4.6	By Nora McHugh	Effect of “long term” increased TNIP1 levels on HaCaT KCs viability and growth

References

1. S. MacNeil, Progress and opportunities for tissue-engineered skin. *Nature.* **445**, 874-880 (2007).
2. R. L. Eckert, E. A. Rorke, Molecular biology of keratinocyte differentiation. *Environ. Health Perspect.* **80**, 109-116 (1989).
3. J. N. Barker, R. S. Mitra, C. E. Griffiths, V. M. Dixit, B. J. Nickoloff, Keratinocytes as initiators of inflammation. *Lancet.* **337**, 211-214 (1991).
4. L. Eckhart, S. Lippens, E. Tschachler, W. Declercq, Cell death by cornification. *Biochim. Biophys. Acta.* **1833**, 3471-3480 (2013).
5. B. J. Aneskievich, E. Fuchs, Terminal differentiation in keratinocytes involves positive as well as negative regulation by retinoic acid receptors and retinoid X receptors at retinoid response elements. *Mol. Cell. Biol.* **12**, 4862-4871 (1992).
6. V. A. Tron *et al.*, p53-regulated apoptosis is differentiation dependent in ultraviolet B-irradiated mouse keratinocytes. *Am. J. Pathol.* **153**, 579-585 (1998).
7. D. D. Bikle, D. Ng, C. L. Tu, Y. Oda, Z. Xie, Calcium- and vitamin D-regulated keratinocyte differentiation. *Mol. Cell. Endocrinol.* **177**, 161-171 (2001).
8. V. Perissi, M. G. Rosenfeld, Controlling nuclear receptors: the circular logic of cofactor cycles *Nat. Rev. Mol. Cell Biol.* **6**, 542-554 (2005).
9. I. Gurevich, A. M. Flores, B. J. Aneskievich, Corepressors of agonist-bound nuclear receptors *Toxicol. Appl. Pharmacol.* **223**, 288-298 (2007).
10. M. Westergaard *et al.*, Modulation of keratinocyte gene expression and differentiation by PPAR-selective ligands and tetradecylthioacetic acid *J. Invest. Dermatol.* **116**, 702-712 (2001).
11. M. Mao-Qiang *et al.*, Peroxisome-proliferator-activated receptor (PPAR)-gamma activation stimulates keratinocyte differentiation *J. Invest. Dermatol.* **123**, 305-312 (2004).
12. M. Schmuth *et al.*, Peroxisome proliferator-activated receptor (PPAR)-beta/delta stimulates differentiation and lipid accumulation in keratinocytes. *J. Invest. Dermatol.* **122**, 971-983 (2004).
13. K. Hanley *et al.*, Farnesol stimulates differentiation in epidermal keratinocytes via PPARalpha. *J. Biol. Chem.* **275**, 11484-11491 (2000).
14. F. O. Nestle, D. H. Kaplan, J. Barker, Psoriasis *N. Engl. J. Med.* **361**, 496-509 (2009).
15. L. G. Komuves *et al.*, Stimulation of PPARalpha promotes epidermal keratinocyte differentiation in vivo. *J. Invest. Dermatol.* **115**, 353-360 (2000).
16. N. S. Tan *et al.*, Critical roles of PPAR beta/delta in keratinocyte response to inflammation. *Genes Dev.* **15**, 3263-3277 (2001).
17. M. Y. Sheu *et al.*, Topical peroxisome proliferator activated receptor-alpha activators reduce inflammation in irritant and allergic contact dermatitis models. *J. Invest. Dermatol.* **118**, 94-101 (2002).
18. H. Green, F. M. Watt, Regulation by vitamin A of envelope cross-linking in cultured keratinocytes derived from different human epithelia. *Mol. Cell. Biol.* **2**, 1115-1117 (1982).
19. L. S. Winterfield, A. Menter, K. Gordon, A. Gottlieb, Psoriasis treatment: current and emerging directed therapies. *Ann. Rheum. Dis.* **64 Suppl 2**, ii87-90; discussion ii91-2 (2005).
20. E. W. Harhaj, V. M. Dixit, Deubiquitinases in the regulation of NF-kappaB signaling *Cell Res.* **21**, 22-39 (2011).

21. C. S. Seitz, Q. Lin, H. Deng, P. A. Khavari, Alterations in NF-kappaB function in transgenic epithelial tissue demonstrate a growth inhibitory role for NF-kappaB. *Proc. Natl. Acad. Sci. U. S. A.* **95**, 2307-2312 (1998).
22. F. C. Victor, A. B. Gottlieb, TNF-alpha and apoptosis: implications for the pathogenesis and treatment of psoriasis. *J. Drugs Dermatol.* **1**, 264-275 (2002).
23. I. Gurevich, B. J. Aneskievich, Liganded RARalpha and RARgamma interact with but are repressed by TNIP1 *Biochem. Biophys. Res. Commun.* **389**, 409-414 (2009).
24. A. M. Flores *et al.*, TNIP1 is a corepressor of agonist-bound PPARs *Arch. Biochem. Biophys.*(2011).
25. I. Gurevich, C. Zhang, N. Francis, B. J. Aneskievich, TNIP1, a Retinoic Acid Receptor Corepressor and A20-binding Inhibitor of NF-kappaB, Distributes to Both Nuclear and Cytoplasmic Locations *J. Histochem. Cytochem.* **59**, 1101-1112 (2011).
26. A. Fritah, M. Christian, M. G. Parker, The metabolic coregulator RIP140: an update *Am. J. Physiol. Endocrinol. Metab.* **299**, E335-40 (2010).
27. L. N. Wei, X. Hu, D. Chandra, E. Seto, M. Farooqui, Receptor-interacting protein 140 directly recruits histone deacetylases for gene silencing *J. Biol. Chem.* **275**, 40782-40787 (2000).
28. C. Mauro *et al.*, ABIN-1 binds to NEMO/IKKgamma and co-operates with A20 in inhibiting NF-kappaB *J. Biol. Chem.* **281**, 18482-18488 (2006).
29. S. Wagner *et al.*, Ubiquitin binding mediates the NF-kappaB inhibitory potential of ABIN proteins *Oncogene.* **27**, 3739-3745 (2008).
30. T. Bouwmeester *et al.*, A physical and functional map of the human TNF-alpha/NF-kappa B signal transduction pathway *Nat. Cell Biol.* **6**, 97-105 (2004).
31. S. Cohen, A. Ciechanover, Y. Kravtsova-Ivantsiv, D. Lapid, S. Lahav-Baratz, ABIN-1 negatively regulates NF-kappaB by inhibiting processing of the p105 precursor *Biochem. Biophys. Res. Commun.* **389**, 205-210 (2009).
32. T. L. Haas *et al.*, Recruitment of the linear ubiquitin chain assembly complex stabilizes the TNF-R1 signaling complex and is required for TNF-mediated gene induction *Mol. Cell.* **36**, 831-844 (2009).
33. J. Gallagher *et al.*, Identification of Naf1/ABIN-1 among TNF-alpha-induced expressed genes in human synoviocytes using oligonucleotide microarrays *FEBS Lett.* **551**, 8-12 (2003).
34. R. P. Nair *et al.*, Genome-wide scan reveals association of psoriasis with IL-23 and NF-kappaB pathways *Nat. Genet.* **41**, 199-204 (2009).
35. J. W. Han *et al.*, Genome-wide association study in a Chinese Han population identifies nine new susceptibility loci for systemic lupus erythematosus *Nat. Genet.* **41**, 1234-1237 (2009).
36. V. Gateva *et al.*, A large-scale replication study identifies TNIP1, PRDM1, JAZF1, UHRF1BP1 and IL10 as risk loci for systemic lupus erythematosus *Nat. Genet.* **41**, 1228-1233 (2009).
37. C. F. He *et al.*, TNIP1, SLC15A4, ETS1, RasGRP3 and IKZF1 are associated with clinical features of systemic lupus erythematosus in a Chinese Han population *Lupus.* **19**, 1181-1186 (2010).
38. A. Kawasaki *et al.*, Association of TNFAIP3 interacting protein 1, TNIP1 with systemic lupus erythematosus in a Japanese population: a case-control association study *Arthritis Res. Ther.* **12**, R174 (2010).
39. Y. Allanore *et al.*, Genome-Wide Scan Identifies TNIP1, PSORS1C1, and RHOB as Novel Risk Loci for Systemic Sclerosis *PLoS Genet.* **7**, e1002091 (2011).
40. K. Gupta, D. Ott, T. J. Hope, R. F. Siliciano, J. D. Boeke, A human nuclear shuttling protein that interacts with human immunodeficiency virus type 1 matrix is packaged into virions *J. Virol.* **74**, 11811-11824 (2000).

41. V. P. Ramirez, I. Gurevich, B. J. Aneskievich, Emerging roles for TNIP1 in regulating post-receptor signaling. *Cytokine Growth Factor Rev.* **23**, 109-118 (2012).
42. M. Favre, C. Butticaz, B. Stevenson, C. V. Jongeneel, A. Telenti, High frequency of alternative splicing of human genes participating in the HIV-1 life cycle: a model using TSG101, betaTrCP, PPIA, INI1, NAF1, and PML *J. Acquir. Immune Defic. Syndr.* **34**, 127-133 (2003).
43. Y. Shiote *et al.*, Multiple splicing variants of Naf1/ABIN-1 transcripts and their alterations in hematopoietic tumors *Int. J. Mol. Med.* **18**, 917-923 (2006).
44. P. C. Encarnacao, V. P. Ramirez, C. Zhang, B. J. Aneskievich, Sp sites contribute to basal and inducible expression of the human TNIP1 (TNFalpha-inducible protein 3-interacting protein 1) promoter. *Biochem. J.* **452**, 519-529 (2013).
45. Y. C. Tung, G. S. Yeo, From GWAS to biology: lessons from FTO *Ann. N. Y. Acad. Sci.* **1220**, 162-171 (2011).
46. T. Berulava, B. Horsthemke, The obesity-associated SNPs in intron 1 of the FTO gene affect primary transcript levels *Eur. J. Hum. Genet.*(2010).
47. L. A. Hindorff *et al.*, Potential etiologic and functional implications of genome-wide association loci for human diseases and traits *Proc. Natl. Acad. Sci. U. S. A.* **106**, 9362-9367 (2009).
48. M. Uddin, M. Sturge, P. Rahman, M. O. Woods, Autosome-wide Copy Number Variation Association Analysis for Rheumatoid Arthritis Using the WTCCC High-density SNP Genotype Data *J. Rheumatol.* **38**, 797-801 (2011).
49. M. S. Hayden, S. Ghosh, Shared principles in NF-kappaB signaling *Cell.* **132**, 344-362 (2008).
50. S. Vallabhapurapu, M. Karin, Regulation and function of NF-kappaB transcription factors in the immune system *Annu. Rev. Immunol.* **27**, 693-733 (2009).
51. G. Dong *et al.*, A20, ABIN-1/2, and CARD11 mutations and their prognostic value in gastrointestinal diffuse large B-cell lymphoma *Clin. Cancer Res.* **17**, 1440-1451 (2011).
52. Genetic Analysis of Psoriasis Consortium & the Wellcome Trust Case Control Consortium 2 *et al.*, A genome-wide association study identifies new psoriasis susceptibility loci and an interaction between HLA-C and ERAP1 *Nat. Genet.* **42**, 985-990 (2010).
53. E. A. Stahl *et al.*, Genome-wide association study meta-analysis identifies seven new rheumatoid arthritis risk loci *Nat. Genet.* **42**, 508-514 (2010).
54. G. Orozco *et al.*, Study of the common genetic background for rheumatoid arthritis and systemic lupus erythematosus *Ann. Rheum. Dis.* **70**, 463-468 (2011).
55. K. Hinata, A. M. Gervin, Y. Jennifer Zhang, P. A. Khavari, Divergent gene regulation and growth effects by NF-kappa B in epithelial and mesenchymal cells of human skin *Oncogene.* **22**, 1955-1964 (2003).
56. M. Halvorsen, J. S. Martin, S. Broadaway, A. Laederach, Disease-associated mutations that alter the RNA structural ensemble *PLoS Genet.* **6**, e1001074 (2010).
57. H. Igarashi *et al.*, A pro-inflammatory role for A20 and ABIN family proteins in human fibroblast-like synoviocytes in rheumatoid arthritis *Immunol. Lett.*(2011).
58. C. A. Dinarello, Anti-inflammatory Agents: Present and Future *Cell.* **140**, 935-950 (2010).
59. E. Sbidian *et al.*, Efficacy and safety of oral retinoids in different psoriasis subtypes: a systematic literature review *J. Eur. Acad. Dermatol. Venereol.* **25 Suppl 2**, 28-33 (2011).
60. L. Michalik, W. Wahli, Peroxisome proliferator-activated receptors (PPARs) in skin health, repair and disease *Biochim. Biophys. Acta.* **1771**, 991-998 (2007).

61. M. Schmuth, Y. J. Jiang, S. Dubrac, P. M. Elias, K. R. Feingold, Thematic review series: skin lipids. Peroxisome proliferator-activated receptors and liver X receptors in epidermal biology *J. Lipid Res.* **49**, 499-509 (2008).
62. W. Huang, C. K. Glass, Nuclear receptors and inflammation control: molecular mechanisms and pathophysiological relevance *Arterioscler. Thromb. Vasc. Biol.* **30**, 1542-1549 (2010).
63. E. Ellinghaus *et al.*, Genome-Wide Meta-Analysis of Psoriatic Arthritis Identifies Susceptibility Locus at REL. *J. Invest. Dermatol.* **132**, 1133-1140 (2012).
64. J. Bowes *et al.*, Confirmation of TNIP1 and IL23A as susceptibility loci for psoriatic arthritis *Ann. Rheum. Dis.*(2011).
65. K. El Bakkouri, A. Wullaert, M. Haegman, K. Heyninck, R. Beyaert, Adenoviral gene transfer of the NF-kappa B inhibitory protein ABIN-1 decreases allergic airway inflammation in a murine asthma model. *J. Biol. Chem.* **280**, 17938-17944 (2005).
66. A. Wullaert *et al.*, Adenoviral gene transfer of ABIN-1 protects mice from TNF/galactosamine-induced acute liver failure and lethality *Hepatology.* **42**, 381-389 (2005).
67. S. Oshima *et al.*, ABIN-1 is a ubiquitin sensor that restricts cell death and sustains embryonic development *Nature.* **457**, 906-909 (2009).
68. J. Zhou *et al.*, A20-binding inhibitor of NF-kappaB (ABIN1) controls Toll-like receptor-mediated CCAAT/enhancer-binding protein beta activation and protects from inflammatory disease *Proc. Natl. Acad. Sci. U. S. A.* **108**, E998-E1006 (2011).
69. S. K. Nanda *et al.*, Polyubiquitin binding to ABIN1 is required to prevent autoimmunity *J. Exp. Med.* **208**, 1215-1228 (2011).
70. S. Zhang, M. Mahalingam, N. Tsuchida, Naf1alpha is phosphorylated in mitotic phase and required to protect cells against apoptosis. *Biochem. Biophys. Res. Commun.* **367**, 364-369 (2008).
71. C. Jonak, G. Klosner, F. Trautinger, Significance of heat shock proteins in the skin upon UV exposure *Front. Biosci.* **14**, 4758-4768 (2009).
72. F. Ritossa, A new puffing pattern induced by temperature shock and DNP in drosophila. *Cellular and Molecular Life Sciences.* **18**, 571-573 (1962).
73. H. H. Kampinga *et al.*, Guidelines for the nomenclature of the human heat shock proteins *Cell Stress Chaperones.* **14**, 105-111 (2009).
74. G. Ravagnan *et al.*, Polydatin, a natural precursor of resveratrol, induces beta-defensin production and reduces inflammatory response. *Inflammation.* **36**, 26-34 (2013).
75. J. L. Curry *et al.*, Innate immune-related receptors in normal and psoriatic skin. *Arch. Pathol. Lab. Med.* **127**, 178-186 (2003).
76. Z. G. Zhao, Q. Z. Ma, C. X. Xu, Abrogation of heat-shock protein (HSP)70 expression induced cell growth inhibition and apoptosis in human androgen-independent prostate cancer cell line PC-3m. *Asian J. Androl.* **6**, 319-324 (2004).
77. J. Hageman, M. A. van Waarde, A. Zylicz, D. Walerych, H. H. Kampinga, The diverse members of the mammalian HSP70 machine show distinct chaperone-like activities. *Biochem. J.* **435**, 127-142 (2011).
78. L. Heldens *et al.*, Protein refolding in peroxisomes is dependent upon an HSF1-regulated function. *Cell Stress Chaperones.* **17**, 603-613 (2012).
79. E. J. Noonan, R. F. Place, C. Giardina, L. E. Hightower, Hsp70B' regulation and function *Cell Stress Chaperones.* **12**, 393-402 (2007).
80. L. Puig, M. T. Fernandez-Figueras, C. Ferrandiz, M. Ribera, J. M. de Moragas, Epidermal expression of 65 and 72 kd heat shock proteins in psoriasis and AIDS-associated psoriasiform dermatitis. *J. Am. Acad. Dermatol.* **33**, 985-989 (1995).

81. L. J. Gomez-Sucerquia, A. Blas-Garcia, M. Marti-Cabrera, J. V. Esplugues, N. Apostolova, Profile of stress and toxicity gene expression in human hepatic cells treated with Efavirenz. *Antiviral Res.* **94**, 232-241 (2012).
82. A. M. Chow, P. Mok, D. Xiao, S. Khalouei, I. R. Brown, Heteromeric complexes of heat shock protein 70 (HSP70) family members, including Hsp70B', in differentiated human neuronal cells. *Cell Stress Chaperones.* **15**, 545-553 (2010).
83. E. J. Noonan, R. F. Place, R. J. Rasoulpour, C. Giardina, L. E. Hightower, Cell number-dependent regulation of Hsp70B' expression: evidence of an extracellular regulator. *J. Cell. Physiol.* **210**, 201-211 (2007).
84. K. Wada, A. Taniguchi, L. Xu, T. Okano, Rapid and highly sensitive detection of cadmium chloride induced cytotoxicity using the HSP70B' promoter in live cells. *Biotechnol. Bioeng.* **92**, 410-415 (2005).
85. K. Wada, A. Taniguchi, T. Okano, Highly sensitive detection of cytotoxicity using a modified HSP70B' promoter. *Biotechnol. Bioeng.* **97**, 871-876 (2007).
86. S. Rohmer, A. Mainka, I. Knippertz, A. Hesse, D. M. Nettelbeck, Insulated hsp70B' promoter: stringent heat-inducible activity in replication-deficient, but not replication-competent adenoviruses. *J. Gene Med.* **10**, 340-354 (2008).
87. J. Bowes, A. Barton, The genetics of psoriatic arthritis: lessons from genome-wide association studies *Discov. Med.* **10**, 177-183 (2010).
88. K. Heyninck, M. M. Kreike, R. Beyaert, Structure-function analysis of the A20-binding inhibitor of NF-kappa B activation, ABIN-1 *FEBS Lett.* **536**, 135-140 (2003).
89. S. Zhang *et al.*, A new ERK2 binding protein, Naf1, attenuates the EGF/ERK2 nuclear signaling *Biochem. Biophys. Res. Commun.* **297**, 17-23 (2002).
90. J. A. Callahan *et al.*, Cutting edge: ABIN-1 protects against psoriasis by restricting MyD88 signals in dendritic cells. *J. Immunol.* **191**, 535-539 (2013).
91. W. H. Boehncke, A. Dahlke, T. M. Zollner, W. Sterry, Differential expression of heat shock protein 70 (HSP70) and heat shock cognate protein 70 (HSC70) in human epidermis *Arch. Dermatol. Res.* **287**, 68-71 (1994).
92. F. Trautinger, I. Trautinger, I. Kindas-Mugge, D. Metze, T. A. Luger, Human keratinocytes in vivo and in vitro constitutively express the 72-kD heat shock protein *J. Invest. Dermatol.* **101**, 334-338 (1993).
93. M. M. Simon *et al.*, Heat shock protein 70 overexpression affects the response to ultraviolet light in murine fibroblasts. Evidence for increased cell viability and suppression of cytokine release *J. Clin. Invest.* **95**, 926-933 (1995).
94. M. Oberringer *et al.*, Differential expression of heat shock protein 70 in well healing and chronic human wound tissue. *Biochem. Biophys. Res. Commun.* **214**, 1009-1014 (1995).
95. P. Boukamp *et al.*, Normal keratinization in a spontaneously immortalized aneuploid human keratinocyte cell line. *J. Cell Biol.* **106**, 761-771 (1988).
96. V. P. Ramirez, B. J. Aneskievich, Transgene Delivery to Cultured Keratinocytes via Replication-Deficient Adenovirus Vectors. *Methods Mol. Biol.*(2013).
97. W. Huang da, B. T. Sherman, R. A. Lempicki, Systematic and integrative analysis of large gene lists using DAVID bioinformatics resources. *Nat. Protoc.* **4**, 44-57 (2009).
98. W. Huang da, B. T. Sherman, R. A. Lempicki, Bioinformatics enrichment tools: paths toward the comprehensive functional analysis of large gene lists. *Nucleic Acids Res.* **37**, 1-13 (2009).
99. F. Minner, Y. Poumay, Candidate housekeeping genes require evaluation before their selection for studies of human epidermal keratinocytes. *J. Invest. Dermatol.* **129**, 770-773 (2009).
100. K. Heyninck *et al.*, The zinc finger protein A20 inhibits TNF-induced NF-kappaB-dependent gene expression by interfering with an RIP- or TRAF2-mediated

transactivation signal and directly binds to a novel NF-kappaB-inhibiting protein ABIN *J. Cell Biol.* **145**, 1471-1482 (1999).
101. S. H. Yuspa, A. E. Kilkenny, P. M. Steinert, D. R. Roop, Expression of murine epidermal differentiation markers is tightly regulated by restricted extracellular calcium concentrations in vitro. *J. Cell Biol.* **109**, 1207-1217 (1989).
102. M. Akerfelt, R. I. Morimoto, L. Sistonen, Heat shock factors: integrators of cell stress, development and lifespan. *Nat. Rev. Mol. Cell Biol.* **11**, 545-555 (2010).
103. H. Saibil, Chaperone machines for protein folding, unfolding and disaggregation. *Nat. Rev. Mol. Cell Biol.* **14**, 630-642 (2013).
104. M. Daugaard, M. Rohde, M. Jaattela, The heat shock protein 70 family: Highly homologous proteins with overlapping and distinct functions. *FEBS Lett.* **581**, 3702-3710 (2007).
105. S. Leppa, R. Kajanne, L. Arminen, L. Sistonen, Differential induction of Hsp70-encoding genes in human hematopoietic cells. *J. Biol. Chem.* **276**, 31713-31719 (2001).
106. E. Noonan, C. Giardina, L. Hightower, Hsp70B' and Hsp72 form a complex in stressed human colon cells and each contributes to cytoprotection. *Exp. Cell Res.* **314**, 2468-2476 (2008).
107. M. Matsuda *et al.*, Prevention of UVB radiation-induced epidermal damage by expression of heat shock protein 70. *J. Biol. Chem.* **285**, 5848-5858 (2010).
108. S. B. Kwon *et al.*, Impaired repair ability of hsp70.1 KO mouse after UVB irradiation *J. Dermatol. Sci.* **28**, 144-151 (2002).
109. A. Sandelin, W. W. Wasserman, Prediction of nuclear hormone receptor response elements. *Mol. Endocrinol.* **19**, 595-606 (2005).
110. M. Podvinec, M. R. Kaufmann, C. Handschin, U. A. Meyer, NUBIScan, an in silico approach for prediction of nuclear receptor response elements. *Mol. Endocrinol.* **16**, 1269-1279 (2002).
111. K. Cartharius *et al.*, MatInspector and beyond: promoter analysis based on transcription factor binding sites. *Bioinformatics.* **21**, 2933-2942 (2005).
112. T. K. Leung, M. Y. Rajendran, C. Monfries, C. Hall, L. Lim, The human heat-shock protein family. Expression of a novel heat-inducible HSP70 (HSP70B') and isolation of its cDNA and genomic DNA. *Biochem. J.* **267**, 125-132 (1990).
113. K. D. Pruitt, T. Tatusova, D. R. Maglott, NCBI Reference Sequence (RefSeq): a curated non-redundant sequence database of genomes, transcripts and proteins. *Nucleic Acids Res.* **33**, D501-4 (2005).
114. W. D. Morgan *et al.*, Two transcriptional activators, CCAAT-box-binding transcription factor and heat shock transcription factor, interact with a human hsp70 gene promoter. *Mol. Cell. Biol.* **7**, 1129-1138 (1987).
115. S. Khalouei, A. M. Chow, I. R. Brown, Stress-induced localization of HSPA6 (HSP70B') and HSPA1A (HSP70-1) proteins to centrioles in human neuronal cells. *Cell Stress Chaperones.*(2013).
116. E. Kolker *et al.*, MOPED: Model Organism Protein Expression Database. *Nucleic Acids Res.* **40**, D1093-9 (2012).
117. B. J. Wu, R. I. Morimoto, Transcription of the human hsp70 gene is induced by serum stimulation. *Proc. Natl. Acad. Sci. U. S. A.* **82**, 6070-6074 (1985).
118. K. Zachova *et al.*, Novel modification of growth medium enables efficient E. coli expression and simple purification of an endotoxin-free recombinant murine hsp70 protein. *J. Microbiol. Biotechnol.* **19**, 727-733 (2009).
119. S. Qiao *et al.*, Thiostrepton is an inducer of oxidative and proteotoxic stress that impairs viability of human melanoma cells but not primary melanocytes. *Biochem. Pharmacol.* **83**, 1229-1240 (2012).

120. M. Sachdeva, Q. Liu, J. Cao, Z. Lu, Y. Y. Mo, Negative regulation of miR-145 by C/EBP-beta through the Akt pathway in cancer cells. *Nucleic Acids Res.* **40**, 6683-6692 (2012).
121. D. Gokhman, I. Livyatan, B. S. Sailaja, S. Melcer, E. Meshorer, Multilayered chromatin analysis reveals E2f, Smad and Zfx as transcriptional regulators of histones. *Nat. Struct. Mol. Biol.* **20**, 119-126 (2013).
122. C. P. Reina, B. Y. Nabet, P. D. Young, R. N. Pittman, Basal and stress-induced Hsp70 are modulated by ataxin-3. *Cell Stress Chaperones.* **17**, 729-742 (2012).
123. S. Koizumi, K. Suzuki, S. Yamaguchi, Heavy metal response of the heat shock protein 70 gene is mediated by duplicated heat shock elements and heat shock factor 1. *Gene.* **522**, 184-191 (2013).
124. G. T. Williams, R. I. Morimoto, Maximal stress-induced transcription from the human HSP70 promoter requires interactions with the basal promoter elements independent of rotational alignment. *Mol. Cell. Biol.* **10**, 3125-3136 (1990).
125. M. Fujimoto *et al.*, HSF4 is required for normal cell growth and differentiation during mouse lens development. *EMBO J.* **23**, 4297-4306 (2004).
126. M. Fujimoto, A. Nakai, The heat shock factor family and adaptation to proteotoxic stress. *FEBS J.* **277**, 4112-4125 (2010).
127. J. Xu, Y. Kawai, I. J. Arinze, Dual role of C/EBPalpha as an activator and repressor of Galphai2 gene transcription. *Genes Cells.* **18**, 1082-1094 (2013).
128. Y. K. Kim *et al.*, Deletion of the inducible 70-kDa heat shock protein genes in mice impairs cardiac contractile function and calcium handling associated with hypertrophy. *Circulation.* **113**, 2589-2597 (2006).
129. I. Gurevich *et al.*, PPARgamma and NF-kappaB regulate the gene promoter activity of their shared repressor, TNIP1 *Biochim. Biophys. Acta.* **1819**, 1-15 (2011).
130. A. J. Parsian *et al.*, The human Hsp70B gene at the HSPA7 locus of chromosome 1 is transcribed but non-functional. *Biochim. Biophys. Acta.* **1494**, 201-205 (2000).
131. K. J. Smith *et al.*, Heat shock protein 70B' (HSP70B') expression and release in response to human oxidized low density lipoprotein immune complexes in macrophages. *J. Biol. Chem.* **285**, 15985-15993 (2010).
132. C. Zhang, I. Gurevich, B. J. Aneskievich, Organotypic modeling of human keratinocyte response to peroxisome proliferators. *Cells Tissues Organs.* **196**, 431-441 (2012).